

# **Study of Antisense Oligonucleotides against Glucose Transporter 5 (Glut 5) on Human Breast Cancer Cells**

**Chung Ka Wing, B.Sc. (Hons)**

A Thesis Submitted in Partial Fulfilment  
of the Requirements for the Degree of  
Master of Philosophy  
in  
Biochemistry

©The Chinese University of Hong Kong

July 2004

The Chinese University of Hong Kong holds the copyright of this thesis. Any person (s) intending to use a part or whole of the materials in the thesis in a proposed publication must seek copyright release from the Dean of the Graduate School.



# Contents

<b>Contents</b>	i
<b>Acknowledgements</b>	v
<b>Abstract</b>	vi
<b>論文摘要</b>	ix
<b>List of Abbreviations</b>	xi
<b>List of Figures</b>	xiii
<b>List of Tables</b>	xv
<b>Chapter 1 Introduction</b>	1
<b>1.1 Breast Cancer</b>	2
1.1.1 Incidence Rate of Breast Cancer	2
1.1.2 Risk Factors Lead to Breast Cancer	5
1.1.3 Conventional Treatments	5
<b>1.2 Relationship between Breast Cancer and Glucose Transporters</b>	7
1.2.1 Importance of Glucose and Fructose	7
1.2.2 Facilitative Glucose Transporters (Gluts) and The Relationship with Breast Cancer	7
<b>1.3 Antisense Oligonucleotides</b>	13
1.3.1 Characteristics of Antisense Oligonucleotides	13
1.3.2 Action Mechanism of Antisense Oligonucleotides	15
1.3.3 Sequence Selection	19
1.3.4 Chemical Modifications of Antisense Oligonucleotides	20
1.3.5 Uptake and Delivery Means of Antisense Oligonucleotides	24
<b>1.4 Objectives of Present Study</b>	26
<b>Chapter 2 Materials and Methods</b>	31
<b>2.1 Materials</b>	32
2.1.1 Cell Lines and Culture Medium	32
2.1.2 Buffers and Reagents	33
2.1.3 Reagents for Transfection	34
2.1.4 Reagents for D-[U <sup>14</sup> C]-Fructose and 2-Deoxy-D-[1- <sup>3</sup> H] Glucose Uptake Assay	35
2.1.5 Reagents for ATP Assay	35
2.1.6 Reagents for RT-PCR	36

2.1.6.1	Reagents for RNA Extraction	36
2.1.6.2	Reagents for Reverse Transcription	36
2.1.6.3	Reagents for Gel Electrophoresis	37
2.1.7	Reagents for Real Time-PCR	38
2.1.8	Reagents and Chemicals for Western Blotting	39
2.1.8.1	Reagents for Protein Extraction	39
2.1.8.2	Reagents for SDS-PAGE	39
2.1.9	Reagents for Flow Cytometry	42
2.1.10	<i>In Vivo</i> Study	43
<b>2.2</b>	<b>Methods</b>	44
2.2.1	Oligonucleotide Design	44
2.2.2	Trypan Blue Exclusion Assay	47
2.2.3	Transfection	47
2.2.4	MTT Assay	47
2.2.5	D-[U <sup>14</sup> C]-fructose and 2-deoxy-D-[1- <sup>3</sup> H] Glucose Uptake Assay	48
2.2.6	Detection of Intracellular ATP Concentration	49
2.2.7	Reverse Transcription-Polymerase Chain Reaction (RT-PCR)	51
2.2.7.1	RNA Extraction by TRIzol Reagent	51
2.2.7.2	Determination of RNA Concentration	51
2.2.7.3	Reverse Transcription	52
2.2.7.4	Polymerase Chain Reaction (PCR)	52
2.2.8	Real-Time PCR	55
2.2.8.1	Analysis of the Real-Time PCR Data	57
2.2.9	Western Blot Analysis	58
2.2.9.1	Protein Extraction	58
2.2.9.2	Protein Concentration Determination	58
2.2.9.3	Western Blotting	60
2.2.10	Flow Cytometry	62
2.2.10.1	Detection of Cell Cycle Pattern with PI	62
2.2.10.2	Detection of Apoptosis with Annexin V/PI	62
2.2.11	<i>In Vivo</i> Study	63
2.2.11.1	Establishment of Tumor-Bearing Animal Model	63
2.2.11.2	Treatment Schedule	63
2.2.11.3	Toxicity of Antisense Oligonucleotides	64



<b>Chapter 3</b>	<b>Results</b>	66
<b>3.1</b>	<b><i>In Vitro</i> Study</b>	67
3.1.1	Effect of Tamoxifen on MCF-7 cells and MDA-MB-231 cells	67
3.1.2	Cytotoxicity of Antisense Oligonucleotides against Glut 5 on MCF-7 cells and MDA-MB-231 cells by MTT Assay	69
3.1.3	Effect of Antisense Oligonucleotides against Glut 5 on Fructose and Glucose Uptake of MCF-7 cells and MDA-MB-231 cells by D-[U <sup>14</sup> C]-Fructose & 2-Deoxy-D-[1- <sup>3</sup> H] Glucose Uptake Assay	77
3.1.4	Effect of Antisense Oligonucleotides against Glut 5 on Intracellular ATP Content of MCF-7 cells and MDA-MB-231 cells by ATP Assay	81
3.1.5	Effect of Antisense Oligonucleotides against Glut 5 on Glut 5 RNA Expression of MCF-7 cells and MDA-MB-231 cells by RT-PCR and Real-Time PCR	83
3.1.5.1	RT-PCR	83
3.1.5.2	Real-Time PCR	87
3.1.6	Effect of Antisense Oligonucleotides against Glut 5 on Glut 5 Protein Expression of MCF-7 cells and MDA-MB-231 cells by Western Blot Analysis	89
3.1.7	Effect of Antisense Oligonucleotides against Glut 5 on Change in Cell Cycle Pattern of MCF-7 cells and MDA-MB-231 cells by Flow Cytometry, Using PI Staining	93
3.1.8	Effect of Antisense Oligonucleotides against Glut 5 on Induction of Apoptosis of MCF-7 cells and MDA-MB-231 cells by Flow Cytometry, Using Annexin V-FITC Staining	98
<b>3.2</b>	<b><i>In Vivo</i> Study</b>	101
3.2.1	Animal Model: Nude Mice	101
3.2.2	Effect of Antisense Oligonucleotides against Glut 5 on the MCF-7 cells-Bearing Nude Mice	101
3.2.2.1	Change of Weight of the Tumor-Bearing Nude Mice	101
3.2.2.2	Tumor Growth Rate	105
3.2.2.3	Glut 5 RNA Expression by Real-Time PCR	109

3.2.2.4	Glut 5 RNA Expression by Western Blotting	111
3.2.3	Assessment of Side Effects of Antisense Oligonucleotides against Glut 5, by Measuring the Plasma Enzyme Level	113
<b>Chapter 4</b>	<b>Discussion</b>	118
<b>4.1</b>	<b>Antisense Oligonucleotides against Glut 5 on Human Breast Cancer</b>	119
4.1.1	Antisense Oligonucleotides Strategy	119
4.1.2	Role of Glut 5 in Breast Cancer	123
4.1.3	Effects of Tamoxifen on MCF-7 and MDA-MB-231	126
<b>4.2</b>	<b><i>In Vitro</i> Study of Antisense Oligonucleotides against Glucose Transporter 5 on Breast Cancer Cells</b>	127
<b>4.3</b>	<b><i>In Vivo</i> Study of Antisense Oligonucleotides against Glucose Transporter 5 on Breast Cancer Cells</b>	135
4.3.1	Effects of Antisense Oligonucleotides against Glut 5 on Body Weight and Tumor Size	137
4.3.2	Expression Level of Glut 5 of the Tumor	138
4.3.3	Assessment of Side Effects of Antisense Oligonucleotides against Glut 5, by Measuring the Plasma Enzymes Level	140
<b>4.4</b>	<b>Possible Mechanism of Antisense Oligonucleotides against Glut 5 on Breast Cancer</b>	141
<b>Chapter 5</b>	<b>Future Prospectus and Conclusions</b>	143
<b>5.1</b>	<b>Future Prospectus of Antisense Oligonucleotides</b>	144
5.1.1	Antisense Oligonucleotides and Treatment of Breast Cancer	144
5.1.2	Role of Glut 5 in Breast Cancer	147
<b>5.2</b>	<b>Conclusions and Remarks</b>	148
	<b>References</b>	151

# Acknowledgments

I would like to express my sincere thanks to my supervisors, Prof. K.P. Fung and Prof. C.Y. Lee for their guidance and precious advice throughout the two-years M.Phil. study.

Besides, I would like to thank Ms. Judy Chan, Ms Jenny Cheung, Ms Virginia Lau, Ms Macey Lee, Ms Julia Lee, Mr. Lion Koon, Ms Ming Lam, Mr. Patrick Tang and Ms Rebecca Tang for their help and valuable advice to my research project. I also wish to thank my friends in BMSB room 316 and in Department of Biochemistry.

Last but not least, I must thank my family and Mr. Johnny Ho for their encouragement and the warmest support in my life.



## Abstract

During breast tumor development, extra energy is required to support the uncontrolled growth. This energy is supplied by increased glucose or fructose uptake, through the agency of facilitative glucose transporters, and their catabolism. By reducing the uptake of these monosaccharides, tumor proliferation would be inhibited as a result of nutrient deprivation. To test this hypothesis, antisense oligonucleotides (AS) against glucose transporter 5 (Glut 5), which is also called fructose transporter, were synthesized to block its expression in breast tumor cells. Antisense treatment represents the regulation of gene expression by short oligonucleotides or oligonucleotide mimics, which relies on various mechanisms including the formation of Watson and Crick hydrogen bonds between the antisense oligomer and the complementary mRNA strand, thereby providing target specificity of the agent.

The sequence of AS(s) were complementary to Glut 5 mRNA, with 15 base pairs in length. The antisense oligonucleotides were then phosphorothioated at each base to increase the stability. In the present study, antisense oligonucleotides were transfected into two human breast tumor cell lines, an estrogen receptor positive cell line MCF-7 and an estrogen receptor negative cell line MDA-MB-231, to investigate the effect of these oligonucleotides on the breast tumor growth, which includes cytotoxic effect, regulation of Glut 5 gene expression, uptake efficiency of

monosaccharides, intracellular ATP content, cell cycle pattern and apoptotic study after AS treatment and *in vivo* study.

For *in vitro* study, it was found that after 72-hour incubation of various concentration of AS, the percentages of survival of MCF-7 cells and MDA-MB-231 cells were decreased in a dose dependent manner. Significant inhibition (>30% in both cell lines) of fructose uptake was observed and was accompanied by the reduction of Glut 5 mRNA and protein level (>40% in both cell lines). The intracellular ATP content was decreased in both MCF-7 cells and MDA-MB-231 cells. In addition, apoptosis was found in both cell lines, with the incidence of phosphatidylserine externalization and the occurrence of apoptotic peaks after 72-hour incubation at IC<sub>50</sub> concentration, namely 220nM, 190nM, 300nM and 220nM for AS 1, AS 2, AS 3 and AS 4 respectively in MCF-7 cells, and 410nM, 400nM, 400nM and 470nM for AS 1, AS 2, AS 3 and AS 4 respectively in MDA-MB-231 cells.

For *in vivo* study, AS was injected to the MCF-7-cells-bearing female nude mice at 20mg/kg/day, just adjacent to the tumor. Treatment of AS decreased the tumor growth rate, when compared with PBS and sense control. The expression of Glut 5 mRNA and protein were also suppressed. Moreover, treatment of AS did not cause any side effects on the liver and heart of the host. In conclusion, AS were effective in



treating breast cancer *in vitro* and *in vivo*. The ultimate goal is to develop an effective approach to human breast cancer treatment by using novel chemically modified antisense oligonucleotides against Glut 5.

## 論文摘要

在乳癌形成過程中，癌細胞需要額外的能量來維持它們的快速生長。葡萄糖和果糖的代謝能為它們帶來能量。癌細胞攝取葡萄糖和果糖主要是透過其細胞膜葡萄糖運輸體(Glucose transporters, Gluts)。我們假設當這些單糖的攝取量減低時，癌細胞的生長速度會降低或令細胞凋亡。因此，我們設計了反義寡核糖核酸 (Antisense oligonucleotides, AS)去抑制乳癌細胞中的葡萄糖運輸體五型(Glut 5)，又稱果糖運輸體的表達。反義寡核糖核酸是一些短少的核糖核酸串，它能夠改變基因的表達，主要是靠建立氫鍵於反義寡核糖核酸與相應的信使核糖核酸(mRNA)之間。

這些長度為十五個鹼鹽基(Base)的反義寡核糖核酸是與 Glut 5 的信使核糖核酸互補的。為了提升寡核糖核酸的穩定性，我們選用了一種經硫化磷酸酯改良的低聚核甘酸。在這項研究中，反義寡核糖核酸被轉移到兩種乳癌細胞包括帶有雌激素受體的 MCF-7 癌細胞，和沒有雌激素受體的 MDA-MB-231 癌細胞，從而研究這些反義寡核糖核酸對乳癌細胞生長影響，包括單糖運輸的效率，細胞內的腺苷三磷酸(ATP)的含量，細胞週期和凋亡測試和動物測試。

在細胞測試中，我們証實在轉移不同濃度的反義寡核糖核酸後七十二小時，MCF-7 癌細胞和 MDA-MB-231 癌細胞的存活率降低了。

隨著劑量的提高，存活率亦相對減少。Glut 5 反義寡核糖核酸 AS 1-4 對 MCF-7 癌細胞的  $IC_{50}$  分別為  $220\mu M$ 、 $190\mu M$ 、 $300\mu M$  和  $220\mu M$ 。而對 MDA-MB-231 癌細胞則為  $410\mu M$ 、 $400\mu M$ 、 $400\mu M$  和  $470\mu M$ 。果糖的攝取量相對地較有義(Sense)序列處理的癌細胞減少了大約百分之三十。與及葡萄糖運輸體信使核糖核酸及蛋白量亦降低了百分之四十。在 MCF-7 和 MDA-MB-231 癌細胞中的腺苷三磷酸含量亦隨之而減少。另外，在利用半數抑制濃度( $IC_{50}$ )去處理癌細胞七十二小時後，磷脂醯絲氨酸(phosphatidylserine)外露，表示癌細胞是透過細胞凋亡的機制而死亡。

在動物測試中，我們將  $20mg/kg/day$  的反義寡核糖核酸注射入含有乳癌腫瘤的裸鼠內，結果，當與磷酸鹽緩衝鹽液(PBS)和有義寡核糖核酸治療的裸鼠比較，在反義寡核糖核酸治療後，腫瘤生長速度下降了。另外，Glut 5 的信使核糖核酸和蛋白量亦減少了。與此同時，反義寡核糖核酸並沒有對裸鼠的心臟和肝臟構成傷害。

總括來說，反義寡核糖核酸有效地治療體內及體外的乳癌，這項研究的最終目的是能夠利用化學改良 Glut 5 反義寡核糖核酸去開發一種治療乳癌的有效方法。

## List of Abbreviations

°C	Degree Celsius
µg	Microgram
µl	Microliter
µM	Micromolar
%	Percentage
ALT	Alanine Transaminase
APS	Ammonium Persulphate
AS	Antisense oligonucleotide
AST	Aspartate Transaminase
ATCC	American Type Culture Collection
ATP	Adenosine Triphosphate
BCA	Bicinchoninic Acid Solution
BSA	Bovine Serum Albumin
cDNA	Complementary Deoxyribonucleic Acid
CK	Creatine Kinase
CO <sub>2</sub>	Carbon Dioxide
CpG	Unmethylated deoxycytidyl-deoxyguanosine dinucleotides
DEPC	Diethyl Pyrocarbonate
DHAP	Dihydroxyacetone Phosphate
DMSO	Dimethylsulfoxide
DNA	Deoxyribonucleic Acid
E-blot buffer	Electroblotting Buffer
ECL	Enhanced Chemiluminescence
EDTA	Ethylene-Diamine-Tetra-Acetic Acid
ER	Estrogen Receptor
F1P	Fructose-1-Phosphate
FBS	Fetal Bovine Serum
FITC	Fluorescein Isothiocyanate
FLSAR	Somatic Cell ATP Releasing Agent
G3P	Glyceraldehyde-3-Phosphate
Glut	Glucose Transporter
HBSS	Hanks' Balanced Salt Solution
HEPES	4-2-Hydroxyethyl-1-Piperazineethanesulfonic Acid
IC <sub>50</sub>	50% Inhibitory Concentration



IGF	Insulin-like Growth Factors
i.p.	Intraperitoneal
i.v.	Intravenous
kDa	Kilo Dalton
LD	Lactate Dehydrogenase
MAPK	Mitogen Activation Protein Kinase
MDR	Multidrug Resistance
MOE	2'-O-Methoxyethyl
mRNA	Messenger RNA
MTT	3-(4,5-dimethylthiazol-2-yl)-2,5-diphenyltetrazoliumbromide
NaCl	Sodium Chloride
NaOAc	Sodium Acetate
NLS	Nuclear Localization Sequence
OD	Optical Density
OMe	2'-O-Methyl
PBS	Phosphate Buffered Saline
PCR	Polymerase Chain Reaction
PI	Propidium Iodide
PNA	Peptide Nucleic Acid
PS	Phosphatidylserine
P/S	Penicillin-streptomycin
PVDS	Polyvinylidene Difluoride
RISC	RNAi Induced Silencing Complex
RNA	Ribonucleic Acid
RNAi	RNA Interference
RNase	Ribonuclease
RPMI	Roswell Park Memorial Institute
RT-PCR	Reverse Transcription PCR
s.c.	Subcutaneous
SGLT	Sodium Linked Glucose Cotransporter
siRNA	Small Interfering RNA
TAE	Tris-Acetate-EDTA
TBS-T	Tris-buffered Saline-Tween-20
TEMED	N,N,N',N'-Tetra-Methylethylenediamine
UV	Ultraviolet
v/v	Volume by Volume
w/v	Weight by Volume



## List of Figures

Figure 1.1	Chart showing the number of new cases per 100 000 female population and incidence rate of breast cancer in Hong Kong	3
Figure 1.2	Chart showing the age-standardized death rate in Hong Kong in recent 20 years	4
Figure 1.3	The proposed two-dimensional structure of Glut family proteins	10
Figure 1.4	Immunolocalization of Glut 5 in human breast tissue	12
Figure 1.5	The formation of DNA triplex after binding of antisense oligonucleotide to the DNA duplex. In consequence, DNA cannot be either replicated or transcribed	16
Figure 1.6	(A) The formation of antisense DNA and mRNA duplex and induction of RNase H cleavage of DNA/RNA hybrid (B) The binding of antisense DNA to the target mRNA and prevent the binding of ribosome by steric hindrance	18
Figure 1.7	Chemical modifications used in antisense oligonucleotides	22
Figure 1.8	Phosphorothioated oligonucleotide	23
Figure 1.9	The growth curve of (A) MCF-7, (B) MDA-MB-231	27
Figure 1.10	The expression pattern of Glut 5 in different breast cancer cell lines.	28
Figure 2.1	Glut 5 mRNA sequence.	45
Figure 2.2	ATP standard curve	50
Figure 2.3	Protein standard curve	59
Figure 3.1	The dose-response curve of tamoxifen on MCF-7 and MDA-MB-231	68
Figure 3.2	Glut 5 mRNA sequence	70
Figure 3.3	Cytotoxicity of AS 1 on (A) MCF-7, (B) MDA-MB-231	71
Figure 3.4	Cytotoxicity of AS 2 on (A) MCF-7, (B) MDA-MB-231	72
Figure 3.5	Cytotoxicity of AS 3 on (A) MCF-7, (B) MDA-MB-231	73
Figure 3.6	Cytotoxicity of AS 4 on (A) MCF-7, (B) MDA-MB-231	74
Figure 3.7	Effect of AS on D-[U <sup>14</sup> C]-Fructose uptake on (A) MCF-7; (B) MDA-MB-231	78
Figure 3.8	Effect of AS on 2-deoxy-D-[1- <sup>3</sup> H] glucose uptake on (A) MCF-7; (B) MDA-MB-231	79
Figure 3.9	Intracellular ATP content of (A) MCF-7, (B) MDA-MB-231 after AS treatment with IC <sub>50</sub> concentration for 72 hours	81

Figure 3.10	mRNA expression of Glut 5 in (A) MCF-7, (B) MDA-MB-231, after AS treatment with IC <sub>50</sub> concentration, 72-hour post-transfection	83
Figure 3.11	Protein expression of Glut 5 in (A) MCF-7, (B) MDA-MB-231, after AS treatment with IC <sub>50</sub> concentration, 72-hour post-transfection	90
Figure 3.12	Cell cycle pattern of MCF-7 after AS treatments, with IC <sub>50</sub> concentration, 72 hour post transfection	94
Figure 3.13	Cell cycle pattern of MDA-MB-231 after AS treatments, with IC <sub>50</sub> concentration, 72 hour post transfection	96
Figure 3.14	Assessment of apoptosis and necrosis after AS treatments with IC <sub>50</sub> concentration, in MCF-7, 72 hour post-transfection, using Annexin V-FITC/PI	99
Figure 3.15	Assessment of apoptosis and necrosis after AS treatments, with IC <sub>50</sub> concentration, in MDA-MB-231, 72 hour post-transfection, using Annexin V-FITC/PI	100
Figure 3.16	Effect of S against Glut 5 on the body weight of the tumor-bearing mice.	102
Figure 3.17	Effect of AS against Glut 5 on the body weight of the tumor-bearing mice	103
Figure 3.18	Comparison of effect of S with AS on body weight of the tumor-bearing mice	104
Figure 3.19	Effect of AS against Glut 5 on the tumor growth in the tumor bearing mice	106
Figure 3.20	Comparison of the tumor volume of AS treatment with S treatment	107
Figure 3.21	Protein expression of Glut 5 of each group of mice with different treatment	112
Figure 3.22	Effect of AS on (A) AST, (B) ALT activities in the plasma of tumor bearing nude mice	116
Figure 3.23	Effect of AS on (A) CK (B) LD activities in the plasma of tumor bearing nude mice	117
Figure 4.1	Flow chart of consequences of antisense oligonucleotides against Glut 5 treatment to tumor bearing nude mice	139
Figure 5.1	Flow chart of consequences of antisense oligonucleotides against Glut 5 treatment	149



## List of Tables

Table 1.1	Tissue distribution of facilitative glucose transporters (Gluts)	8
Table 2.1	The sequence and the region of the antisense or sense oligonucleotides.	43
Table 2.2	Sequences of primers used in PCR	53
Table 2.3	Volume of reagents used in PCR	54
Table 2.4	Volume of reagents for real-time PCR	56
Table 3.1	IC <sub>50</sub> (nM) of AS 1 to AS 4 on MCF-7 and MDA-MB-231	75
Table 3.2	Ratio of band intensity of Glut 5 mRNA of treated sample to negative control of MCF-7	84
Table 3.3	Ratio of band intensity of Glut 5 mRNA of treated sample to negative control of MDA-MB-231	85
Table 3.4	Mean fold change of Glut 5 RNA after AS treatment in MCF-7 and MDA-MB-231, using real-time PCR	88
Table 3.5	Ratio of band intensity of Glut 5 protein of treated sample to negative control of MCF-7	91
Table 3.6	Ratio of band intensity of Glut 5 protein of treated sample to negative control of MDA-MB-231	92
Table 3.7	The percentage distribution of G <sub>1</sub> , S, G <sub>2</sub> /M and Sub G <sub>1</sub> phase of MCF-7 after AS treatments, with IC <sub>50</sub> concentration, 72 hour post transfection	95
Table 3.8	The percentage distribution of G <sub>1</sub> , S, G <sub>2</sub> /M and Sub G <sub>1</sub> phase of MDA-MB-231 after AS treatments, with IC <sub>50</sub> concentration, 72 hour post transfection	97
Table 3.9	The growth rate of tumor in each group and percentage of inhibition on the growth of tumor	108
Table 3.10	Mean fold change of Glut 5 RNA expression from each group of mice with different treatment, by real time PCR	110
Table 3.11	Tissue distribution in plasma of the AST, ALT, CK and LD	114

# **Chapter 1**

## **Introduction**

## **1.1 Breast Cancer**

### **1.1.1 Incidence Rate of Breast Cancer**

Breast cancer is the most common cancer among females in Hong Kong since the early 1990's. It is accounting for almost 20% of all new cases of cancers in females diagnosed in Hong Kong. The incidence rate is increasing during the past 20 years, from 33.1 per 100 000 female population in 1983 to 56.6 per 100 000 in 2000, according to the annual report of the Department of Health (Fig. 1.1). The risk of breast cancer starts to rise from the age of 35, with the peak incidence at age 50 and above. Breast cancer is the third commonest cause of female cancer death in Hong Kong. In 2002, a total of 425 women died from this cancer, accounting for about 9.4% of all cancer deaths in females (Fig. 1.2).



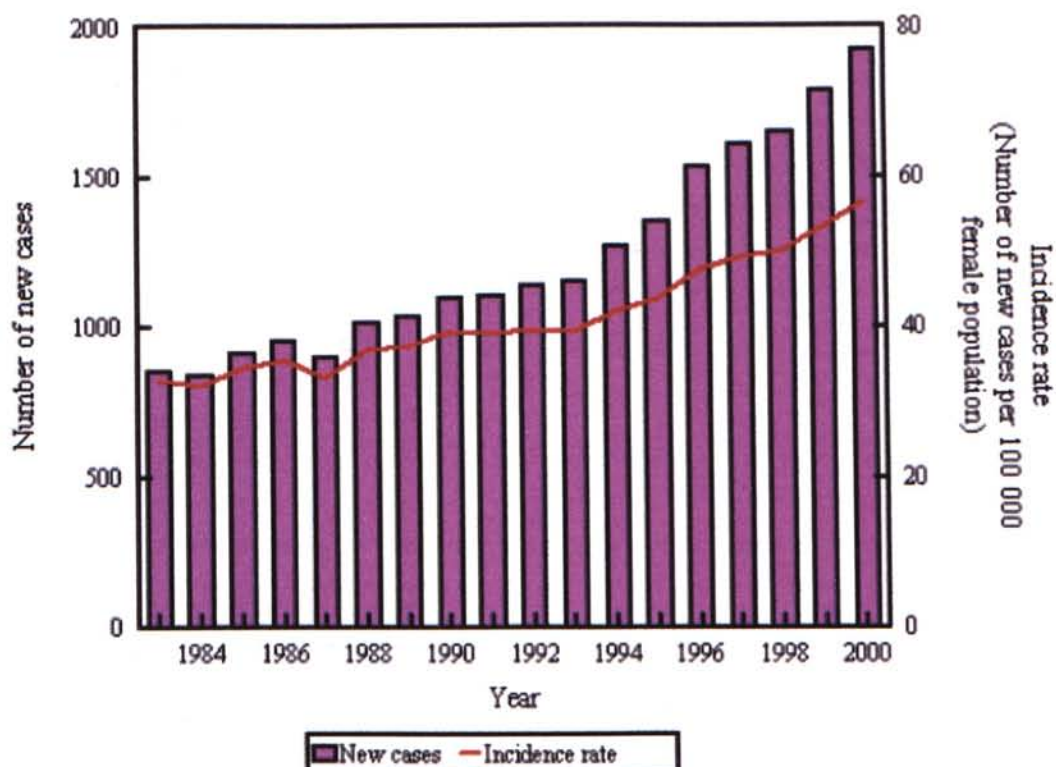


**Figure 1.1**

Chart showing the number of new cases per 100 000 female population and incidence rate of breast cancer in Hong Kong (Adapted from Census and Statistics Department, HKSAR, 2002).

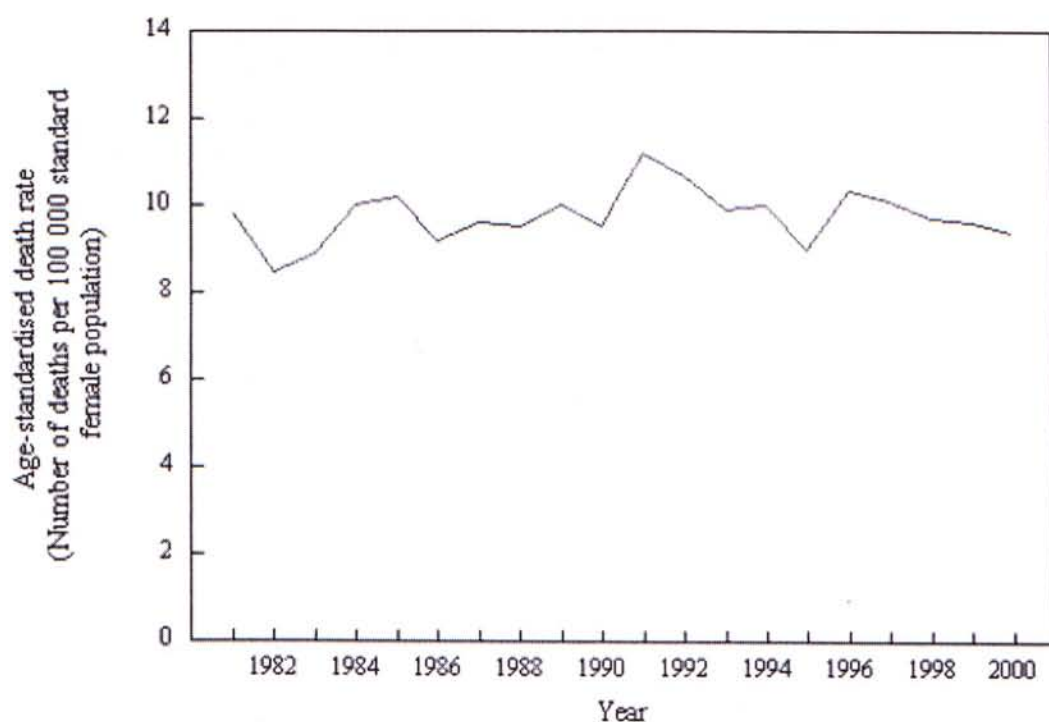


**Figure 1.2**

Chart showing the age-standardized death rate in Hong Kong in recent 20 years (Adapted from Census and Statistics Department, HKSAR).

### **1.1.2 Risk Factors Lead to Breast Cancer**

The risk of having breast cancer is increasing with the age, especially after the menopause. Breast cancer is more common among nulliparous women or women having their first child late. Women who have early menarche and late menopause are also at higher risk. Other risk factors include personal or family history of breast cancer and previous history of certain benign breast diseases. The disease may be related to a high fat diet as well.

### **1.1.3 Conventional Treatments**

In recent years, there has been an advance in treatments against breast cancer. Conventional treatments include surgical removal, radiotherapy, immunotherapy, chemotherapy and hormonal therapy.

Breast cancer is stimulated by the body's own estrogens. Stopping the body's estrogen reaching the breast cells can inhibit growth of tumor or cause apoptosis of the cancer cells. Tamoxifen is the most widely used anticancer drug in treating breast cancer. Tamoxifen stops estrogen stimulating a cancer cell in two main ways. First, it binds to the estrogen receptor (ER) and inhibits the binding of body's own estrogen. Thus, it acts as an estrogen antagonist. It suppresses growth activity, and possibly prevents abnormal growth and the development of breast

cancer ([www.cancernet.co.uk/tamoxifen.htm](http://www.cancernet.co.uk/tamoxifen.htm)).

As its action depends on ER, if a tumor is ER-positive, it is much more likely to respond to tamoxifen. Tamoxifen fails to treat advanced stage breast cancer, which is lack of ER, i.e. ER-negative breast cancer. Besides, tamoxifen has many potential side effects, e.g. occurrence of hot flashes, increase risk of endometrial cancer and thromboembolic disease, etc. Also, many tumors eventually become resistant to treatment with tamoxifen (Sainsbury, 2004).

Based on the high incidence and death rate and the failure of treatment today, novel breast cancer treatment has to be developed.

## **1.2 Relationship between Breast Cancer and Glucose Transporters**

### **1.2.1 Importance of Glucose and Fructose**

Glucose, fructose and other hexoses serve as basic fuel molecules for cancer cells. They were metabolized to provide energy to support the high metabolic rate of cancer cells. The hexoses are unable to diffuse across the cell membranes, and require the actions of transporter proteins for the entry into the cells. Two distinct groups of hexose transporter have been identified and classified basing on their dependence on energy. The first group is sodium-linked glucose co-transporters (SGLTs), which use the energy provided by an electrochemical gradient of sodium, and transport hexoses against a concentration gradient. The second group is facilitative glucose transporter (Gluts), which transport hexoses down a concentration gradient.

### **1.2.2 Facilitative Glucose Transporters (Gluts) and The Relationship with Breast Cancer**

Facilitative glucose transporters (Gluts) were found to have 13 isoforms, Glut 1 to Glut 13 (Joost and Thorens, 2001). The expression pattern of the Gluts was shown in Table 1.1.



**Table 1.1**

Tissue distribution of facilitative glucose transporters (Gluts) (Joost and Thorens, 2001).

<b>Name</b>	<b>Tissue distribution</b>
Glut 1	Present in many tissues; abundant in human erythrocytes, endothelial and many cell lines
Glut 2	Hepatocytes, pancreatic $\beta$ cell, intestine and kidney
Glut 3	Brain
Glut 4	Skeletal muscle, heart and adipose tissue
<b>Glut 5</b>	<b>Intestine, spermatozoa and kidney</b>
Glut 6	Spleen, leukocytes and brain
Glut 7	Microsomal glucose transporter in liver
Glut 8	Testis, brain and blastocyst
Glut 9	Kidney and liver
Glut 10	Liver and pancreas
Glut 11	Heart and skeletal muscle
Glut 12	Heart and prostate
Glut 13	Brain

The Glut proteins contain approximately 500 amino acids, with Glut 1-5 exhibiting 39-65% sequence homology (Mueckler 1994). All Gluts share a common structural motif of 12 transmembrane helices with amino and carboxyl termini located in the cytosol. There is a large loop between transmembrane segments 6 and 7, which divides Glut into 2 parts, the C-terminal domain and N-terminal domain (Gould and Holman, 1993). Also, N-linked glycosylation site is found between segments 1 and 2 (Fig. 1.3).

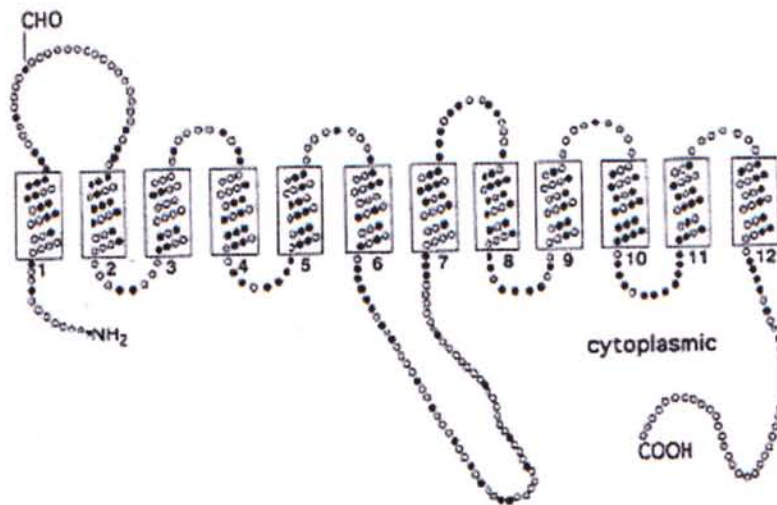


**Figure 1.3**

The proposed two-dimensional structure of Glut family proteins, which consists of 12 membrane-spanning regions with cytoplasmic C-terminal and N-terminal. Also, they all appear to be glycosylated on one of the extracellular loops (Adapted from Olson and Pessin, 1996).

Gluts were found to be over-expressed in many cancers. For example, over-expression of Glut 5 was found in breast cancer cells (Fig. 1.4, Zamora-Leon *et al.*, 1996). Over-expression of Glut was observed in cancer cells because of their different mechanism in the catabolism of hexose. Most cancer cells are anaerobic cells in which catabolism of hexose stopped after glycolysis, and did not further enter Krebs cycle for mass production of energy. Therefore, little energy can be produced by a hexose molecule. In fact, tumor cells require a large amount of energy to support their high growth rate. So, the cells express more glucose transporters as adaptive mechanism in order to survive.

As mentioned in the previous part, expression of Glut 5 was found *in vivo* in human breast cancer but is absent in normal breast tissue (Zamora-Leon *et al.*, 1996). This finding indicated that breast cancer cells may have specialized capacity to transport fructose which is a rare metabolic substrate to be used by only a few human tissues.





**Figure 1.4**

Immunolocalization of Glut 5 in human breast tissue. Glut 5 is shown as a dark blue colour (Adapted from Zamora-Leon *et al.*, 1996).

- (A) Immunohistochemistry of normal breast tissue. Mammary epithelial cells do not express Glut 5 as revealed by basal anti-Glut 5 reactivity;
- (B) Immunohistochemistry of human breast cancer tissue. High-expression of Glut 5 is evidenced by strong anti-Glut 5 immunoreactivity.

## 1.3 Antisense Oligonucleotides

### 1.3.1 Characteristics of Antisense Oligonucleotides

Antisense represents the regulation of gene expression by short oligonucleotides or oligonucleotide mimics, which relies on the formation of Watson and Crick hydrogen bonds between the antisense oligomer and the complementary mRNA strand, thereby providing target specificity of the agent.

Antisense oligonucleotide is a single-stranded, negatively charged DNA, which is designed complementary to the target nucleotide sequence. It forms a duplex with the target nucleotide sequence through the Watson and Crick base pairing.

Antisense oligonucleotide was first introduced by Paterson *et al.* (1977), by inhibiting single-stranded DNA translation in cell free system. It was later discovered that antisense oligonucleotide can be used for the treatment of Rous sarcoma infections (Zamecnik and Stephenson, 1978). From their early work, antisense oligonucleotides have progressed to become a powerful tool in molecular biology and as a therapeutic agent. By pairing with their cognate mRNA, antisense oligonucleotides can knockdown gene expression specifically through several mechanisms which will be discussed later. The antisense oligonucleotide can also be an effective drug. It has been widely accepted as a tool to study gene functions and

to validate drug targets because it is economical and a short experimental cycle is needed (Flaherty *et al.*, 2001). Although the applications of small interfering RNAs (siRNAs) as a new gene knockdown technology have shown significant advantages in some studies, antisense oligonucleotides still remain as a competitive alternative for functional gene validation and drug development (Zhang *et al.*, 2003).

### **1.3.2 Action Mechanism of Antisense Oligonucleotides**

Antisense oligonucleotides are designed to bind to RNA through Watson and Crick hybridization. In general, their size ranges from 12-25 nucleotides in length (Dean and Bennett, 2003). There are multiple mechanisms that can be exploited to inhibit the function of the RNA once the oligonucleotide binds to the target RNA (Crooke, 1999). They are inhibition of transcription and mRNA translation. Inhibition of transcription is by binding of antisense DNA to the DNA duplex by hydrogen bonding and result in formation of DNA triplex. As a consequence, unwinding of the DNA strands and the DNA-polymerase mediated transcription are prevented. Further more, the DNA strands cannot be replicated (Fig. 1.5).



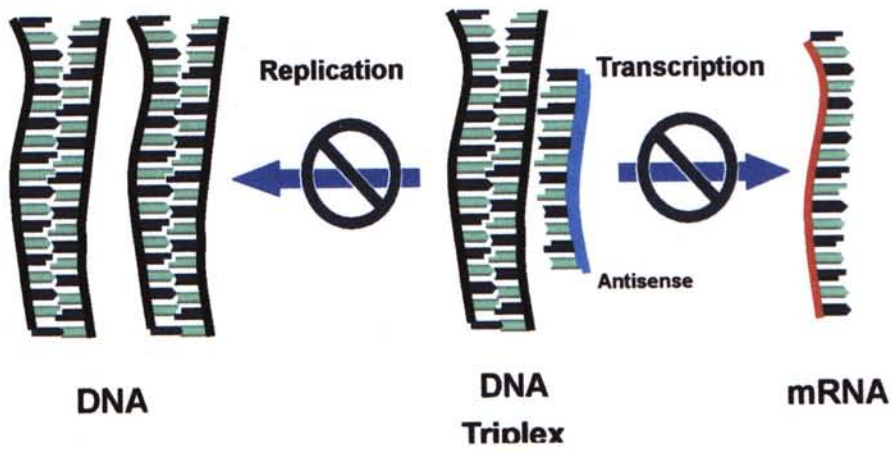


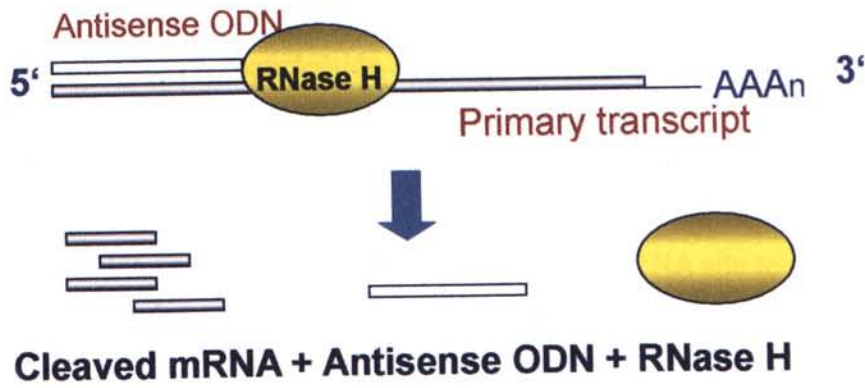
**Figure 1.5**

The formation of DNA triplex after binding of antisense oligonucleotide to the DNA duplex. As a consequence, DNA can neither be replicated nor transcribed.

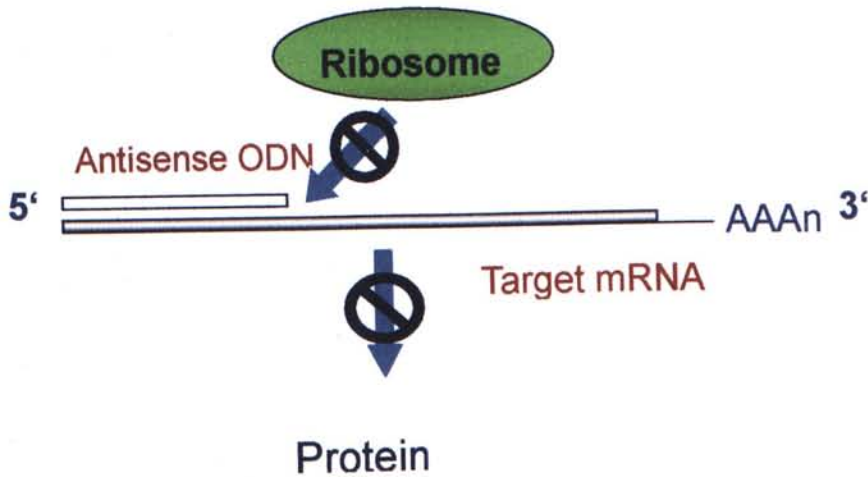
Other action mechanisms of antisense include the inhibition of mRNA translation by RNase H degradation, and modulation of RNA processing and steric hindrance, by blocking pre-mRNA function or interacting with ribosomes (Fig. 1.6A & B).

The best characterized antisense mechanism is RNase H mediated degradation. RNase H is a family of ubiquitously expressed enzymes that cleave the RNA strand of an RNA-DNA hybrid, with at least two forms found in mammalian cells (Lima *et al.*, 2001). The target mRNA sequence is inactivated as an irreversible event since the antisense DNA may degrade several mRNA molecules, through separate hybridizations, resulting in the dissociation of cleaved products.

### Formation of Antisense-mRNA duplex:



(A)



(B)

**Figure 1.6**

(A) The formation of antisense DNA and mRNA duplex and induction of RNase H cleavage of DNA/RNA hybrid.

(B) The binding of antisense DNA to the target mRNA and prevention of the binding of ribosomes by steric hindrance.

### 1.3.3 Sequence Selection

Antisense oligonucleotide sequence selection is the most important step in the application of antisense technology. The effectiveness of an antisense oligonucleotide depends on the accessibility of the mRNA site to which it is intended to bind. Hybridization of antisense oligonucleotide to different regions of mRNA leads to different action mechanisms. For example, antisense complementary to the 5' cap region or the start codon of mRNA can act through steric hindrance and prevent the binding of ribosomes. For the antisense complementary to the coding region of mRNA would trigger RNase H activity. It is necessary to characterize the efficacy, specificity and other properties of antisense oligonucleotides. There are many methods to identify the accessible sites include RNase H mapping, gel shift, oligonucleotide array and random RT priming, as well as computational predictions. Among them, RNase H mapping and random RT priming use short oligonucleotide libraries to determine the accessibility of mRNA have shown promising results (Zhang *et al.*, 2003).



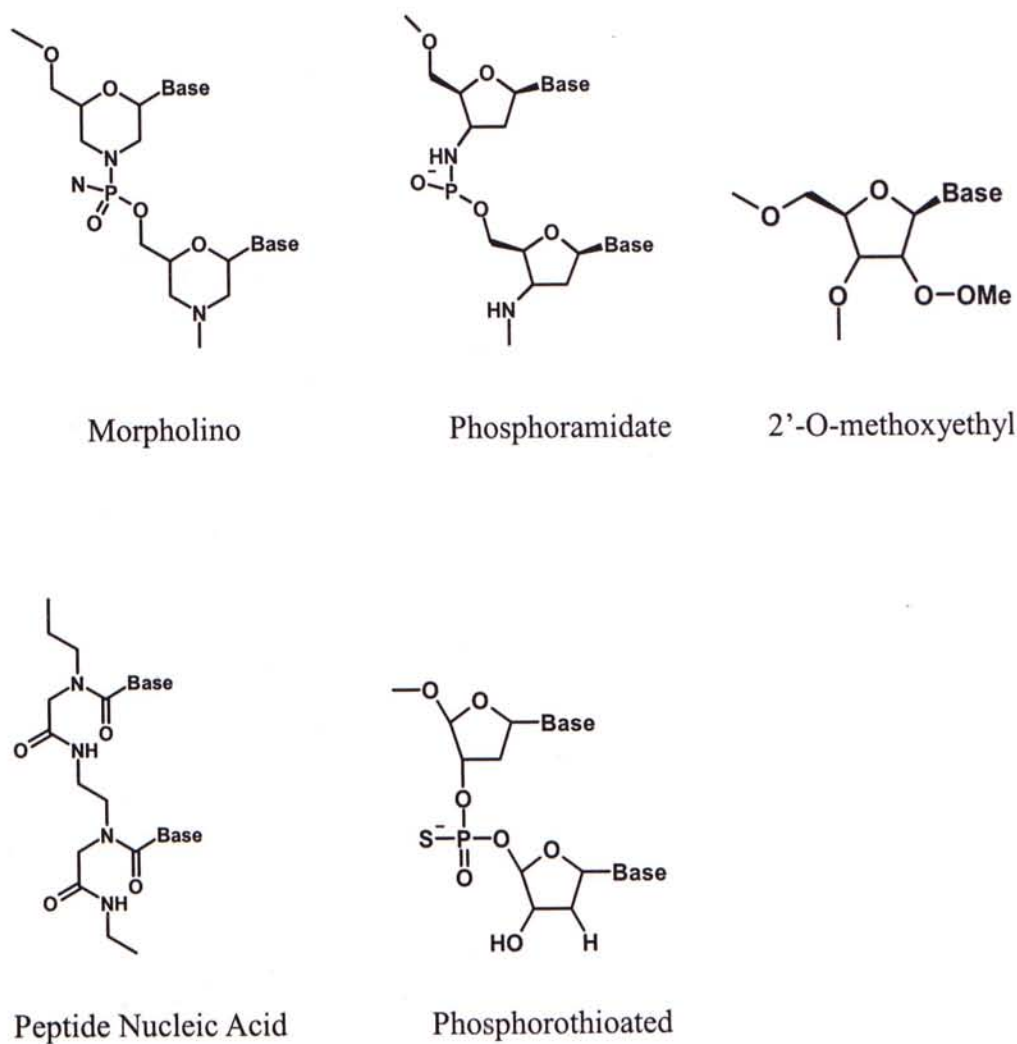
### 1.3.4 Chemical Modifications of Antisense Oligonucleotides

Oligonucleotides exert their activity only by encountering a sufficient intracellular concentration; a sufficient intracellular half-life; serum, body fluids and intracellular nuclease stability; and an efficient cellular uptake and distribution (Alama *et al.*, 1997). Naturally occurring DNA is sensitive to enzymatic degradation by exonuclease and endonucleases, both *in vivo* and *in vitro* (serum-containing medium). In order to prevent rapid degradation by the nucleases, chemical modifications of the natural phosphodiester backbone have been developed.

The three structural elements of oligonucleotides, the base, the phosphodiester group and the sugar, could be modified. Modifications to the base such as a methyl group have been shown to increase the binding affinity for both DNA and RNA (Fig. 1.7) (Flanagan *et al.*, 1999). Modifications to the sugar are useful for enhancing the potency of the oligonucleotide and their pharmacokinetics. The most common modifications are 2'-O-methyl (OMe) and 2'-O-methoxyethyl (MOE) (Fig. 1.7). These modifications result in a 3-10 fold increase in nuclease resistance and decreased toxicity (Geary *et al.*, 2001). Modifications of the phosphate group include phosphorothioated oligonucleotides or "morpholino" modification, which contains a neutral phosphorodiamidate linkage (Fig.1.7) (Summerton *et al.*, 1999). Peptide nucleic acid (PNA), with the sugar-phosphate

backbone is completely replaced with a peptide-based backbone, is a unique modification (Fig. 1.7). This results in a polymer with a neutral backbone that has a high affinity for complimentary nucleic acids and is completely resistant to degradation by nuclease and peptidases (Larsen *et al.*, 1999). Of all the chemical modifications developed, phosphorothioated oligonucleotide is the most extensively studied analogs of the phosphodiester oligonucleotides and was evaluated for their therapeutic potential in human clinical trials (Dean and Bennett, 2003).

In phosphorothioated oligonucleotides, one of the non-bridging oxygen atoms of the phosphate group is replaced with a sulfur atom in order to prevent rapid degradation by nucleases (Fig.1.8). Additionally, phosphorothioated oligonucleotides possess important properties such as binding affinity to target mRNA, cellular uptake, aqueous solubility and the ability to activate RNase H, which is required for antisense activity (Agrawal and Zhao, 1998).

**Figure 1.7**

Chemical modifications used in antisense oligonucleotides.

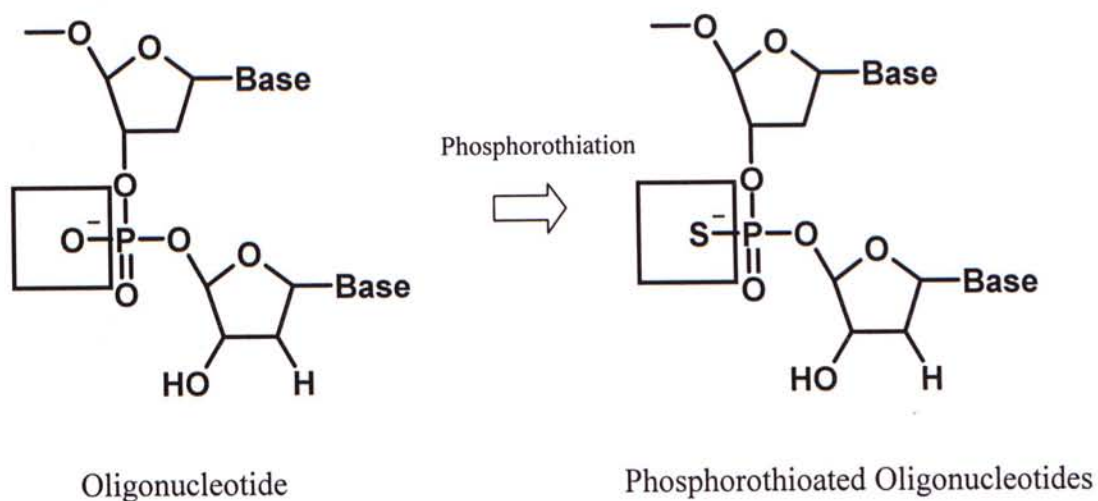


**Figure 1.8**

Phosphorothioated oligonucleotide, one of the non-bridging oxygen atom of the phosphate group is replaced with a sulfur atom in order to prevent rapid degradation by nucleases.



### 1.3.5 Uptake and Delivery Means of Antisense Oligonucleotides

Antisense oligonucleotides are polyanionic, they cannot penetrate the phospholipids bilayer due to their charge and polarity. Delivery vector was developed to mediate the entry and the delivery of antisense oligonucleotides to the target. The vector can also protect the drug from degradation and rapid clearance from the body. The size of vectors must be small to allow intercalation between tissues and to allow intracellular transport. If the vector is too large, this can enhance the clearance of the drug from the body. They must be non-toxic and stable in bloodstream, retain the drug when in the circulation and must release it at its target before elimination. There are many available drug delivery systems either based on natural or synthetic systems and many show great potential in delivering a molecule or drug to the target of interest either in molecular biology research or in therapeutics. The usage of liposomes, protein or peptide constructs and polymers were developed to provide the above properties (Szorka Jr *et al.*, 2000).

Liposomes are small microscopic spheres of concentric, closed phospholipids bilayer enclosing an internal aqueous compartment, like the plasma membrane of cells or of certain organelles. When oligonucleotides are mixed with lipids, complexes form spontaneously due to electrostatic interactions and form a condensed and tight structure (Gershon *et al.*, 1993). The liposome would be

endocytosed and caused disruption of the endosomal membrane, resulting in fusion and expulsion of the contents into cytoplasm (Zelphati *et al.* 1996).

Antisense oligonucleotides can be conjugated to proteins and peptides that have the ability to penetrate the cell membrane without the liposome complex. The oligonucleotides attach by electrostatic interactions to poly-L-Lysines, or other cationic sequence, linked to a carrier molecule that is a ligand for a surface receptor similar to the targeting ligands in liposomes. The peptide complex can be protected from nucleases. A nuclear localization sequence (NLS) can be added to the protein sequence to help bringing the oligonucleotides into the nucleus.

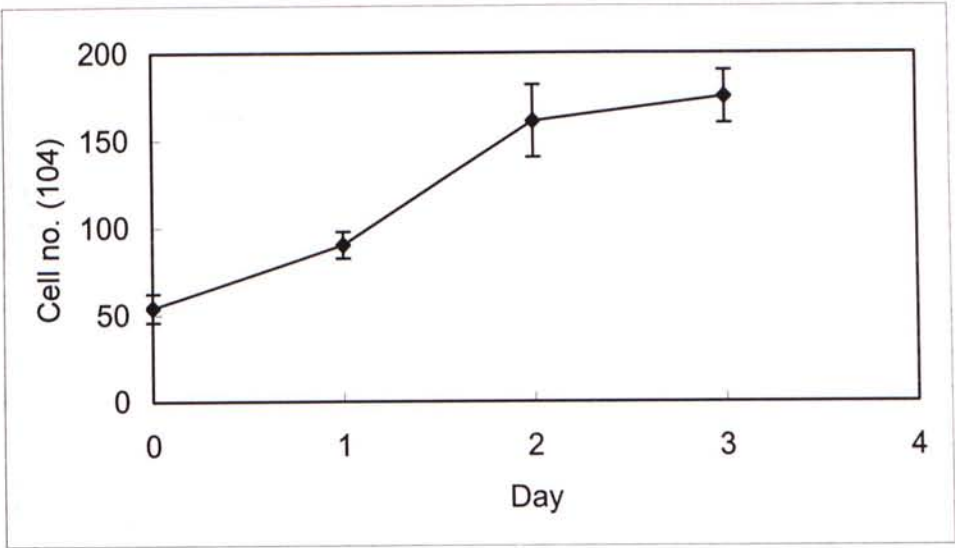
## 1.4 Objectives of Present Study

In the present study, the effects of antisense oligonucleotides against glucose transporter 5 (Glut 5) on two human breast cancer cell lines were investigated.

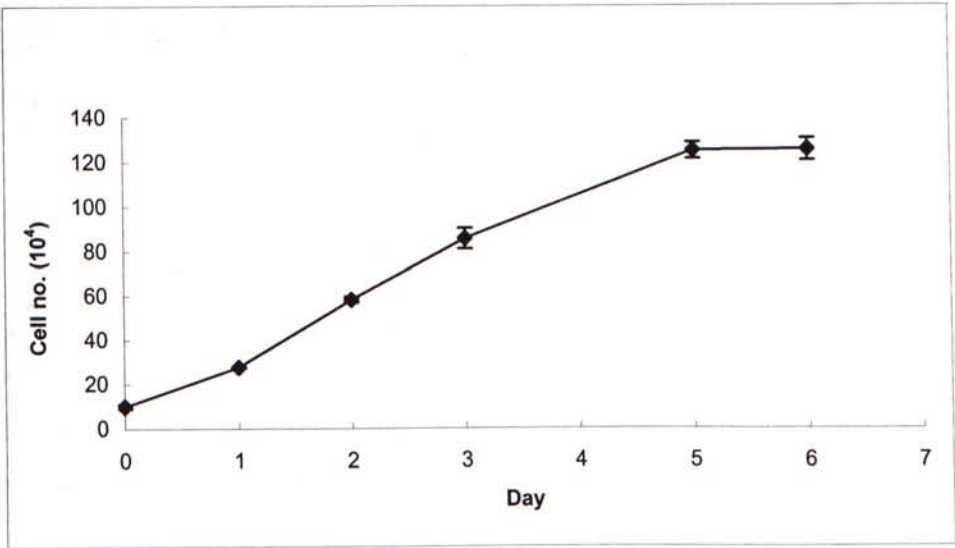
MCF-7 cells possess the characteristics of differentiated mammary epithelium including ability to process estrogen via cytoplasmic estrogen receptors (ER) and the capability of forming domes. Their growth depends on estrogen. This cell line mimics the early stage of breast cancer, which is estrogen dependent. The doubling time is 41 hours (Fig. 1.9A).

It was found that Glut 5 is highly expressed in breast cancer cells. The expression pattern is different in different cell lines (Zamora-Leon *et al.*, 1996). For MCF-7 cells, less Glut 5 were expressed when compared with that of MDA-MB-231 cells (Fig.1.10).

The growth of MDA-MB-231 cells is estrogen independent because they are lack of ER. This cell line mimics the late stage of breast cancer and was found to be more invasive and malignant than MCF-7 cells (Carmeci *et al.*, 1998). The doubling time is 33 hours (Fig. 1.9B).



(A)



(B)

**Figure 1.9**

The growth curve of (A) MCF-7 cells, (B) MDA-MB-231 cells (Adapted from the thesis of Chan KK).  $1 \times 10^5$  cells per well were seeded in a 6-well plate overnight. Then, the cell number was counted by trypan blue exclusion assay on every 24 hours. Each point represents mean  $\pm$  S.D.,  $n=4$ .



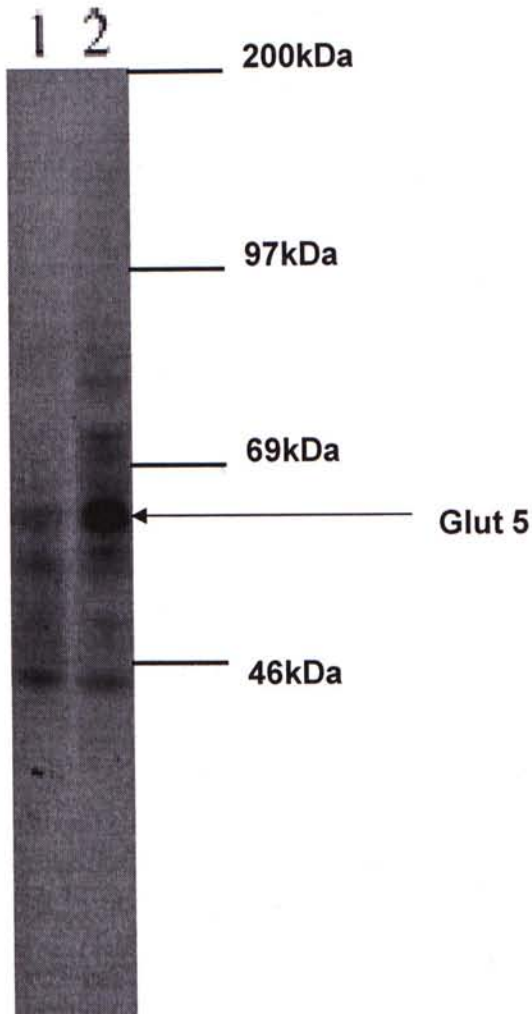


**Figure 1.10**

The expression pattern of Glut 5 in different breast cancer cell lines. Lane 1 is MCF-7 cells and lane 2 is MDA-MB-231 cells. More Glut 5 was expressed in MDA-MB-231 cells when compared with MCF-7 cells (Zamora-Leon *et al.*, 1996).

As mentioned before, glucose transporters play an important role in transporting hexoses into the tumor cells, we hypothesized that blocking the expression of glucose transporters in tumor cells by using antisense oligonucleotides can reduce the nutrient supply. As a result, the growth of tumor may be suppressed due to the lack of nutrients.

Glut 5 was chosen as the target of antisense oligonucleotides because of a couple of reasons. Glut 5 is localized in breast tumor cells, but it is absent in normal breast epithelial cells (Fig. 1.4); also, Glut 5 was only found in a few human normal tissues, i.e. intestine and spermatocytes. There are other isoforms of Gluts in intestine for the uptake of nutrients, e.g. Glut 1, and spermatocytes are found in male only. Targeting Glut 5 in human breast tumor cells in female is highly specific and will not affect the normal function of the surrounding normal breast tissues and other organs in patients. In addition, Glut 5 was expressed in both ER-positive (MCF-7) and -negative cell lines (MDA-MB-231), which mimic the early and late stage breast cancer respectively. It is now known that MDA-MB-231 cells have more Glut 5 than that of MCF-7 cells (Zamora-Leon *et al.*, 1996). This means targeting Glut 5 by antisense oligonucleotide can be used for treating all stages of breast cancer.

Both *in vitro* and *in vivo* effect of Glut 5 antisense oligonucleotides will be investigated. For *in vitro* study, two human breast cancer cell lines will be used.

They are MCF-7 (ER-positive) and MDA-MB-231 (ER-negative). For *in vivo* study, MCF-7-cells-bearing nude mice will be used as animal model. The study will focus on the anti-proliferative effect, and assessment of the probable side effects caused by the antisense oligonucleotides.

The ultimate goal of the project is to develop an effective approach to breast cancer treatment by using novel chemically modified antisense oligonucleotides against Glut 5.

# **Chapter 2**

# **Materials and**

# **Methods**

## **2.1 Materials**

### **2.1.1 Cell Lines and Culture Medium**

#### **Cell Lines: MCF-7 and MDA-MB-231**

The MCF-7 and MDA-MB-231 cell lines were purchased from American Type Culture collection (ATCC, Rockville, MD, USA). Both cell lines were cultured in complete RPMI 1640 medium (Gibco BRL, USA), which was supplemented with 10% fetal bovine serum (v/v, FBS, Gibco BRL, USA) and 1% penicillin-streptomycin (v/v, PS, 10 000U/ml, Gibco BRL, USA). The cells were maintained at 37°C in a humidified atmosphere of 5% CO<sub>2</sub>/95% air.

#### **Roswell Park Memorial Institute Tissue Culture Medium 1640 (RPMI 1640 Medium, Gibco BRL, USA)**

RPMI 1640 medium was prepared by dissolving the powder which contains phenol red, L-glutamine and 0.5mM HEPES in 1L of dH<sub>2</sub>O. The medium was supplemented with 2g of NaHCO<sub>3</sub>. The pH was adjusted to 7.2. The medium was then filtered by 0.22  $\mu$ m bottle-top filter (Millipore). The complete RPMI 1640 medium was supplemented with 10% fetal bovine serum (v/v, FBS, Gibco BRL, USA) and 1% penicillin-streptomycin (v/v, PS, 10 000U/ml, Gibco BRL, USA).



## 2.1.2 Buffers and Reagents

### Trypsin-EDTA Solution

Trypsin-EDTA solution, containing 0.25% trypsin and 1 mM EDTA-tetrasodium in HBSS without  $\text{Ca}^{2+}$  and  $\text{Mg}^{2+}$ , was purchased from Gibco BRL, USA.

### Trypan Blue Solution

Trypan blue solution was purchased from Sigma Chemical Co. It contained 0.4% (w/v) trypan blue dissolved in 0.817% NaCl and 0.06%  $\text{K}_2\text{PO}_4$ .

### 10x Tris-Glycine

10x tris-glycine was prepared by dissolving 30.3g tris and 144g glycine in 1L  $\text{dH}_2\text{O}$ . The pH was adjusted to 8.3 and was stored at 4°C.

### Normal Saline: 0.9% (w/v) Sodium Chloride (NaCl)

0.9% NaCl was prepared by dissolving 9g of solid form of NaCl in 1L of  $\text{dH}_2\text{O}$ . It was stored at room temperature.

### Phosphate Buffered Saline (PBS)

PBS was prepared by mixing 136mM NaCl, 2.7mM KCl, 1.5mM  $\text{KH}_2\text{PO}_4$  and 8mM  $\text{Na}_2\text{PO}_4$ . The chemicals are dissolved in  $\text{ddH}_2\text{O}$ . The pH was adjusted to 7.4 and the solution was sterilized by autoclaving. It was stored at room temperature.

### Tris Buffered Saline (TBS)

TBS was prepared by dissolving 12.114g Tris and 87.66g NaCl in 1L  $\text{dH}_2\text{O}$ . The pH was adjusted to 8 and stored at 4°C.

### **Tetrazolium Salt 3-(4,5-Dimethylthiazol-2-yl)-2,5-Diphenyltetrazolium Bromide (MTT, Sigma) Solution**

MTT was prepared by dissolving it in PBS at concentration of 5mg/ml. The solution was then filtered by a 0.22  $\mu$  m filter (Millipore).

### **Tris-acetate (TAE) Buffer**

TAE was prepared as 50x concentrated stock solution by dissolving 242g Tris base, 57.1ml glacial acetic acid and 100ml 0.5M EDTA (pH 8.0) in 1L dH<sub>2</sub>O.

### **Tris-EDTA (TE) Buffer**

TE was prepared by mixing 10mM Tris-Cl and 1mM EDTA in dH<sub>2</sub>O. The pH was adjusted to 7.4.

## **2.1.3 Reagents for Transfection**

### **Oligofectamine reagent (Invitrogen Co. Ltd.)**

Oligofectamine reagent was purchased from Invitrogen Co. Ltd. It was diluted with plain medium prior to use, according to the manufacturer's manual. It was stored at 4°C.

## 2.1.4 Reagents for D-[U<sup>14</sup>C]-Fructose and 2-Deoxy-D-[1-<sup>3</sup>H]

### Glucose Uptake Assay

#### D-[U<sup>14</sup>C]-Fructose and 2-Deoxy-D-[1-<sup>3</sup>H] Glucose

D-[U<sup>14</sup>C]-fructose (200  $\mu$  Ci/ml) and 2-deoxy-D-[1-<sup>3</sup>H] glucose (1.0mCi/ml) were purchased from Amersham Biosciences Ltd. They were stored at -20°C and 4°C respectively.

## 2.1.5 Reagents for ATP Assay

Intracellular ATP concentration was detected by using Bioluminescent somatic cell ATP assay kit, which was purchased from Sigma Chemical Co. This kit employed for the bioluminescent determination of the ATP released from a suspension of viable somatic cells:

FLSAR

Intracellular ATP  $\longrightarrow$  Free ATP

Firefly Luciferase

Free ATP + Luciferin  $\rightleftharpoons$  Adenyl-luciferin + PPi

Mg<sup>2+</sup>

Adenyl-luciferin + O<sub>2</sub>  $\longrightarrow$  Oxyluciferin + AMP + CO<sub>2</sub> + Light

The light emitted is proportional to the ATP present.

The kit contains ATP assay mix, ATP assay mix dilution buffer, 10X somatic cell ATP releasing agent (FLSAR) and ATP standard (0.9mg). ATP assay mix should be dissolved in 5ml of autoclaved dH<sub>2</sub>O, and diluted for 25 folds with ATP assay mix dilution buffer. The ATP assay mix dilution buffer should be dissolved in 50ml of autoclaved dH<sub>2</sub>O before use. The kit was stored at -20°C.

## **2.1.6 Reagents for RT-PCR**

### **2.1.6.1 Reagents for RNA Extraction**

#### **TriZOL Reagent (Invitrogen Co. Ltd.)**

Trizol reagent was purchased from Invitrogen Co. Ltd. It was stored at 4°C for optimal performance.

#### **Chloroform**

Chloroform was purchased from BDH Laboratory Supplies, UK. It was stored at room temperature and in a flammable liquid safety cabinet.

#### **Isopropanol**

Isopropanol was purchased from BDH Laboratory Supplies, UK. It was stored at room temperature and in a flammable liquid safety cabinet.

#### **DEPC-treated Double Distilled Water (0.1%)**

DEPC-treated double distilled water was prepared by mixing 1ml of diethyl pyrocarbonate (DEPC, purchased from Sigma Chemical Co.) to 1L of ddH<sub>2</sub>O in a fume hood and was stirred overnight to destroy RNase. It was then autoclaved to destroy DEPC.

### **2.1.6.2 Reagents for Reverse Transcription**

#### **Thermoscript™ RT-PCR System for 1<sup>st</sup>-strand cDNA Synthesis Kit (Invitrogen Co. Ltd)**

Thermoscript™ RT-PCR system for 1<sup>st</sup>-strand cDNA synthesis kit was purchased from Invitrogen Co. Ltd. This kit contains oligo dT (0.5 µg/µl), 10X RT buffer



(200mM Tris-HCl (pH 8.4), 500mM KCl), 0.1M DTT, 10mM dNTP mix, Thermoscript<sup>TM</sup> RT(50U/  $\mu$ l), RNase<sup>TM</sup> OUT recombinant ribonuclease inhibitor (40U/  $\mu$ l) and *E. coli* RNase H (2U/  $\mu$ l).

#### ***Taq* polymerase (5000U/ml)**

*Taq* polymerase was purchased from Amersham Biosciences Ltd. It is a single-subunit enzyme purified from the thermophilic bacterium *Thermus aquaticus*. The assay condition was according to the manufacturer's manual. It was stored at -20 °C.

### **2.1.6.3 Reagents for Gel Electrophoresis**

#### **1% Agarose Gel (w/v)**

1% agarose gel was prepared by dissolving 1g agarose (Sigma Chemical Co.) in 100ml TAE. It was boiled until the agarose was melted. The gel was cooled down to about 50°C and 10  $\mu$ l of ethidium bromide (Amersham Biosciences Ltd.) was added. It was then poured into a cast gel system.

#### **6x DNA Loading Dye**

6x DNA loading dye was prepared by mixing 0.25% bromophenol blue (v/v), 0.25% xylene cyanol FF (v/v) and 30% glycerol (v/v) in dH<sub>2</sub>O.

#### **100 Base-Pair DNA Marker**

100 Base-Pair DNA Marker was prepared by mixing 3  $\mu$ l of 1  $\mu$ g/  $\mu$ l of the 100 base-pair DNA marker (Amersham Biosciences Ltd.), 4  $\mu$ l of 6x DNA loading dye



and 5  $\mu$ l autoclaved dH<sub>2</sub>O.

### **QIAquick Gel Extraction Kit (Qiagen)**

QIAquick gel extraction kit was used for purification of cDNA in the agarose gel. The kit contains QIAquick spin columns, buffer QG, buffer PE, buffer EB, and collection tube. 40ml of absolute ethanol should be added to buffer PE before use. It was stored at room temperature.

## **2.1.7 Reagents for Real-Time PCR**

### **TaqMan® Universal PCR Master Mix (Applied Biosystems HK Ltd.)**

TaqMan universal PCR master mix was purchased from Applied Biosystems HK Ltd. and contained AmpliTaq Gold® DNA Polymerase, AmpErase® UNG, dNTPs with dUTP, Passive Reference I, and optimized buffer components. It was stored at 4°C.

### **Assays-on-Demand™ 18S rRNA Gene Expression (Applied Biosystems HK Ltd.)**

Assays-on-Demand™ 18S rRNA gene expression was purchased from Applied Biosystems HK Ltd. It is the primers for 18S rRNA and labeled with a fluorescence dye "VIC". It was stored at -20°C.

### **Assays-on-Demand™ Glut 5 Gene Expression (Applied Biosystems HK Ltd.)**

Assays-on-Demand™ Glut 5 gene expression that was purchased from Applied Biosystems HK Ltd. It contains the primers for Glut 5 labeled with a fluorescence dye "FAM". It was stored at -20°C.

## **2.1.8 Reagents and Chemicals for Western Blotting**

### **2.1.8.1 Reagents for Protein Extraction**

#### **Protein Lysis Buffer**

Lysis buffer was prepared by mixing 21  $\mu$ g/ml aprotinin, 5  $\mu$ g/ml leupeptin, 5mM  $MgCl_2$ , 1mM PMSF, 1% SDS, 1mM sodium meta-vanadate and 10mM tris buffer (pH 7.4) in PBS. It was stored at room temperature.

#### **Protein Standard (2mg/ml)**

Protein standard was prepared by dissolving 0.002g bovine serum albumin (BS) in 1ml  $dH_2O$ . It was stored at  $-20^{\circ}C$ .

#### **Bicinchoninic acid (BCA) solution (Sigma Chemical Co.)**

BCA solution was purchased from Sigma Chemical Co. and was stored at room temperature.

#### **Reagent B**

Reagent B was prepared by dissolving 4g of  $CuSO_4 \cdot 5H_2O$  in 100ml  $dH_2O$ . It was stored at room temperature. Mixture of BCA solution and reagent B should be freshly prepared each time.

### **2.1.8.2 Reagents for SDS-PAGE**

#### **10% Ammonium Persulfate (APS)**

APS was prepared by dissolving 1g ammonium persulfate in 10ml  $dH_2O$ . It was stored at  $-20^{\circ}C$ .

**4x Lower Gel Buffer**

4x lower gel buffer was prepared by dissolving 181.6g Tris and 4g SDS in 1L of dH<sub>2</sub>O. The pH was adjusted to 8.8 and it was stored at room temperature.

**4x Upper Gel Buffer**

4x upper gel buffer was prepared by dissolving 60.6g Tris and 4g SDS in 1L of dH<sub>2</sub>O. The pH was adjusted to 8.8 and it was stored at room temperature.

**12.5% Separating Gel for SDS-PAGE**

12.5% separating gel was prepared by mixing 1.0825 ml of dH<sub>2</sub>O, 1.6675 ml of 30% acrylamide, 1ml of 4X upper gel buffer, 4.65  $\mu$ l of TEMED and 20  $\mu$ l of 10% APS.

Mixture should be freshly prepared for each experiment.

**4.5% Stacking Gel for SDS-PAGE**

4.5% stacking gel was prepared by mixing 1.2ml of dH<sub>2</sub>O, 0.3ml of 30% acrylamide, 0.5ml 4X lower gel buffer, 2.65  $\mu$ l of TEMED and 15  $\mu$ l of 10% APS. Mixture should be freshly prepared for each experiment.

**2x SDS Loading Dye**

2x SDS loading dye was prepared by dissolving 2% (w/v) SDS, 10% sucrose, 0.002% bromophenol blue and 62.5mM Tris in dH<sub>2</sub>O. The pH was adjusted to 6.8. Then the loading buffer was supplemented with 5% (v/v) 2-mercaptoethanol and stored at 4°C.

### **10x SDS Running Buffer**

10x SDS running buffer was prepared by dissolving 30.3g Tris, 144g glycine and 10g SDS in 1L of dH<sub>2</sub>O.

### **Rainbow™ Coloured Protein Molecular Weight Marker**

Rainbow™ coloured protein molecular weight marker was purchased from Amersham Biosciences Ltd.

### **Polyvinylidene Difluoride (PVDF) Western Blotting Membrane**

PVDF membrane with a pore size of 0.45 µm was purchased from Millipore corporation.

### **Electroblotting Buffer**

Electroblotting buffer was prepared by mixing 66.7ml of 10x Tris-glycine, 100ml methanol and 500ml of dH<sub>2</sub>O.

### **Tris-Buffered Saline with 0.1% Tween-20 (TBST)**

Tris-Buffered Saline with 0.1% Tween-20 (TBST) was prepared by mixing 1ml of Tween-20 in 1L TBS.

### **Blocking Solution**

Blocking solution was prepared by dissolving 1g of non-fat milk powder in 10ml of TBST. It was stored at 4°C.



### **Primary and Secondary Antibodies**

The primary antibodies included mouse monoclonal anti-human  $\beta$ -actin and rabbit anti-human Glut 5 were purchased from Sigma and Research Diagnostics respectively. They were stored at -20°C. The secondary antibodies included anti-mouse IgM and goat anti-rabbit IgG HRP were purchased from Pharmigen and Santa Cruz Biotechnology Inc. respectively. They were stored at 4°C.

### **Enhanced Chemiluminescence (ECL) Assay**

Enhanced chemiluminescence (ECL) assay kit was purchased from Amersham Biosciences Ltd. It was stored at 4°C.

## **2.1.9 Reagents for Flow Cytometry**

### **TACS™ Annexin V Kits (Trevigen, Inc.)**

TACS™ Annexin V Kits was purchased from Trevigen, Inc. The kit contains Annexin V-FITC, 10X Binding Buffer and propidium iodide. It was stored at 4°C.

### **Propidium Iodide (PI)**

Propidium iodide was purchased from Sigma Chemical Co. It was reconstituted in PBS (2mg/ml).

### **Ribonuclease A (RNase A)**

Ribonuclease A (RNase A) was purchased from Sigma Chemical Co. It was dissolved in TE buffer (5mg/ml, pH 7.4).



### **2.1.10 *In Vivo* Study**

#### **Animal Model: Balb/c Nude Mice**

Female nude mice aged 4-6 weeks were used as animal models for *in vivo* study. The mice were bred at the Laboratory Animal Services Center of The Chinese University of Hong Kong under pathogen-free condition.

#### **Sodium Pentobarbital Solution**

Sodium pentobarbital solution was prepared by dissolving 25mg of sodium pentobarbital in 1 ml of sterile PBS. It was stored at 4°C.

#### **Heparin Solution**

Heparin solution was prepared by dissolving 50 units of heparin in 1 ml of sterile PBS. It was stored at 4°C.

#### **Antisense Oligonucleotides**

AS 2 (Sequence: 5' ATG TGG CGA CTC TGC 3') and its sense sequence (5' GCA GAG TCG CCA CAT 3') were used.

## 2.2 Methods

### 2.2.1 Oligonucleotide Design

In this project, 5 oligonucleotide sequences with 15 base pairs were designed. One of them is a sense sequence and the others are antisense. Sense sequence is used to illustrate the non-specific effect. They are all complementary to human glucose transporter 5 cDNA sequence (Fig.2.1). The sequence and the region of the antisense or sense oligonucleotides are shown in table 2.1. The selected sequences were checked against their specificity to Glut 5 by using a program called “Blast” in NCBI. The website is <http://www.ncbi.nlm.nih.gov>. In order to increase the stability, the sequences designed were then modified to phosphorthioated-oligonucleotide, with a sulfur ion replaced the oxygen ion in the phosphate group, as mentioned in section 1.3.4, fig. 1.8.

```

1  cttctctctc cattcagtgc acgcgttact ttggctaaaa ggaggtgagc ggcactctgc
61  ccttccagag caagcatgga gcaacaggat cagagcatga aggaaggag gctgacgctt
121 gtgcttgccc tggcaaccct gatagctgcc ttgggtcat ccttccagta tgggtacaac
181 gtggctgctg tcaactcccc agcactgctc atgcaacaat ttacaatga gacttactat
241 ggtaggaccg gtgaattcat ggaagacttc cccttgacgt tgctgtggtc tgtaaccgtg
301 tccatgtttc catttgagg gtttatcgga tccctcctgg tcggccctt ggtgaataaa
361 ttgggcagaa aaggggcctt gctgttcaac aacatatttt ctatcgtgcc tgcgatctta
421 atgggatgca gcagagtcgc cacatcattt gagcttatca ttatttccag acttttgggtg
481 ggaatatgtg caggtgtatc ttccaacgtg gtcccatgt acttagggga gctggccctt
541 aaaaacctgc ggggggctct cgggggtggg cccagctct tcatcactgt tggcatcctt
601 gtggcccaga tctttggctc tcggaatctc cttgcaaacg tagatggctg gccgatcctg
661 ctggggctga ccggggctcc cgcggcgtg cagctccttc tgctgcctt cttcccagag
721 agccccaggt acctgctgat tcagaagaaa gacgaagcgg ccgccaagaa agccctacag
781 acgctgcgcg gctgggactc tgtggacagg gaggtggccg agatccggca ggaggatgag
841 gcagagaagg ccgcggtctt catctcctg ctgaagctgt tccgatgcg ctgctgcgc
901 tggcagctgc tgtccatcat cgtcctcatg ggcgccagc agctgtcgg cgtcaacgct
961 atctactact acgcggacca gatctacctg agcgccggcg tgccggagga gcacgtgcag
1021 tacgtgacgg ccggcaccgg ggccgtgaac gtggatcatga ccttctgcgc cgtgttcgtg
1081 gtggagctcc tgggtcggag gctgctgctg ctgctgggt tctccatctg cctcatagcc
1141 tgctgcgtgc tcactgcagc tctggcactg caggacacag tgtcctggat gccatacatc
1201 agcatcgtct gtgtcatctc ctacgtcata ggacatgccc tcggggccag tcccataccc
1261 gcgctgctca tcactgagat cttcctgcag tcctctcggc catctgcctt catggtgggg
1321 ggagctgtgc actggctctc caacttcacc gtgggcttga tcttccggt catccaggag
1381 ggctcggcc cgtacagctt cattgtcttc gccgtgatct gcctcctcac caccatctac
1441 atcttcttga ttgtcccga gaccaaggcc aagacgttca tagagatcaa ccagattttc
1501 accaagatga ataagggtgc tgaagtgtac ccggaagagg aggaactgaa agagcttcca
1561 cctgtcactt cggaacagt actctggaga ggaagccagt ggagctggtc tgccagggggc
1621 tcccacttt ggctatttt tctgacttct agctgtctgt gaatatccag aaataaaaaca
1681 actctgatgt ggaatgcagt cctcatctcc agcctccca cccagtgagg aactgtgcaa
1741 agggctgcct tgctgttctt gaagctgggc tgtctctctc catgttggcc tgtcaccaga
1801 cccagatcaa ttaaacagct ggtcctccac ttgtgtggt cagccttcgt gtggctcctg
1861 gtaacgtggc tccaccttga tgggtcaacc ttgtgtggc tcctggtaac ataacaacaa
1921 cagttactat agtggtgaga tgggaaggaat caaattttgc cagagaaact aactcggtgg
1981 cccaacagg tcttccgggg ccatgggcat ttgttttagag ccaaattcat cctcttacca
2041 gatccttttc cagaaatacc tgtctaggaa ggtgtgatgt cagaaacaat gacatccaga
2101 aagctgagga acaggttcct gtggagacac tgagtcagaa ttcttcatcc aaattatttt
2161 gttagtggaa aatggaattg cttctgtgta gtcaataaaa tgaacctgat cacttttc

```

**Figure 2.1**

Glut 5 mRNA sequence. The complementary sequences of AS 1 to AS 4 were in bold fonts.

**Table 2.1**

The sequences and the regions of the antisense or sense oligonucleotides. They are named as S, AS 1 to AS 4. They can hybridize to different regions of the Glut 5 cDNA sequence.

<b>Name</b>	<b>Region</b>	<b>Sequence (5'→ 3')</b>
Sense (S)	70-84	GCA AGC ATG GAG CAA
Antisense 1 (AS 1)	70-84	TTG CTC CAT GCT TGC
Antisense 2 (AS 2)	431-445	ATG TGG CGA CTC TGC
Antisense 3 (AS 3)	1221-1235	TGT CCT ATG ACG TAG
Antisense 4 (AS 4)	1572-1586	CAG AGT CAC TGT TCC



### 2.2.2 Trypan Blue Exclusion Assay

0.4% trypan blue solution was mixed with 10  $\mu$ l of cell suspension. Then, 10  $\mu$ l was transferred to the hemacytometer. The viable cells, which were not stained, were counted in a square of hemacytometer. The cell concentration (cells/ml) was calculated as follows:

$$\text{Cells per ml} = \text{Number of cell} \times 10^4 \times \text{Dilution factor}$$

### 2.2.3 Transfection

The cationic lipid, oligofectamine reagent (Invitrogen Co. Ltd.) was used as carrier to deliver the antisense oligonucleotides into the cells. The procedure of transfection was performed according to the manufacturer's manual. Briefly, oligofectamine reagent was first diluted with plain RPMI and was allowed to stand at room temperature for 5 minutes. In this 5 minutes, the oligonucleotides were diluted with serum free RPMI. Then the diluted oligofectamine and oligonucleotides were mixed and incubated for 15 minutes at room temperature to allow the formation of lipid-oligonucleotide complex. During the incubation period, the medium in the culture plate was replaced by serum free RPMI to facilitate transfection. After 15 minutes, the complexes were added to the cells and incubated for 4 hours at 37°C. By the end of incubation, serum was added to increase the volume. Two or three days later, the plate could be used for assaying.

### 2.2.4 MTT assay

$8 \times 10^3$  cells per well were seeded onto a 96-well plate in 100  $\mu$ l RPMI supplemented with 10% FBS (v/v). At the time of seeding and during transfection,



no antibiotics were used. This can help cell growth and allow transfection with rinsing the cells if they are to be transfected in the presence of serum. After 24 hours, transfection could be carried out. After 48 or 72 hours, the medium in each well was removed and each well was washed with PBS once. Then, 30  $\mu$ l of MTT solution (5mg/ml) was added to each well and the plate was incubated at 37°C for 2 hours. After incubation, the MTT was discarded and 100  $\mu$ l DMSO was added to dissolve the crystals and further incubated for 30 minutes at room temperature. The absorbance at 540nm was then measured by an ELISA plate reader (BIO-RAD). The blank was set using 100  $\mu$ l of DMSO only.

### **2.2.5 D-[U<sup>14</sup>C]-Fructose and 2-Deoxy-D-[1-<sup>3</sup>H] Glucose Uptake Assay**

4x10<sup>4</sup> cells per well were seeded onto a 24-well plate in 500  $\mu$ l RPMI supplemented with 10% FBS (v/v). One day later, transfection could be carried out. After 48 or 72 hours, D-[U<sup>14</sup>C]-fructose and 2-deoxy-D-[1-<sup>3</sup>H] glucose uptake assay can be performed. The procedure in Wu *et al.* (1998) was followed, with modifications. Firstly, the medium in each well was discarded and each well was washed with PBS once. Then 0.5ml PBS (0.5ml glucose-free RPMI, Gibco BRL, USA, for glucose uptake assay) was added to each well and incubated at 37°C for 1 hour to release the endogenous fructose or glucose. After incubation, 0.1mM fructose and 0.5  $\mu$  Ci D-[U<sup>14</sup>C]-fructose (0.1mM 2-deoxy-glucose and 0.5  $\mu$  Ci 2-deoxy-D-[1-<sup>3</sup>H] glucose for glucose uptake assay, Amersham Biosciences Ltd.) in 1ml PBS was added to each well and incubated at 37°C for 15 minutes. The PBS was discarded and each well was washed with 10mM fructose (10mM

deoxy-glucose) in normal saline twice. After that, 100  $\mu$ l 0.5mM NaOH was added to each well to lyse the cell and the plate was shaken at room temperature for 15 minutes. Finally, 100  $\mu$ l 0.5mM HCl was added for neutralization. Volume of 120  $\mu$ l was added to the scintillation vial containing 4ml scintillation fluid for counting and 20  $\mu$ l was used for protein concentration determination using BCA method.

$$\text{Amount of fructose (glucose) uptake} = \frac{\text{Count per minute (cpm)}}{\text{Amount of protein (} \mu \text{g)}} \quad (\text{cpm}/\mu \text{g})$$

### 2.2.6 Detection of Intracellular ATP Concentration

Intracellular ATP concentration was detected by using Bioluminescent somatic cell ATP assay kit (Sigma Chemical Co.).  $8 \times 10^4$  cells were seeded in a well of a 12-well culture plate. One day later, transfection can be carried out. 72 hours later, the medium in each well was removed and washed with PBS twice. 0.3ml 1X somatic cell ATP releasing agent was added to each well and the plate was shaken by orbital shaker (KikaLabotechnik) in 300 mot/min for 3 minutes. At the same time, 0.1ml of ATP assay mix solution was added to a reaction vial and allowed to stand at room temperature for 3 minutes to hydrolyze the endogenous ATP. Then, 0.1ml of cell lysate or ATP standard (or dH<sub>2</sub>O as blank) was transferred to the reaction vial, and the amount of light emitted (L) was measured immediately with a luminometer (Lumat LB 9501, Berthold). Standard curve of ATP concentration should be plotted against the L (Fig. 2.2). The amount of protein in the lysate was also measured by BCA method.

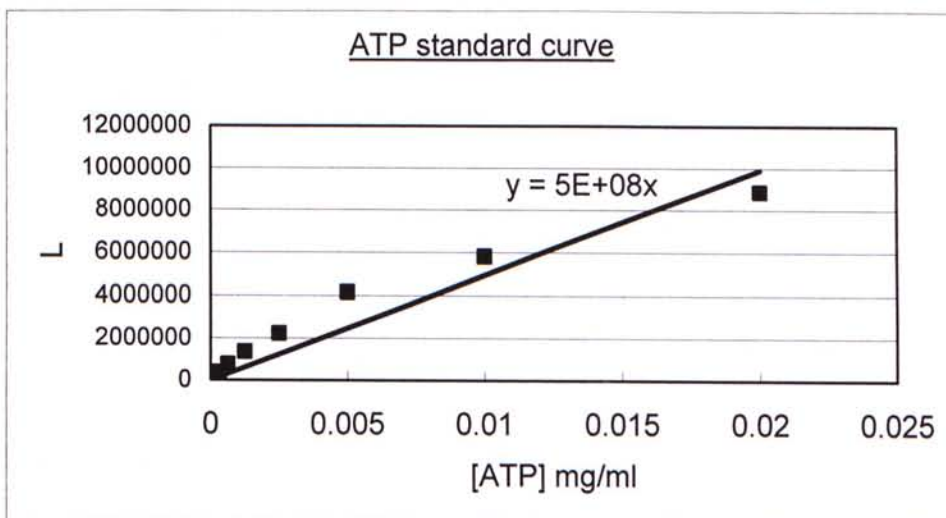


**Figure 2.2**

ATP standard curve. The equation of the trend line is for calculation of the ATP concentration in samples. The total ATP per  $\mu$ g of protein can be calculated as follows:

$$[\text{ATP}] (\text{mg/ml}) = L \text{ of sample} / 5 \times 10^8$$

$$\text{Total ATP per mg of protein} = \frac{[\text{ATP}] \text{mg/ml} \times 0.3 \text{ml}}{\text{Amount of protein (mg)}}$$



## 2.2.7 Reverse Transcription- Polymerase Chain Reaction (RT-PCR)

### 2.2.7.1 RNA Extraction by TRIzol Reagent (Invitrogen Co. Ltd.)

1.6x10<sup>5</sup> cells per well were seeded onto 6-well plate in 2ml RPMI supplemented with 10% FBS (v/v). 1 day later, transfection could be carried out. After 72 hours, the medium was removed and washed each well with PBS once. 1ml of TRIzol reagent was added to each well and the cells were lysed by pipetting up and down for several times. The lysate was transferred to a clean microfuge tube and was kept at 4 °C to prevent rapid degradation of RNA. Then, 200  $\mu$ l of chloroform was added to each tube and the tube was vortex vigorously for 15 seconds. The tube was then centrifuged at 13 600 x g for 15 minutes at 4 °C. After centrifugation, the upper colourless aqueous phase contains RNA and was poured into a new clean microfuge tube. 500  $\mu$ l of isopropanol was added to the tube and incubated at -20 °C for more than 1 hour. After incubation, the sample was centrifuged at 13 600 x g for 15 minutes at 4 °C. The supernatant was removed and 1ml of ice-cold 75% ethanol was added to wash the pellet. The 75% ethanol was then removed and 20  $\mu$ l of DEPC H<sub>2</sub>O was added to dissolve the RNA. RNA should be kept at -80 °C.

### 2.2.7.2 Determination of RNA Concentration

The RNA concentration can be measured spectrophotometrically, at 260nm and 280nm. The spectrophotometric assessment of RNA concentration is based on the strong absorption of light at 260nm of RNA. The absorption was measured at the peak of the RNA spectra and concentrations could be calculated by using the following equations: \* [RNA] ( $\mu$  g/ml) = 40/(1/ O.D.<sub>260</sub>).



The purity of the RNA can be reflected by the concentration of protein in the sample. This is achieved by measuring absorbance at 280nm. A pure sample of RNA should have a ratio of absorbance at 260/280nm exceeding 1.75 for further analytical purposes.

\* For dsDNA:  $[DNA] (\mu g/ml) = 50/(1/O.D._{260})$

### 2.2.7.3 Reverse Transcription

Reverse transcription was performed by using the Thermoscript™ RT-PCR system for 1<sup>st</sup>-strand cDNA synthesis kit. The procedure in manufacturer's manual was followed. Briefly, 1  $\mu$ l of oligo dT, 2  $\mu$ l of 10mM dNTP mix, 2  $\mu$ g of RNA, and DEPC H<sub>2</sub>O were mixed to give the volume of 12  $\mu$ l in total. The RNA and primer were denatured at 65°C for 5 minutes and chilled in ice. Then, 4  $\mu$ l of 5X cDNA synthesis buffer, 1  $\mu$ l of 0.1M DTT, 1  $\mu$ l of RNaseOut™ (40U/ $\mu$ l), 1  $\mu$ l of DEPC H<sub>2</sub>O and 1  $\mu$ l of Thermoscript™ RT (15U/ $\mu$ l) were added to each tube. The sample was then transferred to a thermocycler (ABI) preheated to 50 °C for 1 hour and the reaction was terminated by incubating at 85 °C for 5 minutes. Finally, 1  $\mu$ l of RNase H was added and further incubated at 37 °C for 20 minutes. The product, cDNA, can be stored at -20 °C.

### 2.2.7.4 Polymerase Chain Reaction (PCR)

Amplification of target genes from the cDNA was performed using the primers in table 2.2. The reagents used in PCR was listed in table 2.3.

**Table 2.2**

Sequences of primers used in PCR. These sequences were checked by the “Blast” program of NCBI for homology.

Genes	Direction	Primer sequence	Product size
$\beta$ -actin	Forward	5' CCT CGC CTT TGC CGA TCC 3'	700b.p.
	Reverse	5' GGA TCT TCA TGA GGT AGT CAG TC 3'	
Glut 5	Forward	5' CGT GCC TGC GAT CTT AAT GGG 3'	581b.p.
	Reverse	5' TAG ATC TGG TCC GCG TAG TAG 3'	

**Table 2.3**  
Volume of reagents used in PCR.

Reagent	Volume added ( $\mu$ l)
cDNA	5
10X PCR buffer	2.5
2.5mM dNTP	2.5
2.5mM Forward primer	2.5
2.5mM Reverse primer	2.5
High grade DMSO	1.5
Taq polymerase	0.2
Autoclaved dH <sub>2</sub> O	8.3
Total	25

The reaction mix (Table 2.3) was then undergone PCR by PCR machine (Applied Biosystem). Thermocycling was carried out as follows:

For $\beta$ -actin,	For Glut 5,
94°C for 5 minutes	94°C for 5 minute
94°C for 1 minute	94°C for 1 minute
63°C for 40 seconds	52°C for 50 seconds
72 °C for 40 seconds	72 °C for 50 seconds
72 °C for 10 minutes	72 °C for 10 minutes
<div style="display: flex; justify-content: space-around; align-items: center;"> <div style="text-align: center;"> <math>\left. \begin{array}{l} 94^{\circ}\text{C for 1 minute} \\ 63^{\circ}\text{C for 40 seconds} \\ 72^{\circ}\text{C for 40 seconds} \end{array} \right\} \text{Repeat for 28 cycles}</math> </div> <div style="text-align: center;"> <math>\left. \begin{array}{l} 94^{\circ}\text{C for 1 minute} \\ 52^{\circ}\text{C for 50 seconds} \\ 72^{\circ}\text{C for 50 seconds} \end{array} \right\} \text{Repeat for 45 cycles}</math> </div> </div>	

Amplification products were stored at -20°C and then resolved in 1% agarose gel.

## 2.2.8 Real-Time PCR

RNA extraction, determination of RNA concentration and reverse transcription were followed the procedure described in section 2.2.7.1-2.2.7.3. Amplification of target genes from the cDNA was performed with reagents listed in table 2.4. Samples were loaded in triplicate. Real-time PCR was run in ABI PRISM® 7000 Sequence Detection System. The reaction mix (Table 2.4) was then undergone PCR by ABI PRISM® 7700 Sequence Detection System (Applied Biosystem). Thermocycling was carried out as follows:

Stage 1: 50°C for 2 minutes	
Stage 2: 95 °C for 10 minutes	
Stage 3: 95°C for 15 seconds	} Repeat for 50 cycles
60°C for 1 minute	



**Table 2.4**

Volume of reagents for real-time PCR.

Reagent	Volume added ( $\mu$ l)
cDNA	1
TaqMan® Universal PCR Master Mix	5
Assays-on-Demand™ Glut 5 Gene Expression	0.5
Assays-on-Demand™ 18s rRNA Gene Expression	0.25
dH <sub>2</sub> O	3.25
Total	10

### 2.2.8.1 Analysis of the Real-Time PCR Data

The endpoint of real time PCR analysis is the threshold cycle ( $C_T$ ).

Threshold cycle ( $C_T$ ) is the cycle number at which the fluorescence emission exceeds the fixed threshold. The initial amount of target template is inversely proportional to the  $C_T$ .  $C_T$  was determined by using the computer program “Sequence Detection Systems, Version 1.9, by Applied Biosystem”. The expression level of the target gene which is represented by “Mean fold change” can be calculated as follows:

$$\text{Mean fold change} = 2^{-\Delta\Delta C_T}$$

Where  $\Delta\Delta C_T = \Delta C_T$  of target gene of sample  $-\Delta C_T$  of target gene control

$$\Delta C_T = C_T \text{ of target gene} - C_T \text{ of 18S rRNA}$$

(Livak and Schmittgen, 2001).

Mean fold change of target gene represents the amount of target gene. Mean fold change of negative control was set to be 1. For down-regulation of target gene, the mean fold change is ranged from 0-1; for up-regulation of target gene, the mean fold change is greater than 1.

## **2.2.9 Western Blot Analysis**

### **2.2.9.1 Protein Extraction**

$8 \times 10^4$  cells were seeded on 100mm culture dish. 1 day later, transfection can be carried out. 72 hours later, cells were collected and were washed twice with PBS. 100  $\mu$ l of lysis buffer was added and allowed to stand on ice for 3 hours. Then, samples were boiled for 10 minutes and centrifuged at  $13\,600 \times g$  for 10 minutes at 4°C. Finally, the supernatant was collected and stored at -20°C.

### **2.2.9.2 Protein Concentration Determination**

The protein concentration can be determined by bicinchoninic acid (BCA) protein assay. 1  $\mu$ l of each sample was mixed with 9  $\mu$ l of dH<sub>2</sub>O in a 96-well plate. Bovine serum albumin (BSA) was used to establish the protein standard curve. Both protein samples and BSA standard were done in triplicate. BCA reaction mixture was composed of BCA solution and reagent B in the ratio of 50:1. 200  $\mu$ l of BCA mixture was added to each well and incubated at 37°C for 30 minutes. After incubation, the absorbance at 540 nm was measured by ELISA plate reader (Bio-Rad). Standard curve of protein amount was plotted against the OD<sub>540nm</sub> (Fig. 2.3), and the amount of protein in the sample can be calculated by the equation of the trend line.

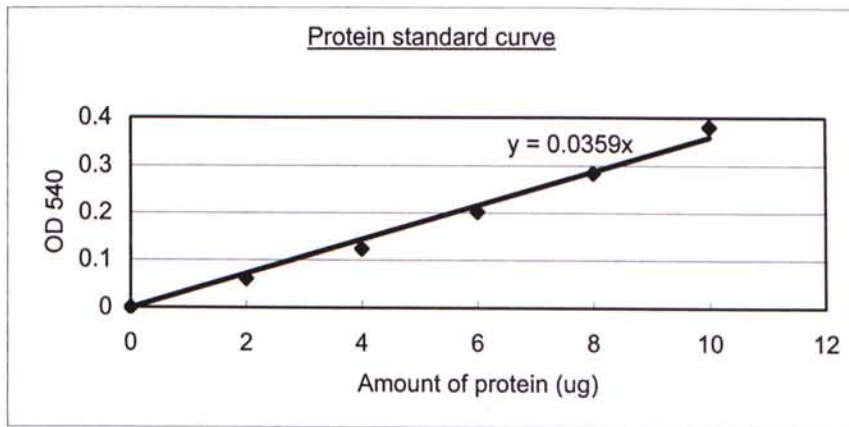


**Figure 2.3**

Protein standard curve. 2-10  $\mu$ g of BSA was added to each well in 96 well plate. 200  $\mu$ l of BCA mixture was added to each well and incubated at 37°C for 30 minutes. After incubation, the absorbance at 540 nm was measured by ELISA plate reader (Bio-Rad).



### 2.2.9.3 Western Blotting

#### SDS-PAGE

The apparatus of 3D vertical electrophoresis system (Bio-Rad) was set according to manufacturer's manual. 12.5% polyacrylamide separating gel was set with 1.0825 ml of dH<sub>2</sub>O, 1.6675 ml of 30% acrylamide, 1ml of 4X upper gel buffer, 4.65  $\mu$ l of TEMED and 20  $\mu$ l of 10% APS. 4.5% stacking gel was set with 1.2ml of dH<sub>2</sub>O, 0.3ml of 30% acrylamide, 0.5ml 4X lower gel buffer, 2.65  $\mu$ l of TEMED and 15  $\mu$ l of 10% APS.

According to the BSA standard curve, equal amount of protein samples (25-40  $\mu$ g) were used for SDS-PAGE. Protein samples were mixed with equal volume of 2 x SDS loading dye and boiled for 10 minutes. Then samples were loaded to the well of the polyacrylamide gel with rainbow coloured protein molecular marker (Amersham Bioscience Ltd.). The gel was then run at 120V for 90 minutes. The upper stacking gel was removed.

#### Transfer of Protein to PVDF Membrane by Electroblothing

Semi-Dry Electrophoretic Transfer Cell (semi-dry blotter, BioRad) was set referring to the steps in the manual. PVDF membrane (0.45  $\mu$ m) (Immobilon, Millipore) was used for electroblothing. The dry PVDF membrane was soaked in absolute methanol for re-hydration. The membrane was then put in E-blot buffer for a few seconds. Three pieces of Whatman 3mm papers were soaked in E-Blot buffer and put onto the platinum anode. The membrane was put onto the Whatman 3mm papers followed by the acrylamide gel. Another 3 pieces of E-blot buffer-soaked 3mm paper were put onto the gel. The proteins were transferred at

constant current at 0.15A for 2 gels for 45 minutes.

### **Probing Proteins with Antibodies**

After transfer of protein to the PVDF membrane, the membrane should be blocked with 10% non-fat milk (in TBS-T) at room temperature for 2 hours. Then, it was washed with TBS-T for 15 minutes for 3 times. Primary antibody, 0.6  $\mu$ l of mouse anti-human  $\beta$ -actin or 3  $\mu$ l of rabbit anti-Glut 5 in 3ml 10% non-fat milk was added for probing at room temperature for 2 hours. After probing, the membrane was washed with TBS-T for 15 minutes for 3 times and probed with secondary antibody (conjugated with horseradish peroxidase) at room temperature for 1 hour. The membrane was washed again with TBS-T for 15 minutes for 3 times and it was ready for ECL detection.

### **Enhanced Chemiluminescence (ECL) Assay**

ECL assay was used for detection of probed proteins. ECL detection reagent 1 and reagent 2 (Amersham) were mixed in the ratio of 1:1 and the membrane was immersed in the mixture for 90 seconds. Then the membrane was wrapped and put into the Hypersensitive film cassette (Amersham) followed by a Fuji Medical x-ray film (Super Rx, Fuji) in dark with various exposure time. The film was then developed by a film processor (M35 X-OMAT, Kodak).

## **2.2.10 Flow Cytometry**

A computer program, WinMDI, was used for data analysis.

### **2.2.10.1 Detection of Cell Cycle Pattern with PI**

$4 \times 10^5$  cells were seeded in a 60 mm culture dish with serum free RPMI to synchronize the cells. 1 day later, transfection can be carried out. 72 hours later, cells were harvested and washed with PBS. Cells were then fixed with 1 ml of 70% ethanol at 4°C overnight. After fixation, the cells were centrifuged at 300 x g for 5 minutes to remove the ethanol. Cells were then resuspended in 0.46 ml freshly prepared propidium iodide solution containing propidium iodide (43 µg/ml) and RNase A (1mg/ml) and incubated in dark at 37°C for 30 minutes. After incubation, the cells were analyzed by FACSsort flow cytometer (Becton Dickinson).

### **2.2.10.2 Detection of Apoptosis with Annexin V/PI**

The detection of apoptosis was performed by using TACS™ Annexin V-FITC kit (Trevigen, Inc.).  $4 \times 10^5$  cells were seeded in a 60 mm culture dish. 1 day later, transfection could be carried out. 72 hours later, cells were harvested and washed with PBS.  $5 \times 10^5$  cells were used for the assay. 10 µl of 10X binding buffer, 10 µl of PI, 1 µl of Annexin V-FITC conjugate and 79 µl of dH<sub>2</sub>O were added to a sample and incubated in the dark at room temperature for 15 minutes. After incubation, 400 µl of 1X binding buffer was added to the sample and the sample was analyzed by FACSsort flow cytometer (Becton Dickinson).



## 2.2.11 *In Vivo* Study

### 2.2.11.1 Establishment of Tumor-Bearing Animal Model

Female nude mice were used for investigating the *in vivo* effect of the antisense oligonucleotides against Glut 5.  $1 \times 10^7$  cells were inoculated subcutaneously (s.c.) into the anterior part of the nude mice and allowed to grow for 5-10 days. The weight of the mice, size of tumor should be measured before treatment. Treatments were started when the tumor size reached about 4mm x 4mm x 3mm ( $\sim 50\text{mm}^3$ ).

### 2.2.11.2 Treatment Schedule

The mice were divided into 3 groups, 10 mice per group, randomly. Groups included (1) PBS-Control group, (2) Sense-control group and (3) Antisense group.

For sense and antisense group, 20mg/kg/day of oligonucleotides were injected s.c., adjacent to the tumor in each nude mice for 8 doses, every other day. For PBS-control group, 0.1ml of PBS was injected. The antisense oligonucleotides were administrated into the tumor-bearing mice s.c., with constant volume of 0.1ml/mouse/injection.

After 8 doses, the mice were sacrificed. The weight of the mice should be recorded. The mice were first anesthetized by intra-peritoneal (i.p.) injection of 0.1ml pentobarbital. Then, the mice could be dissected and 0.5-0.8ml whole blood was withdrawn from the heart. The blood was transferred to a 1.5ml microfuge tube which contained 20  $\mu\text{l}$  of heparin and was centrifuged at  $1000 \times g$  for 10 minutes at 4°C. After centrifugation, the plasma was transferred to a clean microfuge tube and



stored at 4 °C until enzyme assay was performed.

On the other hand, the tumor should be taken out and the volume was measured. The volume of tumor was calculated as follows:

$$\text{Volume of tumor (mm}^3\text{)} = \text{Length (mm)} \times \text{Width (mm)} \times \text{Height (mm)}$$

The tumor was homogenized and then RNA or protein was extracted from the homogenate, following the procedure in section 2.2.9.

### **2.2.11.3 Toxicity of Antisense Oligonucleotides**

To assess the toxicity of antisense oligonucleotides after treatment, plasma enzymes activities were measured. After the above treatment, the mice were sacrificed and plasma was collected. The activities of 4 plasma enzymes, creatine kinase (CK), lactate dehydrogenase (LDH), alanine transaminase (ALT) and aspartate transaminase (AST), were measured by enzymatic diagnostic kits (Sigma). Increased activities of CK and LDH indicate heart tissue damage. While the increases of ALT and AST indicate liver tissue damage.

The procedures of measuring the enzymatic activities were according to the protocol of the enzymatic kits. Briefly, for measuring CK and LDH activities, 25  $\mu$ l of plasma was mixed with 500  $\mu$ l of CK or LDH reagent, respectively. The mixture was then incubated at 30°C for 3 minutes and 30 seconds for CK and LDH, respectively. The absorbance was measured at 340 nm by spectrophotometer (Beckman) for 2 minutes and 1 minute for CK and LDH, respectively at 30 seconds interval. For measuring AST and ALT, 100  $\mu$ l of plasma was mixed with 1 ml AST or ALT reagent and incubate at 37°C for 1 minute. Absorbance was measured at 340 nm at 30 seconds interval for 2 minutes.

The enzymatic activities were calculated as follows:

$$\text{Enzymatic activity (U/L)} = (\Delta A \text{ per min} \times TV \times 1000) / (6.22 \times LP \times SV)$$

where  $\Delta A \text{ per min}$  = change in absorbance per minute at 340 nm  
 TV = total reaction volume (ml)  
 LP = light path  
 6.22 = millimolar absorptivity of NADPH at 340 nm  
 SV = sample volume  
 1000 = conversion of units per ml to per liter

thus, CK (U/L) =  $\Delta A \text{ per min} \times 8200$   
 LDH (U/L) =  $\Delta A \text{ per min} \times 3376$   
 AST (U/L) =  $\Delta A \text{ per min} \times 1768$   
 ALT (U/L) =  $\Delta A \text{ per min} \times 1768$

The mean value of the plasma enzymatic activities of the same group was then plotted against the corresponding treatments.

# **Chapter 3**

## **Results**

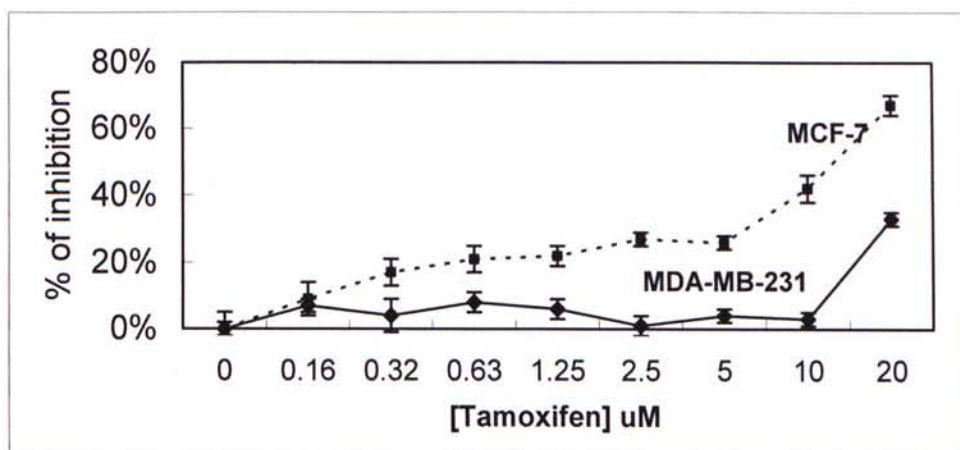
### **3.1 *In Vitro* Study**

#### **3.1.1 Effect of Tamoxifen on the Growth of MCF-7 and MDA-MB-231 cells**

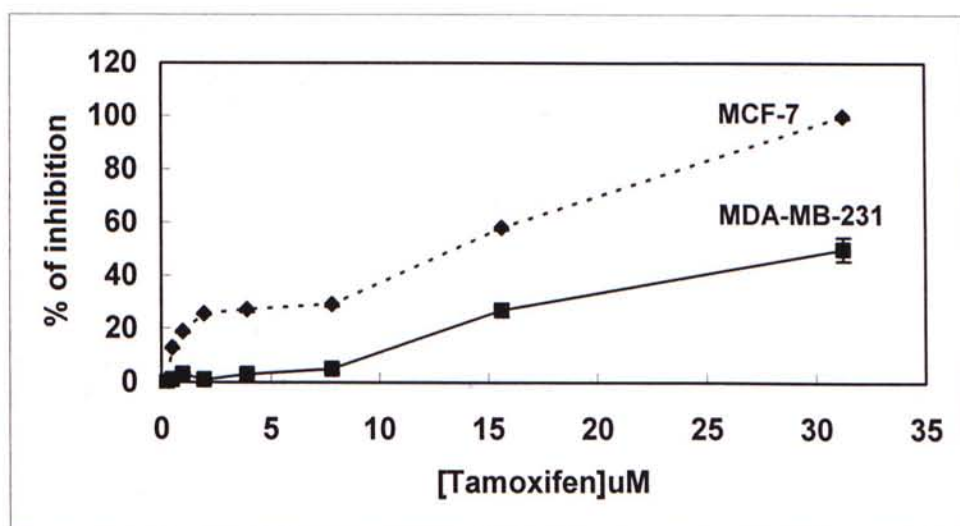
Tamoxifen is the most common anti-cancer drug for treating breast cancer. It has been used for more than 20 years. Tamoxifen works against the effects of estrogen on the breast cancer cells, i.e. anti-estrogen, and exerts its actions through the estrogen receptors (ER). Therefore, it is efficient to treat early stage, ER-positive breast cancer but not advanced stage, ER-negative, breast cancer.

The cytotoxic effects of tamoxifen on MCF-7 cells and MDA-MB-231 cells were investigated using MTT assays (Fig. 3.1). After 48 or 72 hour incubation, the  $IC_{50}$  of tamoxifen on MCF-7 cells were 15 $\mu$ M and 12.5 $\mu$ M respectively. For MDA-MB-231 cells, the  $IC_{50}$  of tamoxifen were 40 $\mu$ M and 35 $\mu$ M respectively.





(A)



(B)

**Figure 3.1**

The dose-response curve of tamoxifen on MCF-7 and MDA-MB-231 cells (Each point represents mean  $\pm$  S.D.,  $n = 6$ ).

(A) Incubated for 48 hours (obtained from the thesis of Chan KK).

(B) Incubated for 72 hours

$1 \times 10^4$  cells per well were seeded on 96-well plates. After 24 hours, 100mM tamoxifen (in 100% EtOH) was diluted to certain concentrations with RPMI 1640 medium supplemented with 10% FBS and 5% PS. 200  $\mu$ l of diluted tamoxifen was added to each well and incubated for 72 hours. Then, MTT assay could be performed.

### **3.1.2 Cytotoxicity of Antisense Oligonucleotides against Glut 5 on MCF-7 cells and MDA-MB-231 cells by MTT Assay**

The cytotoxic effects of various concentrations of antisense oligonucleotides (AS), namely 200nM, 400nM, 600nM, 800nM and 1  $\mu$  M, AS 1 to AS 4, flanking different regions of the Glut 5 mRNA (Fig.3.2), were investigated by MTT assay. All AS caused cytotoxic effects after 72-hour of incubation on both cell lines in a dose dependent manner. AS 1, which is complementary to the start codon exhibited an  $IC_{50}$  of 220nM on MCF-7 cells, while it gave 410nM on MDA-MB-231 cells (Fig. 3.3). AS 2, which is complementary to the coding region near 5' end exhibited an  $IC_{50}$  of 190nM on MCF-7 cells, while it exhibited 400nM on MDA-MB-231 cells (Fig. 3.4). AS 3, which is complementary to the coding region near 3' end, exhibited an  $IC_{50}$  of 300nM on MCF-7 cells, while it exhibited 400nM on MDA-MB-231 cells (Fig. 3.5). AS 4, which is complementary to the stop codon exhibited an  $IC_{50}$  of 220nM on MCF-7 cells, while it exhibited 470nM on MDA-MB-231 cells (Fig. 3.6). The  $IC_{50}$  of all AS on both cell lines were summarized in table 3.1.

```

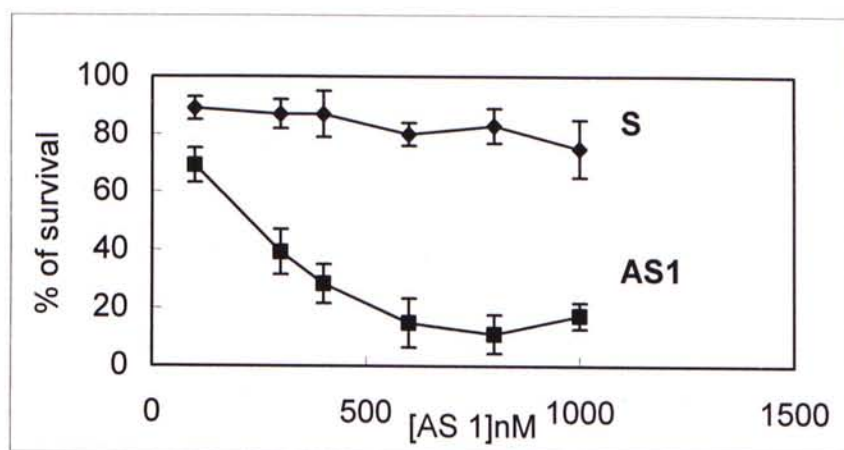
1  cttctctctc cattcagtgc acgcgttact ttggctaaaa ggaggtgagc ggcactctgc
61  ccttccagag caagcatgga gcaacaggat cagagcatga aggaagggag gctgacgctt
121 gtgcttgccc tggcaaccct gatagctgcc tttgggtcat ccttccagta tgggtacaac
181 gtggctgctg tcaactcccc agcactgctc atgcaacaat tttacaatga gacttactat
241 ggtaggaccg gtgaattcat ggaagacttc cccttgacgt tgctgtggtc tgtaaccgtg
301 tccatgtttc catttgagg gtttatcgga tccctcctgg tcggccccctt ggtgaataaa
361 tttggcagaa aaggggcctt gctgttcaac aacataatct ctatcgtgcc tgcgatctta
421 atgggatgca gcagagtcgc cacatcattt gagcttatca ttatttccag acttttggtg
481 ggaatatgtg caggtgtatc ttccaacgtg gtcccatgt acttagggga gctggccccct
541 aaaaacctgc ggggggctct cgggggtggg cccagctct tcatcactgt tggcatcctt
601 gtggcccaga tctttggtct tcggaatctc cttgcaaacg tagatggctg gccgatcctg
661 ctggggctga ccggggctcc cgcggcgctg cagctccttc tgctgccctt cttccccgag
721 agccccaggt acctgctgat tcagaagaaa gacgaagcgg ccgccaagaa agccctacag
781 acgctgcgcg gctgggactc tgtggacagg gaggtggcgg agatccggca ggaggatgag
841 gcagagaagg ccgcgggctt catctccgtg ctgaagctgt tccgatgcg ctcgctgcgc
901 tggcagctgc tgtccatcat cgtcctcatg ggcggccagc agctgtcggg cgtcaacgct
961 atctactact acgcggacca gatctacctg agcgcggcg tgccggagga gcacgtgcag
1021 tacgtgacgg ccggcaccgg ggccgtgaac gtggtcatga ccttctgcgc cgtgttcgtg
1081 gtggagctcc tgggtcggag gctgctgctg ctgctgggt tctccatctg cctcatagcc
1141 tgctgcgtgc tactgcagc tctggcactg caggacacag tgtcctggat gccatacatc
1201 agcatcgtct gtgtcatctc ctacgtcata ggacatgcc tcgggccag tcccataccc
1261 gcgctgctca tactgagat cttcctgcag tcctctcggc catctgcctt catggtgggg
1321 ggcagtgtgc actggctctc caacttcacc gtgggcttga tcttcccgtt catccaggag
1381 ggcctcggcc cgtacagctt cattgtcttc gccgtgatct gcctcctcac caccatctac
1441 atcttcttga ttgtcccga gaccaaggcc aagacgttca tagagatcaa ccagattttc
1501 accaagatga ataaggtgtc tgaagtgtac ccgaaaaagg aggaactgaa agagcttcca
1561 cctgtcactt cggaacagt actctggaga ggaagccagt ggagctggtc tgccaggggc
1621 tccccacttt ggcttatttt tctgacttct agctgtctgt gaatatccag aaataaaaca
1681 actctgatgt ggaatgcagt cctcatctcc agcctcccca cccagtggg aactgtgcaa
1741 agggctgcct tgctgttctt gaagctgggc tgtctctctc catgttggcc tgtcaccaga
1801 cccgagtcaa ttaaacagct ggtcctccac tttgctggtt cagccttcgt gtggctcctg
1861 gtaacgtggc tccacctga tgggtcaacc tttgtgtggc tcctggtaac ataacaacaa
1921 cagttactat agtggtgaga tgggaaggaat caaatcttgc cagagaaact aactcggtgg
1981 ccccaacagg tcttccgggg ccattgggcat ttgttttagag ccaaattcat cctcttacca
2041 gatccttttc cagaaatacc tgtctaggaa ggtgtgatgt cagaaacaat gacatccaga
2101 aagctgagga acaggttcct gtggagacac tgagtcagaa ttcttcatcc aaattatttt
2161 gttagtggaa aatggaattg cttctgtgta gtcaataaaa tgaacctgat cacttttc

```

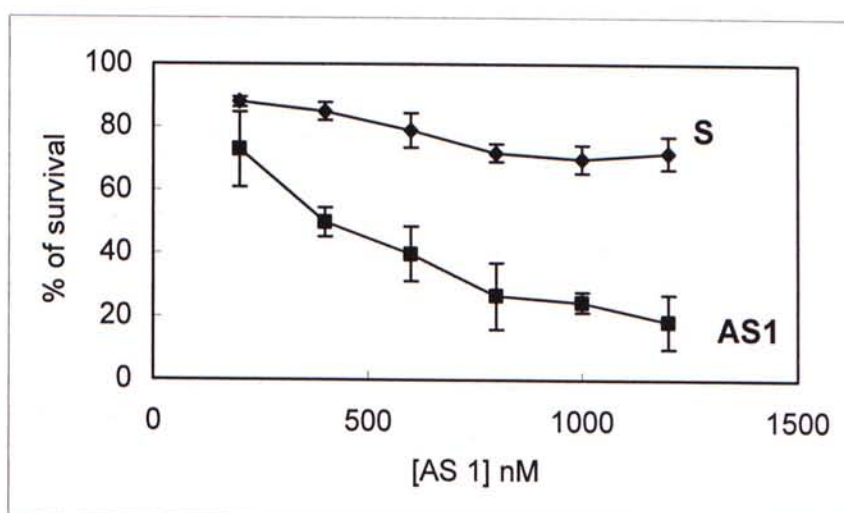
**Figure 3.2**

Glut 5 mRNA sequence. The complementary sequences of AS 1 to AS 4 were in bold fonts.





(A)



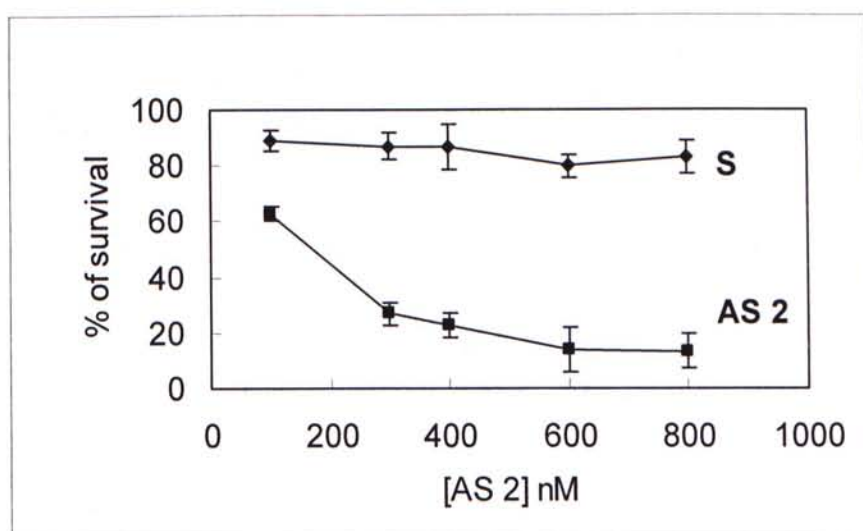
(B)

**Figure 3.3**

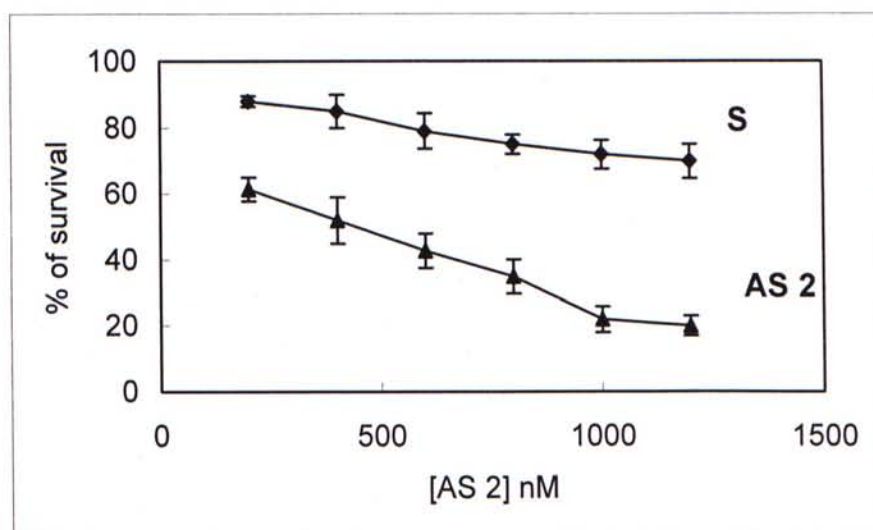
Cytotoxicity of AS 1 on (A) MCF-7 cells, (B) MDA-MB-231 cells.

$7 \times 10^3$  cells were seeded on each well of 96-well plate. On the next day, transfections of 100nM to  $1.2 \mu\text{M}$  of AS 1, with oligofectamine, were carried out. After 72 hours incubation, MTT assays were done. The value for untreated control cells was set at 100%. Data shown were mean  $\pm$  S.D.,  $n=6$ . The  $\text{IC}_{50}$  can be obtained from the graph.





(A)

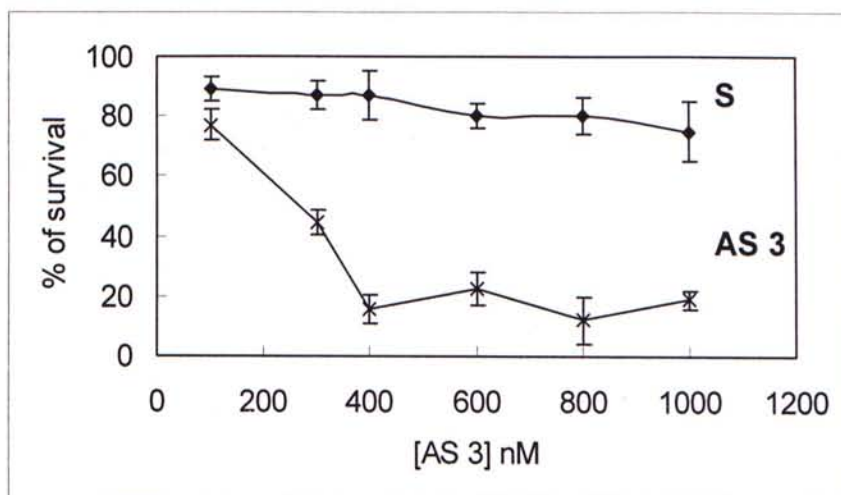


(B)

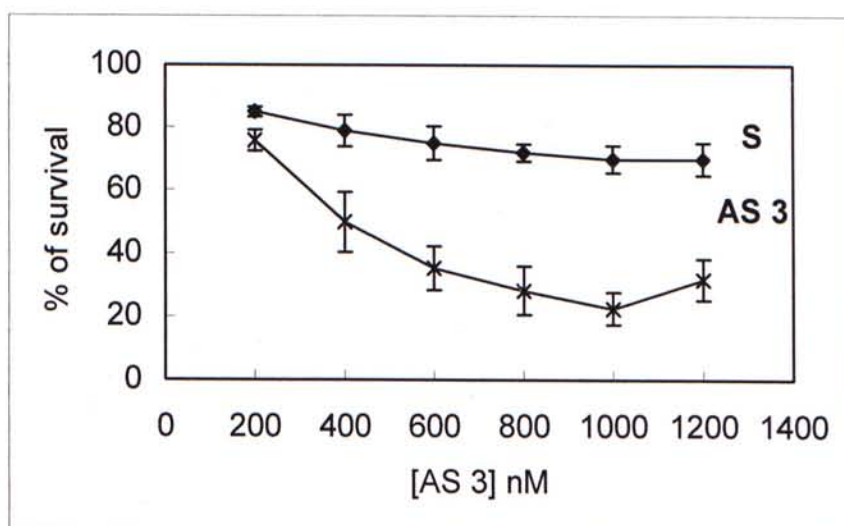
**Figure 3.4**

Cytotoxicity of AS 2 on (A) MCF-7 cells, (B) MDA-MB-231 cells.

$7 \times 10^3$  cells were seeded on each well of 96-well plate. On the next day, transfections of 100nM to 1.2 $\mu$ M of AS 2, with oligofectamine, were carried out. After 72 hours incubation, MTT assays were done. The value for untreated control cells was set at 100%. Data shown were mean  $\pm$  S.D.,  $n=6$ . The  $IC_{50}$  can be obtained from the graph.



(A)

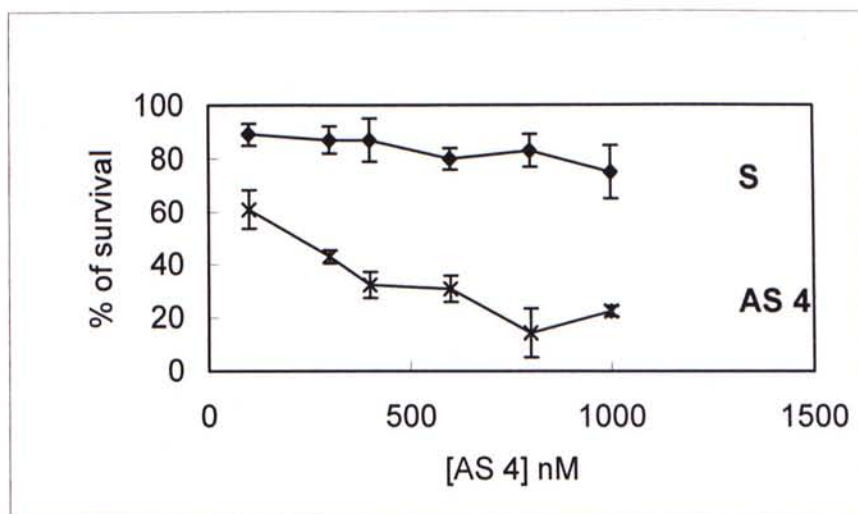


(B)

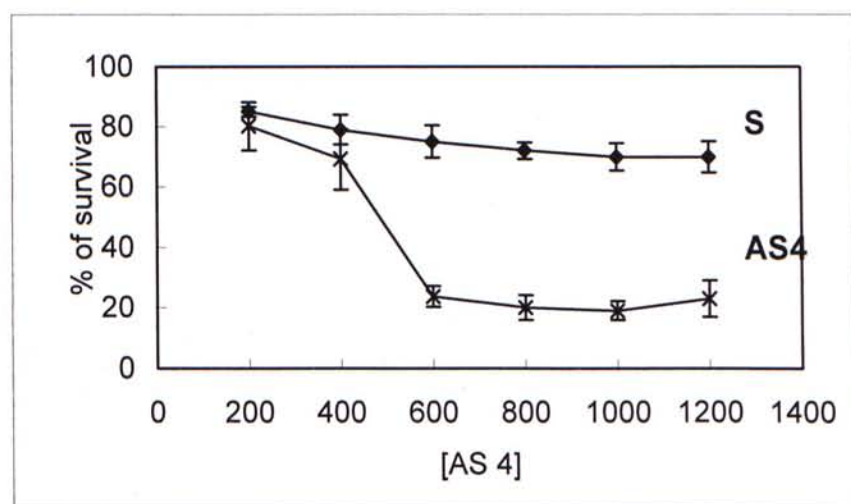
**Figure 3.5**

Cytotoxicity of AS 3 on (A) MCF-7 cells, (B) MDA-MB-231 cells.

$7 \times 10^3$  cells were seeded on each well of 96-well plate. On the next day, transfections of 100nM to  $1.2 \mu\text{M}$  of AS 3, with oligofectamine, were carried out. After 72 hours incubation, MTT assays were done. The value for untreated control cells was set at 100%. Data shown were mean  $\pm$  S.D.,  $n=6$ . The  $\text{IC}_{50}$  can be obtained from the graph.



(A)



(B)

**Figure 3.6**

Cytotoxicity of AS 4 on (A) MCF-7 cells, (B) MDA-MB-231 cells.

$7 \times 10^3$  cells were seeded on each well of 96-well plate. On the next day, transfections of 100nM to  $1.2 \mu\text{M}$  of AS 4, with oligofectamine, were carried out. After 72 hours incubation, MTT assays were done. The value for untreated control cells was set at 100%. Data shown were mean  $\pm$  S.D.,  $n=6$ . The  $\text{IC}_{50}$  can be obtained from the graph.

**Table 3.1**

IC<sub>50</sub> (nM) of AS 1 to AS 4 on MCF-7 cells and MDA-MB-231 cells. The IC<sub>50</sub> values were obtained from the MTT assay, after 72-hour incubations.

	IC <sub>50</sub> (nM)	
Cell line	MCF-7 cells	MDA-MB-231 cells
AS 1	220	410
AS 2	190	400
AS 3	300	400
AS 4	220	470



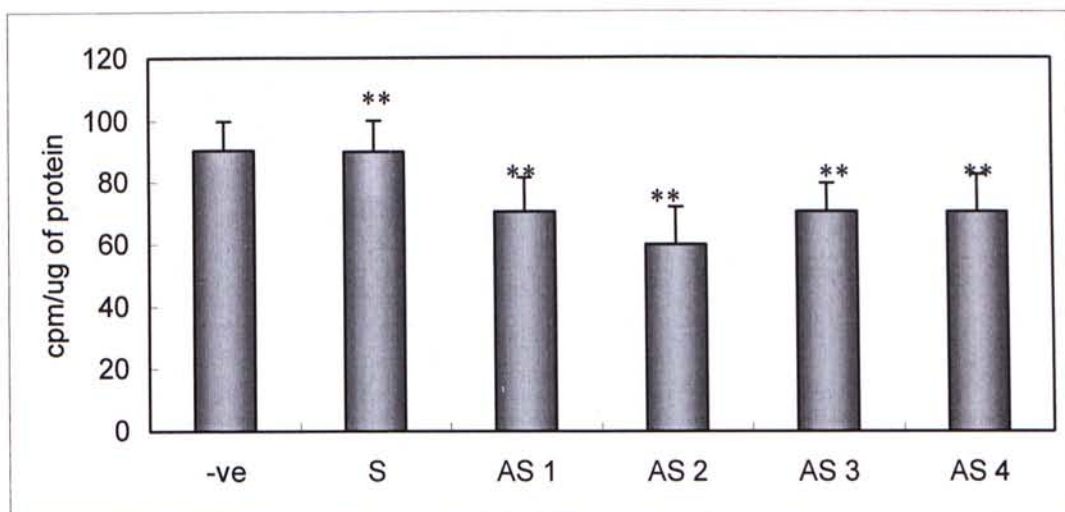
### **3.1.3 Effect of Antisense Oligonucleotides against Glut 5 on Fructose and Glucose Uptake of MCF-7 Cells and MDA-MB-231 Cells by D-[U<sup>14</sup>C]-Fructose and 2-Deoxy-D-[1-<sup>3</sup>H] Glucose Uptake Assay**

Glut 5 is responsible for transport fructose in the intestine and sperm. In the previous part, it was found that AS against Glut 5 caused a cytotoxic effect in breast cancer cell lines in a dose dependent manner. We hypothesized that AS against Glut 5 can down-regulate the mRNA and protein expression of the target gene and thus decrease the fructose uptake in the cells. Therefore, D-[U<sup>14</sup>C]-fructose and 2-deoxy-D-[1-<sup>3</sup>H] glucose uptake assays were performed to test whether the fructose and glucose uptake level decrease after AS treatment in both cell lines. The procedure was described in section 2.2.5.

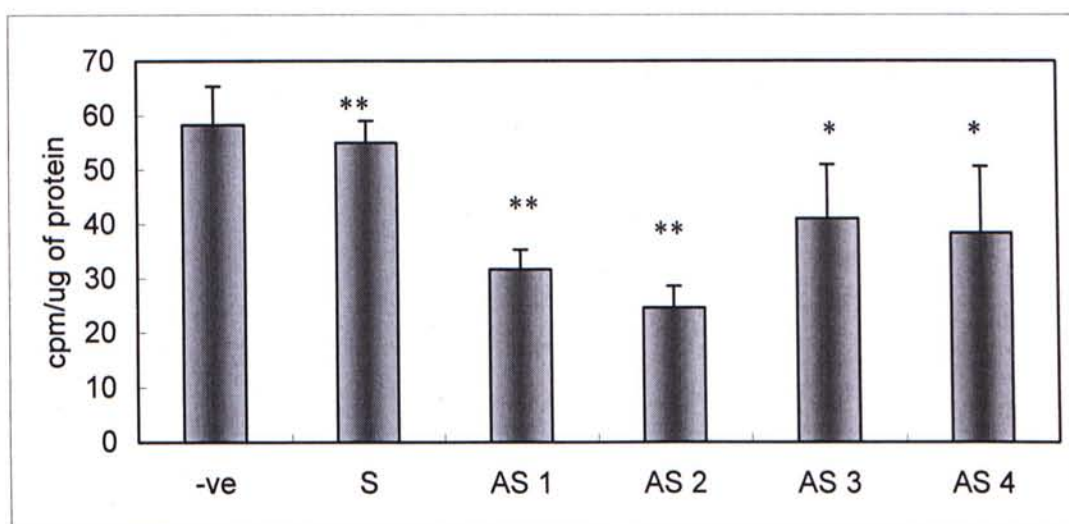
For MCF-7 cells, after treatment of AS, the fructose uptake was decreased when compared with that of the negative control and the sense control, after 72 hours of transfection (Fig. 3.7A). For MDA-MB-231 cells, a similar result was obtained (Fig. 3.7B).

2-deoxy-D-[1-<sup>3</sup>H] glucose uptake assay was also done to test whether the AS affect glucose transport in the cancer cells, followed the procedure described in Chan *et al.* (1999). It can be also used to test the specificity of the AS. If the AS only

hybridized only to Glut 5, the glucose uptake level should not be decreased, as Glut 5 is a fructose transporter, rather than a glucose transporter. It is more specific and effective in transporting fructose (Tatibouet *et al.*, 2000). For MCF-7 cells, after treatment of AS, the glucose uptake was not reduced significantly, when compared with the negative control and the sense control, after 72 hours of transfection (Fig. 3.8A). For MDA-MB-231 cells, a similar result was observed (Fig. 3.8B).



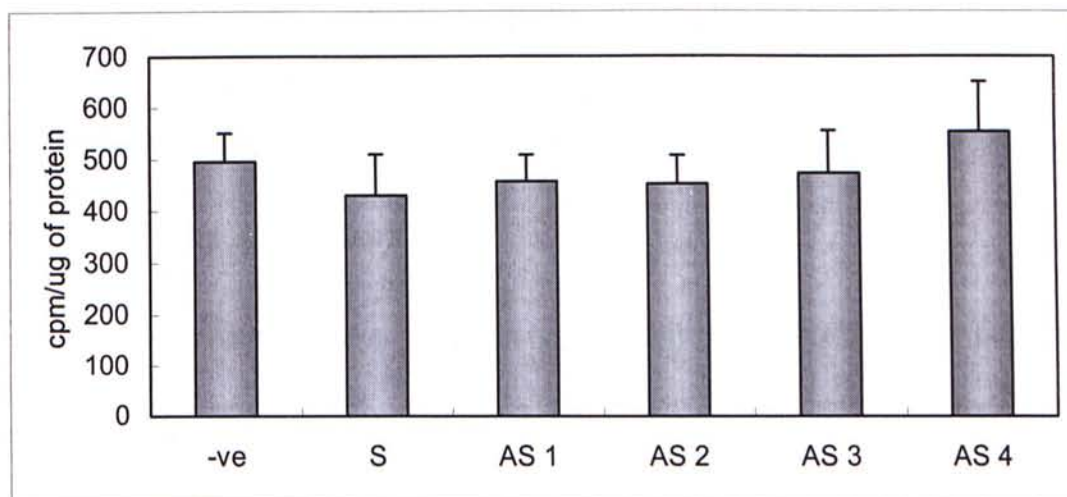
(A)



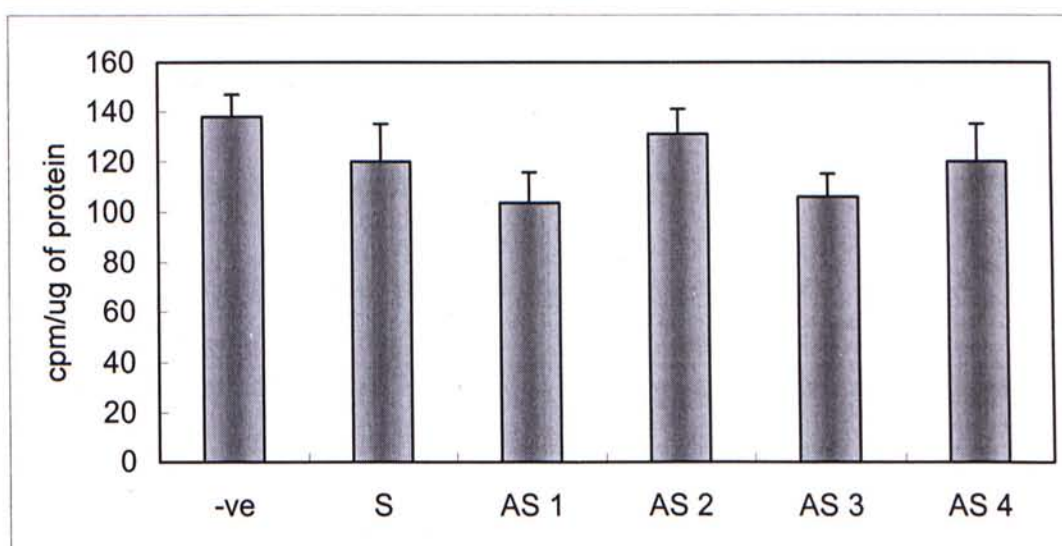
(B)

**Figure 3.7**

Effect of AS on D-[U<sup>14</sup>C]-fructose on (A) MCF-7 cells; (B) MDA-MB-231 cells. The procedure was described in section 2.2.5. Data shown were mean  $\pm$  S.D.,  $n = 4$ . (Student's  $t$ -test: \*  $p < 0.05$ , \*\*  $p < 0.01$ ).



(A)



(B)

**Figure 3.8**

Effect of AS on 2-deoxy-D-[1-<sup>3</sup>H] glucose uptake on (A) MCF-7 cells; (B) MDA-MB-231 cells. The procedure was described in section 2.2.5. Data shown were the mean  $\pm$  S.D., n=4. (Student's *t*-test: S, AS 1-4,  $P < 0.01$ ).

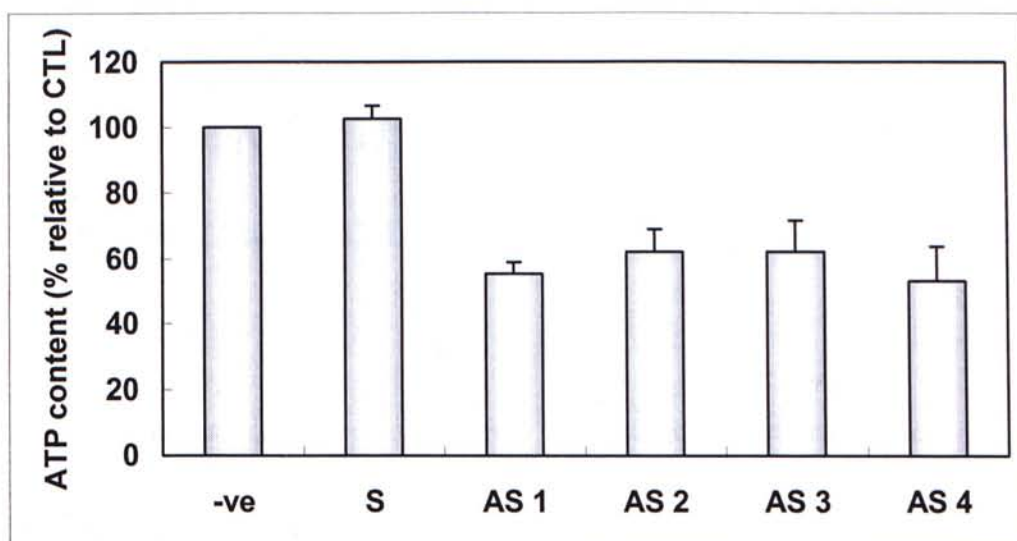


### **3.1.4 Effect of Antisense Oligonucleotides against Glut 5 on Intracellular ATP Content of MCF-7 Cells and MDA-MB-231 Cells by ATP Assay**

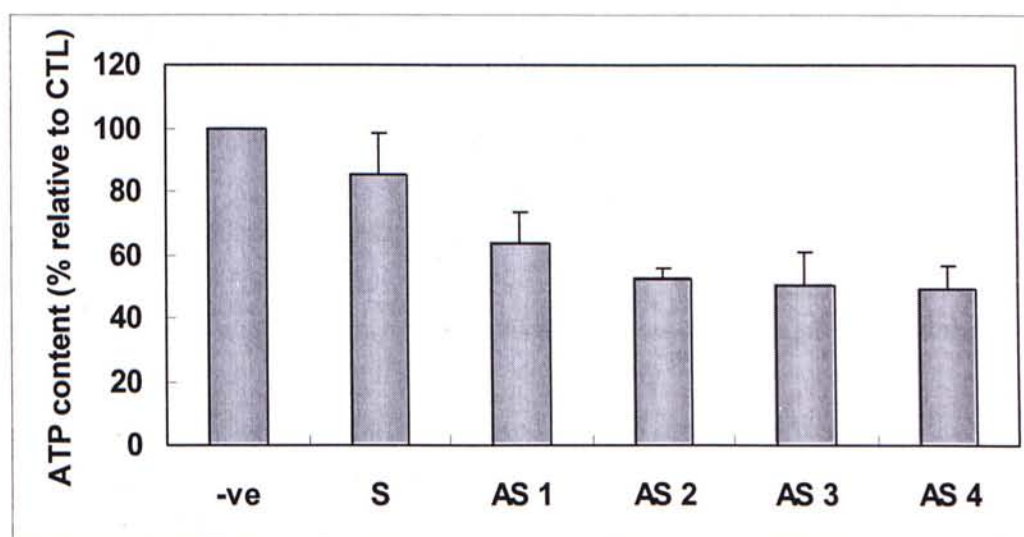
As mentioned above, Glut 5 is highly expressed in breast cancer cells, but absent in normal breast cells (Zamora-Leon *et al.*, 1996). This finding indicated that breast cancer cells may have a specialized capacity to transport fructose which is a rare metabolic substrate to be used by only a few human tissues. If fructose is the metabolic substrate for the breast cancer cells, the ATP content in the cells should be changed upon the inhibition of fructose uptake. Therefore, intracellular ATP assay was done to investigate the effect of AS on the breast cancer cells.

The intracellular ATP level was measured by Bioluminescent somatic cell ATP assay kit (Sigma Chemical Co.). The procedure was described in section 2.2.6. Standard curve of ATP concentration should be plotted against the light emitted (L) (Fig. 2.2). The amount of protein in the lysate was also measured by the BCA method.

For MCF-7 cells, after treatment of AS, the intracellular ATP content was reduced significantly, from 50-60%, when compared with the negative control and the sense control, after 72 hours of transfection (Fig. 3.9A). For MDA-MB-231 cells, a similar result was observed (Fig. 3.9B).



(A)



(B)

**Figure 3.9**

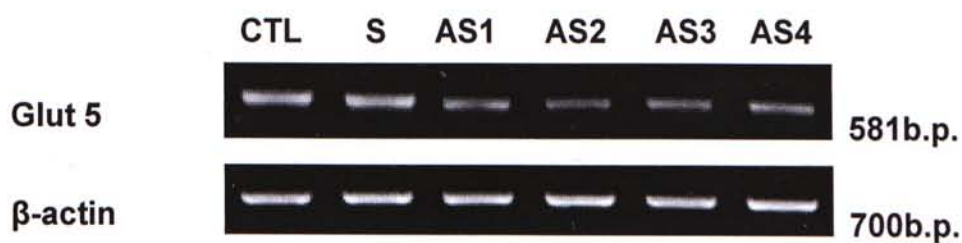
Intracellular ATP content of (A) MCF-7 cells, (B) MDA-MB-231 cells after AS treatment with  $IC_{50}$  concentration for 72 hours. The procedure was described in section 2.2.6. Data shown were mean  $\pm$  S.D.,  $n=4$ . (Student's  $t$ -test: S, AS 1-4,  $P<0.01$ ).

### **3.1.5 Effect of Antisense Oligonucleotides against Glut 5 on Glut 5 RNA Expression of MCF-7 Cells and MDA-MB-231 Cells by RT-PCR and Real-Time PCR**

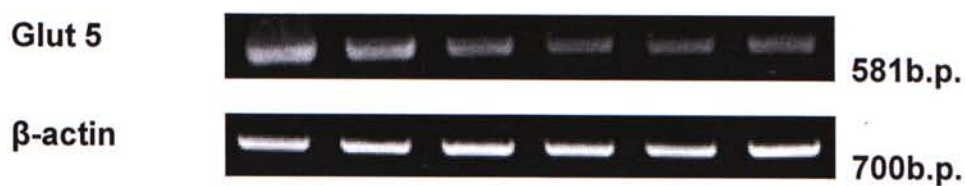
#### **3.1.5.1 RT-PCR**

Theoretically, AS can suppress the target gene expression in both transcriptional and translational levels. To investigate whether AS against Glut 5 can suppress the Glut 5 RNA level, RT-PCR was performed. After AS 1-4 treatments, the total RNA from the cells were extracted and reverse transcribed to cDNA. Two pairs of primers were used, namely  $\beta$ -actin and Glut 5. They gave the product of approximately 600bp and 700bp respectively. The mRNA levels after AS treatments of both cell lines were shown in Fig. 3.10 and Tables 3.2 and 3.3 showed the ratio of the band intensity of Glut 5 of the treated sample compared to that of the negative control. The band intensity was measured by a densitometer.

From the result, it can be shown that in MCF-7 cells, there was a down-regulation of Glut 5 RNA expression after AS treatment with  $IC_{50}$  concentration, 72 hour post-transfection, when compared with that of negative control. Similar results were obtained for MDA-MB-231 cells (Fig.3.10B). It suggested that Glut 5 can suppress the expression of Glut 5 mRNA in both cell lines.



(A)



(B)

**Figure 3.10**

mRNA expression of Glut 5 in (A) MCF-7 cells, (B) MDA-MB-231 cells, after AS treatment with  $IC_{50}$  concentration, 72-hour post-transfection. The procedure was described in section 2.2.7.



**Table 3.2**

Ratio of band intensity of Glut 5 mRNA of treated sample compared to that of the negative control of untreated MCF-7 cells (Fig. 3.10). The band intensity was measured by a densitometer. The experiment was repeated for three times and data shown were mean  $\pm$  S.D.

	Band Intensity		Ratio
	$\beta$ -actin	Glut 5	
<b>Negative Control</b>	29840	25580	-
<b>S</b>	27410	24160	1.03 $\pm$ 0.02
<b>AS 1</b>	30450	15020	0.58 $\pm$ 0.05
<b>AS 2</b>	31060	10350	0.39 $\pm$ 0.01
<b>AS 3</b>	24970	12380	0.58 $\pm$ 0.03
<b>AS 4</b>	27810	14210	0.60 $\pm$ 0.02

**Table 3.3**

Ratio of band intensity of Glut 5 mRNA of treated sample compared to that of the negative control of untreated MDA-MB-231 cells (Fig. 3.10). The band intensity was measured by a densitometer. The experiment was repeated for three times and data shown were mean  $\pm$  S.D.

	Band Intensity		Ratio
	$\beta$ -actin	Glut 5	
<b>Negative Control</b>	33500	29230	-
<b>S</b>	31870	24160	$0.87 \pm 0.05$
<b>AS 1</b>	37350	14210	$0.44 \pm 0.03$
<b>AS 2</b>	35320	10760	$0.35 \pm 0.02$
<b>AS 3</b>	33290	10960	$0.38 \pm 0.04$
<b>AS 4</b>	39790	13600	$0.39 \pm 0.02$

### 3.1.5.2 Real-Time PCR

The expression of Glut 5 RNA was investigated using real-time PCR. Real-time RT-PCR can be used for quantitation of the initial amount of template specifically. The real-time PCR system is based on the detection and quantitation of a fluorescent reporter. This signal increases in direct proportion to the amount of PCR product in a reaction. By recording the amount of fluorescence emission at each cycle, it is possible to monitor the PCR reaction during exponential phase where the first significant increase in the amount of PCR product correlates to the initial amount of target template. Threshold cycle ( $C_T$ ) is the cycle number at which the fluorescence emission exceeds the fixed threshold. The initial amount of target template is inversely proportional to the  $C_T$ . The expression level of the target gene which is represented by “Mean fold change” can be calculated as follows:

$$\text{Mean fold change} = 2^{-\Delta\Delta C_T}$$

Where  $\Delta\Delta C_T = \Delta C_T$  of target gene of sample  $-\Delta C_T$  of target gene control

$$\Delta C_T = C_T \text{ of target gene} - C_T \text{ of 18S rRNA}$$

Mean fold change of target gene represents the amount of target gene. Mean fold change of negative control was set to be 1. For down-regulation of target gene,

the mean fold change is ranged from 0-1; for up-regulation of target gene, the mean fold change is greater than 1.

To detect the initial amount of Glut 5 RNA after AS treatment, primers for Glut 5 conjugated with a fluorescence dye “FAM” and primers for 18S rRNA conjugated with “VIC” were used. 18S rRNA was used for normalization and calculation.

The mean fold changes of Glut 5 RNA expression after AS 1-4 treatments in MCF-7 cells and MDA-MB-231 cells were tabulated in Table 3.4. In both cell lines, the mean fold changes of all AS treatments were less than 1. This showed that Glut 5 RNA expression was reduced after AS treatments.



**Table 3.4**

Mean fold change of Glut 5 RNA after AS 1-4 treatments in MCF-7 cells and MDA-MB-231 cells, using real-time PCR. The procedure was described in section 2.2.8. Data shown were mean  $\pm$  S.D., n = 3.

	<b>Mean Fold Change</b>	
<b>Treatment</b>	<b>MCF-7 Cells</b>	<b>MDA-MB-231Cells</b>
<b>Negative Control</b>	1	1
<b>S</b>	0.86 $\pm$ 0.05	1.074 $\pm$ 0.08
<b>AS 1</b>	0.574 $\pm$ 0.02	0.653 $\pm$ 0.05
<b>AS 2</b>	0.523 $\pm$ 0.03	0.624 $\pm$ 0.05
<b>AS 3</b>	0.553 $\pm$ 0.06	0.533 $\pm$ 0.04
<b>AS 4</b>	0.437 $\pm$ 0.03	0.604 $\pm$ 0.03

### **3.1.6 Effect of Antisense Oligonucleotides on Glut 5 Protein Expression of MCF-7 Cells and MDA-MB-231 Cells by Western Blot Analysis**

As mentioned before, AS can suppress the target gene expression in both transcriptional and translational levels. To investigate whether AS against Glut 5 can suppress the Glut 5 protein level, Western blot analysis was performed, according to the procedure described in section 2.2.9. The protein levels after AS 1-4 treatments of both cell lines were shown in Fig. 3.11 and Tables 3.5 and 3.6 showed the ratios of the band intensity of Glut 5 protein of treated sample to that of the negative control. The band intensity was measured by a densitometer.

From the result, it can be shown that in MCF-7 cells, there was a suppression of Glut 5 protein level after AS 1-4 treatments with respective  $IC_{50}$  concentrations, 72 hour post-transfection, when compared with that of the negative control (Fig.3.11A). Similar results were obtained for MDA-MB-231 cells (Fig. 3.11B). It suggested that Glut 5 can inhibit the expression of Glut 5 protein in both cell lines.

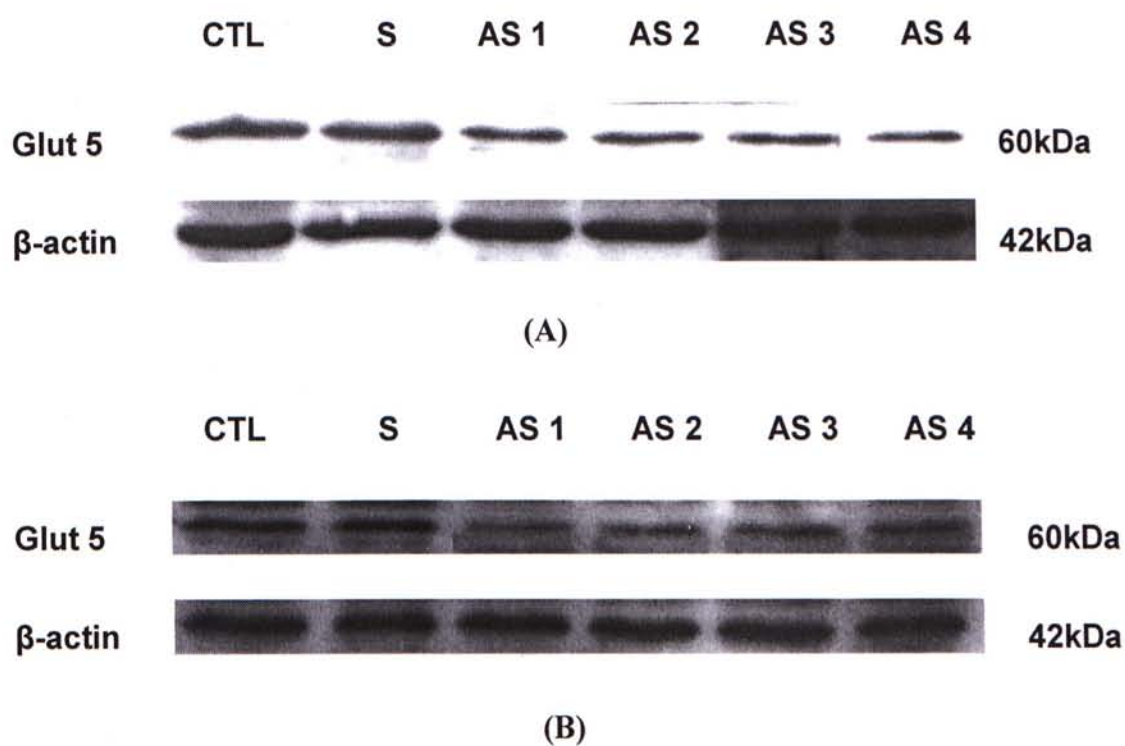


**Figure 3.11**

Protein expression of Glut 5 in (A) MCF-7 cells, (B) MDA-MB-231 cells, after AS 1-4 treatments with respective  $IC_{50}$  concentrations, 72-hour post-transfection. The procedure was described in section 2.2.9.

**Table 3.5**

Ratio of band intensity of Glut 5 protein of treated sample to that of the negative control of untreated MCF-7 cells (Fig. 3.11). The band intensity was measured by a densitometer. The experiment was repeated for three times and data shown were mean  $\pm$  S.D.

	Band Intensity		Ratio
	$\beta$ -actin	Glut 5	
<b>Negative Control</b>	116800	78530	-
<b>S</b>	113600	76580	$1.00 \pm 0.03$
<b>AS 1</b>	119400	51920	$0.65 \pm 0.04$
<b>AS 2</b>	124000	44780	$0.54 \pm 0.04$
<b>AS 3</b>	136300	45430	$0.50 \pm 0.07$
<b>AS 4</b>	135600	44330	$0.49 \pm 0.07$



**Table 3.6**

Ratio of band intensity of Glut 5 protein of treated sample to that of the negative control of untreated MDA-MB-231 cells (Fig.3.11). The band intensity was measured by a densitometer. The experiment was repeated for three times and data shown were mean  $\pm$  S.D.

	Band Intensity		Ratio
	$\beta$ -actin	Glut 5	
Negative Control	135600	127200	-
S	130500	125900	1.03 $\pm$ 0.02
AS 1	131800	87770	0.71 $\pm$ 0.06
AS 2	123310	72980	0.63 $\pm$ 0.03
AS 3	121400	73460	0.65 $\pm$ 0.4
AS 4	121400	77270	0.68 $\pm$ 0.04

### **3.1.7 Effect of Antisense Oligonucleotides against Glut 5 on Change in Cell Cycle Pattern of MCF-7 Cells and MDA-MB-231 Cells by Flow Cytometry, Using PI Staining**

To investigate whether AS treatment alter the cell cycle pattern of MCF-7 and MDA-MB-231 cells, flow cytometry using propidium iodide (PI) was used. PI is the most common dye to assess the DNA content quantitatively. PI binds to DNA and emits red fluorescence which can be detected by flow cytometer FL-2 channel. We can estimate the percentage of cells in sub  $G_1$ ,  $G_1$ , S and  $G_2/M$  phase using a computer program WinMDI.

The cell cycle patterns of MCF-7 cells after AS 1-4 treatments, 72 hours post transfection, were shown in Fig. 3.12 and the percentage of each phase was tabulated in Table 3.7. From the result, it was found that there is no accumulation of cell population in  $G_1$ , S and  $G_2/M$  phase, but in sub  $G_1$  phase (Fig. 3.12 and Table 3.7). For MDA-MB-231, similar results were obtained (Fig. 3.13 and Table 3.8). For both cell lines, no cell cycle arrest was observed in all treatments, but there might be apoptosis of the treated cells, as there was an accumulation of cells in the sub  $G_1$  phase.

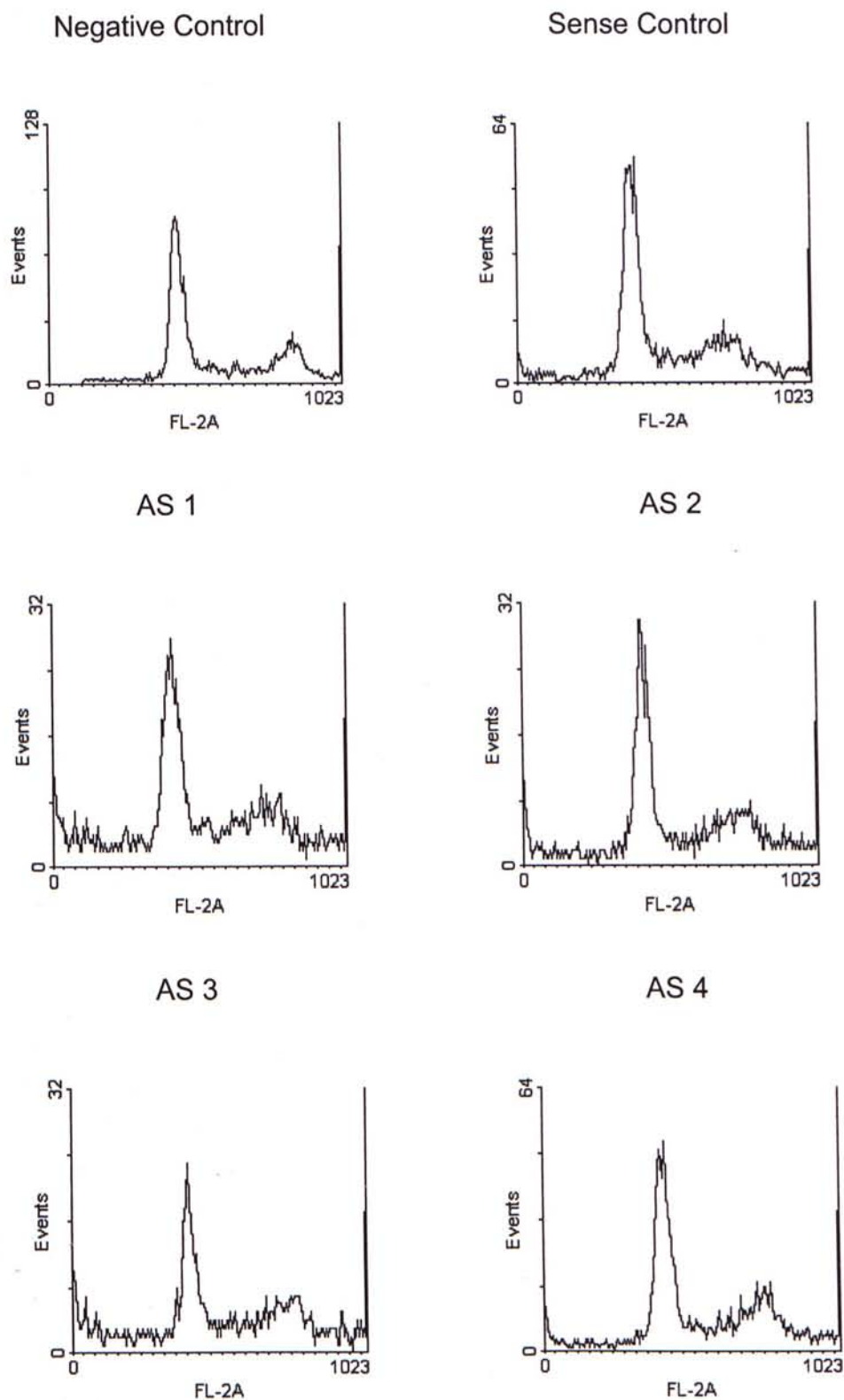


**Figure 3.12**

Cell cycle pattern of MCF-7 cells after AS 1-4 treatments, with respective  $IC_{50}$  concentrations, 72 hours post transfection. The procedure was described in section 2.2.10.1.

**Table 3.7**

The percentage distribution of G<sub>1</sub>, S, G<sub>2</sub>/M and Sub G<sub>1</sub> phase of MCF-7 cells after AS 1-4 treatments, with respective IC<sub>50</sub> concentration, 72 hours post transfection.

Phase	G <sub>1</sub>	S	G <sub>2</sub> /M	Sub G <sub>1</sub>
Negative control	48.73	15.63	16.05	1.92
Sense	50.28	14.56	16.67	4.28
AS 1	45.80	13.91	13.46	14.47
AS 2	45.98	14.4	14.92	12.70
AS 3	42.12	13.98	15.51	14.24
AS 4	48.35	14.73	13.54	8.56



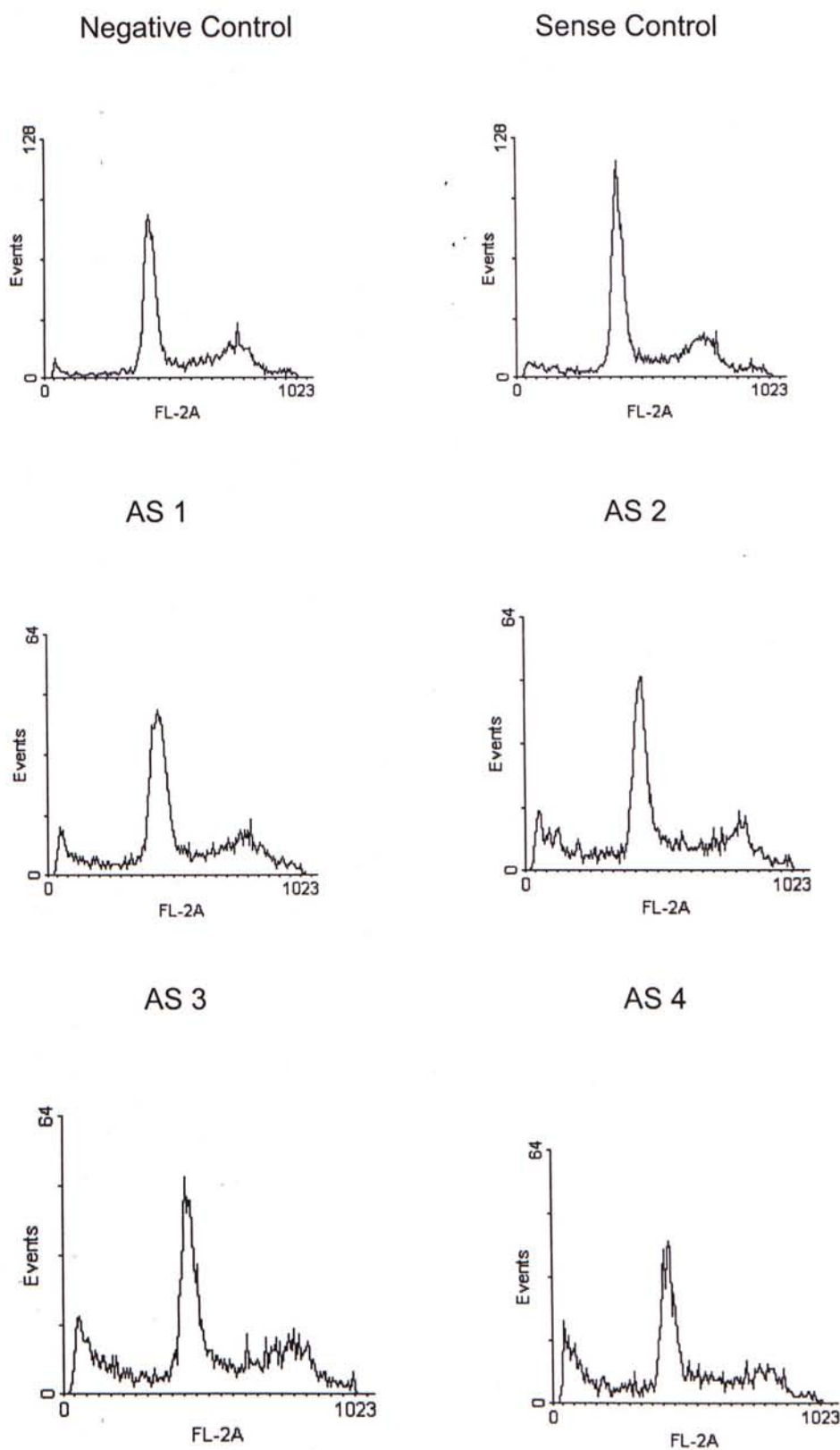


**Figure 3.13**

Cell cycle pattern of MDA-MB-231 cells after AS 1-4 treatments, with respective  $IC_{50}$  concentrations, 72 hours post transfection. The procedure was described in section 2.2.10.1.

**Table 3.8**

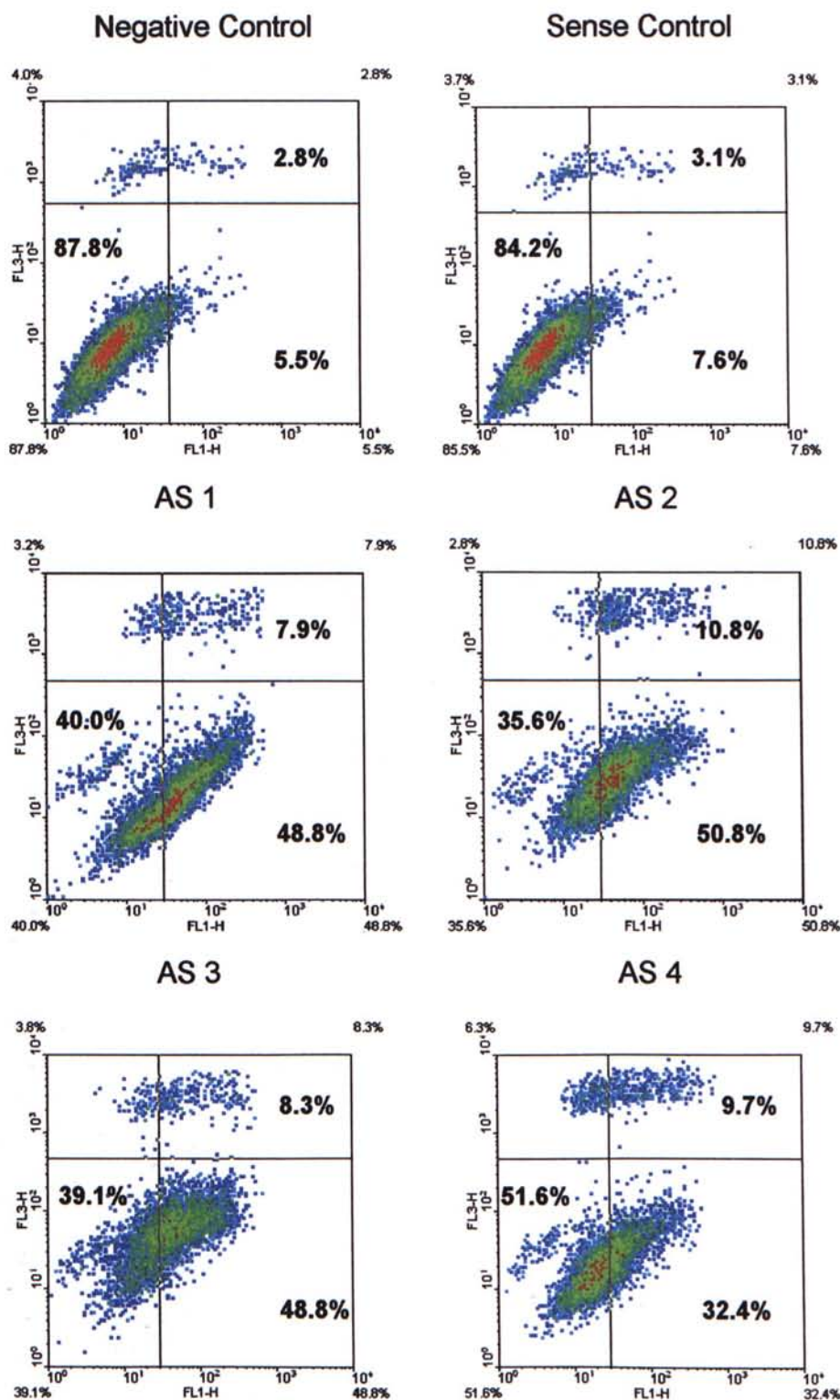
The percentage distribution of G<sub>1</sub>, S, G<sub>2</sub>/M and Sub G<sub>1</sub> phase of MDA-MB-231 cells after AS 1-4 treatments, with respective IC<sub>50</sub> concentration, 72 hours post transfection.

Phase	G <sub>1</sub>	S	G <sub>2</sub> /M	Sub G <sub>1</sub>
Negative control	53.85	11.57	22.06	3.02
Sense	54.63	11.22	20.93	3.72
AS 1	38.48	12.52	18.02	25.38
AS 2	37.49	11.57	15.44	30.52
AS 3	33.04	12.13	14.94	33.48
AS 4	32.58	12.72	16.06	31.48

### **3.1.8 Effect of Antisense Oligonucleotides against Glut 5 on Induction of Apoptosis of MCF-7 Cells and MDA-MB-231 Cells by Flow Cytometry, Using Annexin V-FITC Staining**

To investigate whether AS treatment to MCF-7 cells and MDA-MB-231 cells induce apoptosis, flow cytometry using Annexin V-FITC staining was performed. Annexin V is a specific phosphatidylserine (PS) binding protein, in which PS are normally found in the inner membrane of the plasma membrane and is externalized to the outer surface of the membrane during apoptosis. Annexin V is conjugated to FITC which emits green fluorescence and can be detected by FL-1 channel of the flow cytometer. At the same time, PI was used to identify the dead cells and detected by FL-3. Early apoptotic cells are annexin V positive but PI negative, while late apoptosis and necrosis cells are both annexin V and PI positive.

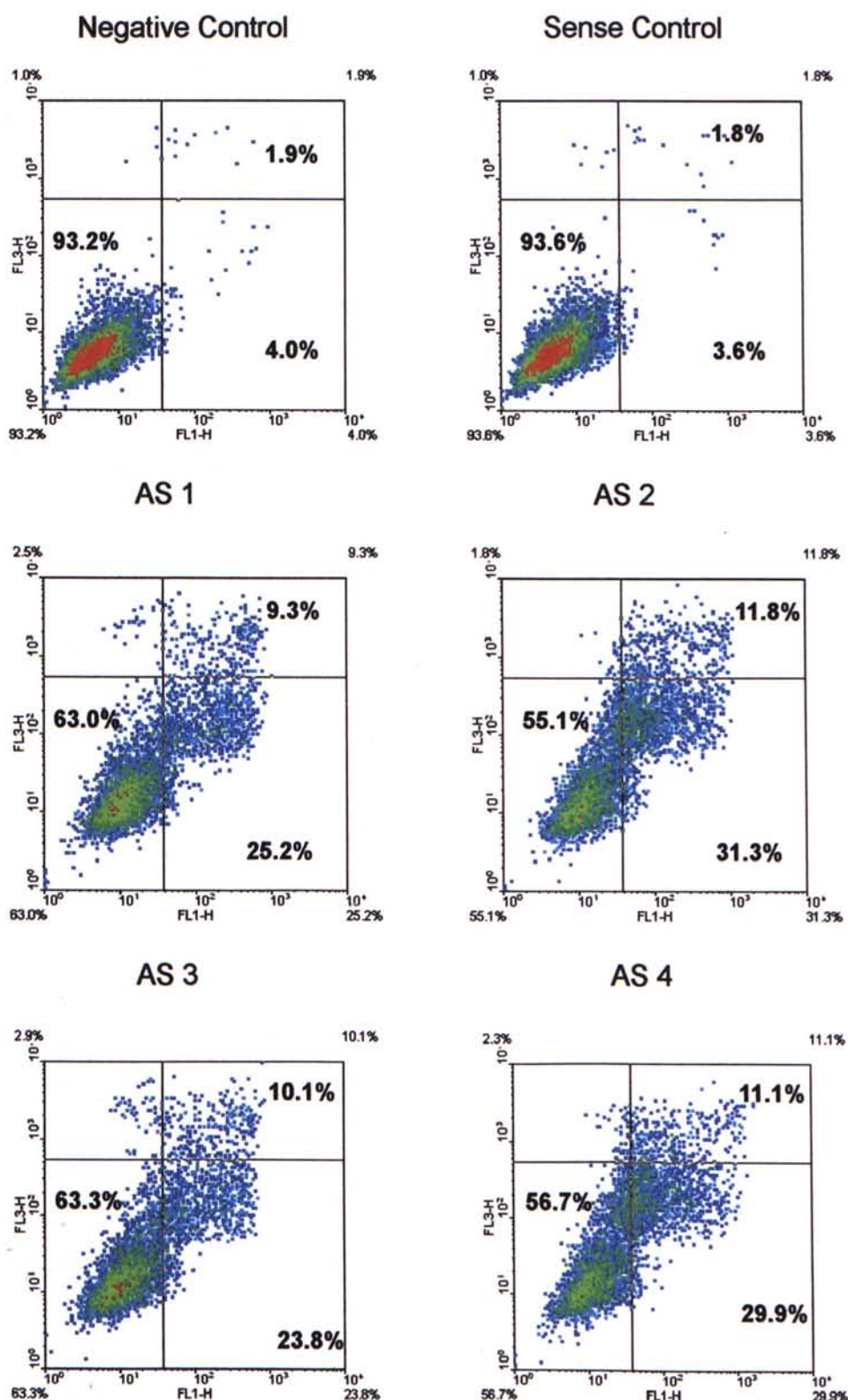
The detection of apoptosis and necrosis after AS 1-4 treatments with respective  $IC_{50}$  concentration, 72 hours post-transfection of MCF-7 cells and MDA-MB-231 cells were shown in Fig.3.14 and Fig.3.15. From the results, it suggested that all AS 1-4 induced apoptosis after 72 hours recovery for both cell lines.



**Figure 3.14**

Assessment of apoptosis and necrosis in MCF-7 cells, after AS 1-4 treatments with respective  $IC_{50}$  concentration, 72 hours post-transfection using Annexin V-FITC/PI. The procedure was described in section 2.2.10.2.



**Figure 3.15**

Assessment of apoptosis and necrosis in MDA-MB-231 cells, after AS 1-4 treatments with respective  $IC_{50}$  concentration, 72 hours post-transfection using Annexin V-FITC/PI. The procedure was described in section 2.2.10.2.

## **3.2 *In Vivo* Study**

### **3.2.1 Animal Model: Nude Mice**

Tumor bearing female nude mice, aged 4-6 weeks, were used as animal model. As the MCF-7 cells are dependent on estrogen for growth, a 0.72mg, 60-day releasing 17 $\beta$ -estradiol pellet (Innovative Research of America) was inoculated s.c. into the anterior part before inoculation of cancer cells. The establishment of tumor-bearing animal model and the treatment schedule in section 2.2.9 were followed.

### **3.2.2 Effect of Antisense Oligonucleotides against Glut 5 on the MCF-7 Cells-Bearing Nude Mice**

#### **3.2.2.1 Change of Body Weight of the Tumor-Bearing Nude Mice**

The weight of the tumor-bearing mice in all groups were recorded before each time of injection (Fig. 3.16, 3.17 & 3.18). First injection day was noted as Day 0. Data shown were mean $\pm$  S.D., n=10. From the results, the body weights of the mice remained quite constant during the whole treatment.

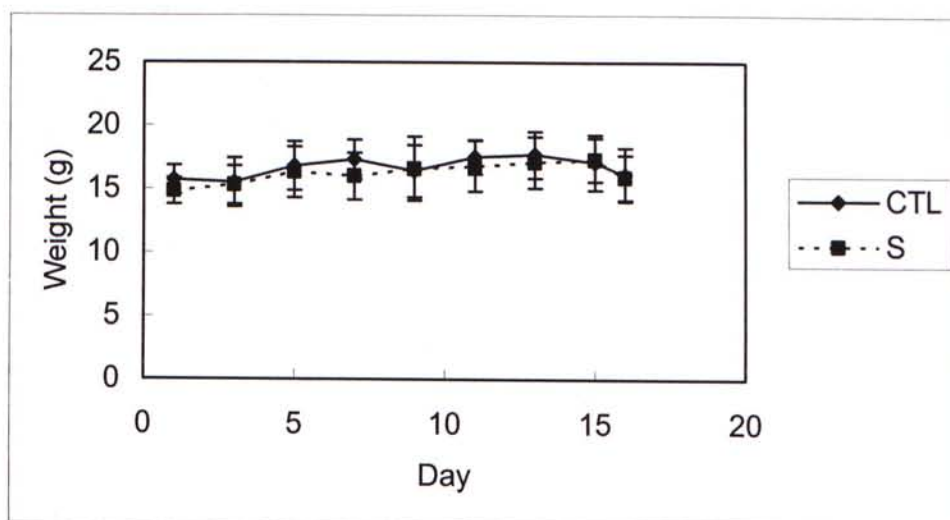


**Figure 3.16**

Effect of S against Glut 5 on the body weights of the MCF-7 cells-bearing nude mice. First injection day was noted as Day 0. Data shown were mean  $\pm$  S.D.,  $n=10$ .

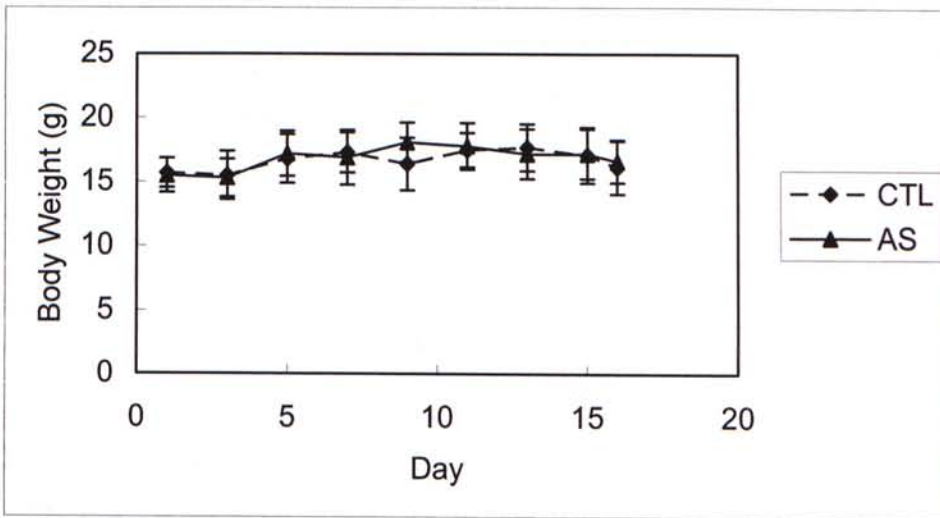


**Figure 3.17**

Effect of AS against Glut 5 on the body weights of the MCF-7 cells-bearing nude mice. First injection day was noted as Day 0. Data shown were mean  $\pm$  S.D., n=10.



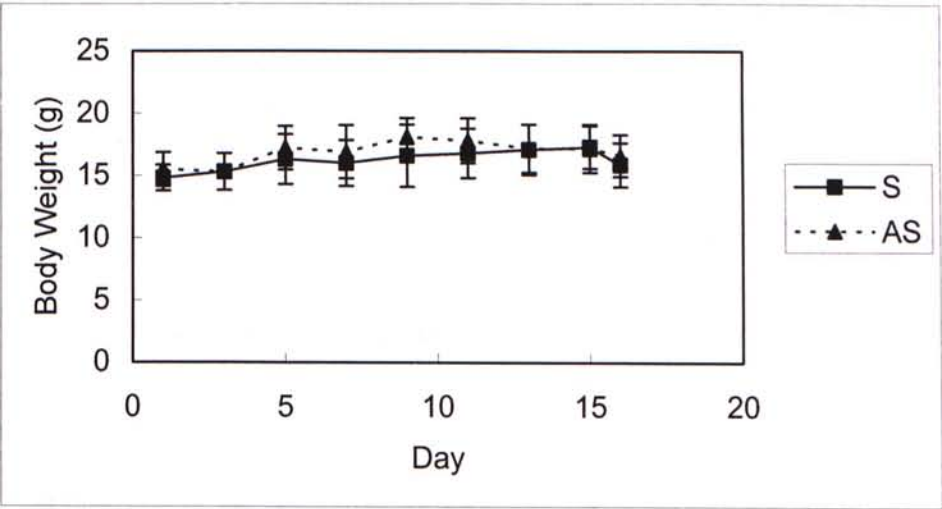


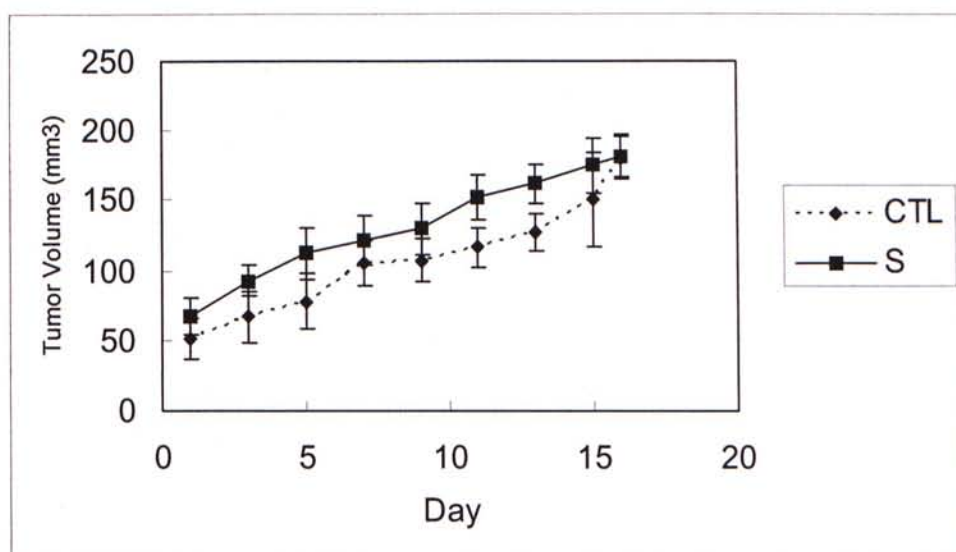
**Figure 3.18**  
Comparison of effect of S with AS on body weights of the MCF-7 cells-bearing nude mice. First injection day was noted as Day 0. Data shown were mean $\pm$  S.D., n=10.

### 3.2.2.2 Tumor Growth Rate

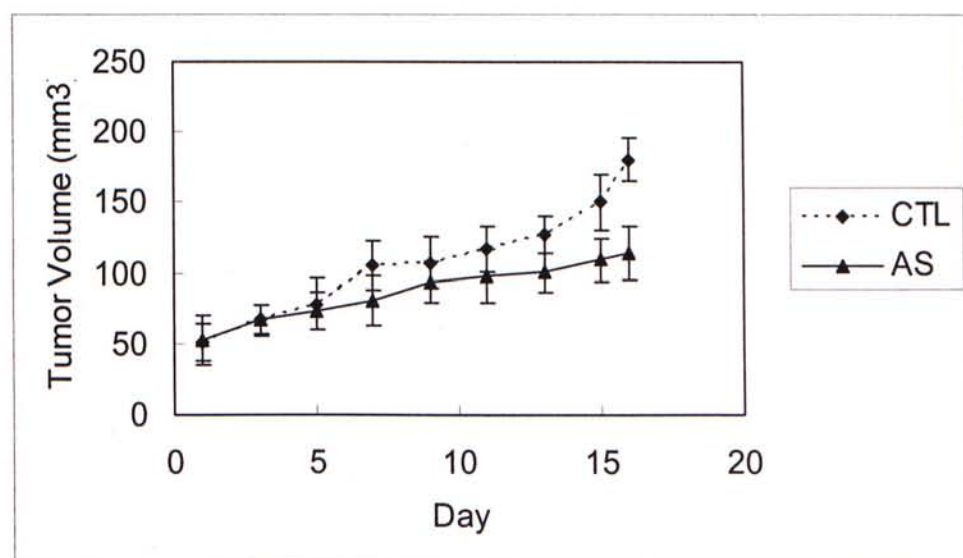
The tumor volume of the MCF-7 cells-bearing nude mice in all groups were recorded before each time of injection (Fig. 3.19 & 3.20). First injection day was noted as Day 0. Data shown were mean $\pm$  S.D., n=10. The growth rate of the tumor and percentage of inhibition of tumor growth was shown in Table 3.9.

After 8 doses, on day 16, the tumor-bearing mice were sacrificed and the tumor was excised. The tumor volume of each mouse in each group was recorded (Fig. 3.19 & 3.20).

From the results, it showed that after AS treatment, the tumor volume still increased progressively, but with less growth rate when compared with the sense control and PBS control. The percentage of inhibition of growth was tabulated in Table 3.9.



(A)



(B)

**Figure 3.19**

Effect of AS against Glut 5 on the tumor growth in the MCF-7 cells-bearing nude mice. The procedure was described in section 2.2.11. First injection day was noted as Day 0. Data shown were mean  $\pm$  S.D.,  $n=10$ . (Student's  $t$ -test:  $P<0.01$ ).

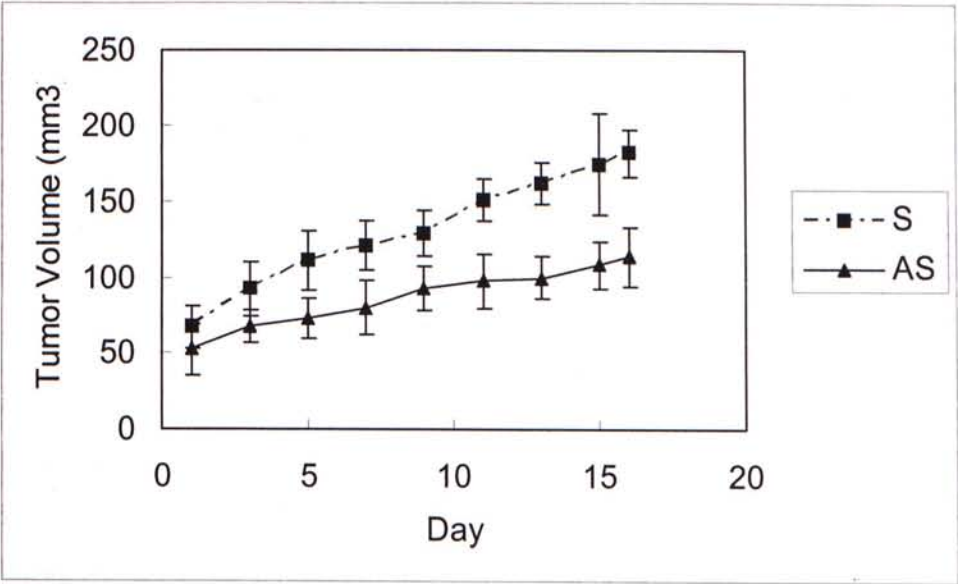


**Figure 3.20**  
Comparison of the tumor volume of AS treatment with S treatment in MCF-7 cells-bearing nude mice. First injection day was noted as Day 0. Data shown were the mean $\pm$  S.D., n=10. (Student's *t*-test:  $P<0.01$ ).

**Table 3.9**  
The growth rate of tumor in each group and percentage of inhibition on the growth of tumor in MCF-7 cells-bearing nude mice (with respect to PBS control).

	<b>Growth rate</b>  <b>(mm<sup>3</sup>/day)</b>	<b>% of inhibition</b>  <b>(Respect to PBS CTL)</b>
<b>PBS control</b>	7.4912	--
<b>Sense</b>	7.2187	-0.8%
<b>Antisense</b>	3.845	37%



### 3.2.2.3 Glut 5 RNA Expression by Real-Time PCR

The expression of Glut 5 RNA in the tumor was investigated using real-time PCR. Total RNA was extracted from the tumor homogenate obtained on day 16 and reverse transcribed to cDNA which is the template for the PCR. The  $C_T$  values of each group of mice with different treatments were tabulated in table 3.10. From the results, it showed that  $C_T$  values increased after AS treatment, when compared with that of the PBS control and sense control.

**Table 3.10**

Mean fold change of Glut 5 RNA expression from each group of MCF-7 cells-bearing mice with different treatments, by real time PCR. Data shown were mean  $\pm$  S.D., n = 3.

Treatment	Mean Fold Change
PBS CTL	1
Sense	1.131 $\pm$ 0.12
Antisense	0.495 $\pm$ 0.03

#### **3.2.2.4 Glut 5 Protein Expression by Western Blotting**

The Glut 5 protein expression level after AS treatment to the MCF-7 cells-bearing nude mice was investigated by Western blotting. Total protein was extracted from the tumor homogenate obtained on day 16, using the procedure in section 2.2.9. The Glut 5 protein expression level was shown in Fig. 3.21. As expected, the protein level was decreased with AS treatment, when compared with that of the PBS and sense control.

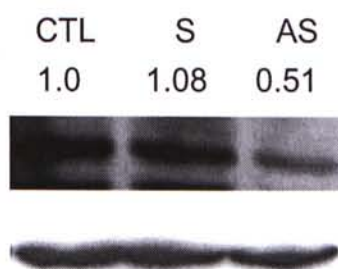


**Figure 3.21**

Protein expression of Glut 5 of each group of MCF-7 cells-bearing mice with different treatments.

### **3.2.3 Assessment of Side Effects of Antisense Oligonucleotides against Glut 5, by Measuring the Plasma Enzymes Level**

To assess the side effects of AS on the internal organs of MCF-7 cells-bearing nude mice, measurement of plasma enzymes activities can be used as the diagnostic tool. To detect heart damage, creatine kinase (CK) and lactate dehydrogenase (LD) can be used. To detect liver damage, aspartate transaminase (AST) and alanine transaminase (ALT) can be used. The tissue distribution of these enzymes is shown in table 3.11. These enzymes are normally absent or only small amount are present in the plasma. The increase in the plasma enzyme activities means that there is some damage of the corresponding tissues.



**Table 3.11**

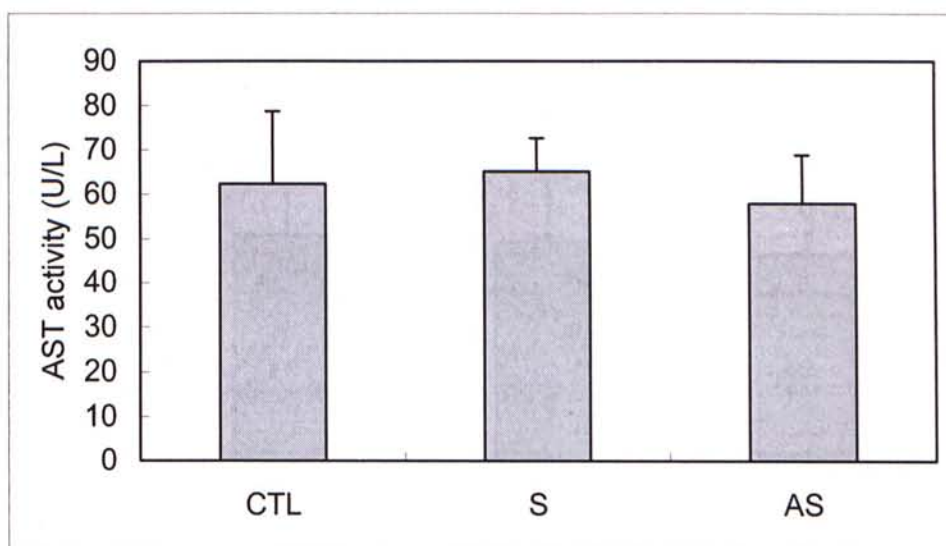
Tissue distribution in plasma of the AST, ALT, CK and LD.

<b>Enzyme</b>	<b>Tissue Distribution</b>
<b>AST</b>	Liver cells, cardiac cells, skeletal muscle and erythrocytes.
<b>ALT</b>	Large amount in liver, lesser extent in skeletal muscle, kidney and heart
<b>CK</b>	High concentration in cardiac cells, low concentration in skeletal muscle and in brain
<b>LD</b>	High concentration in cardiac cells, low concentration in skeletal muscle, liver, kidney, brain and erythrocytes

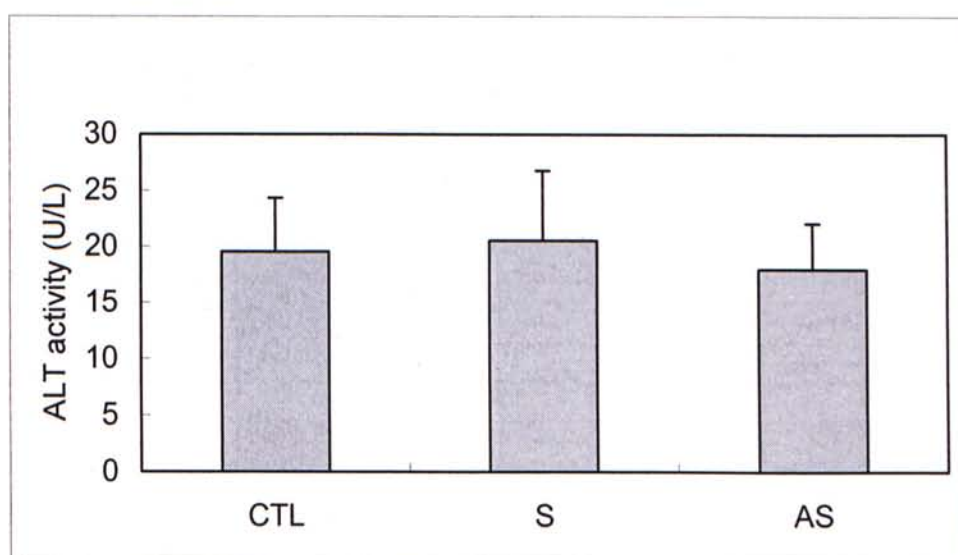
After AS treatment for 15 days, there was no significant change of AST & ALT activities in the plasma (Fig.3.22), when compared with that of the PBS control and sense control. This means that no liver damage was detected in the MCF-7 cells-bearing nude mice after AS treatment.

Similarly, there is no significant change of CK & LD activities in the plasma (Fig.3.23), when compared with that of the PBS control and sense control. This means that no heart damage was detected in these mice after AS treatment.

In addition, no death, hemolysis and gastrointestinal toxicity occurred in all groups.



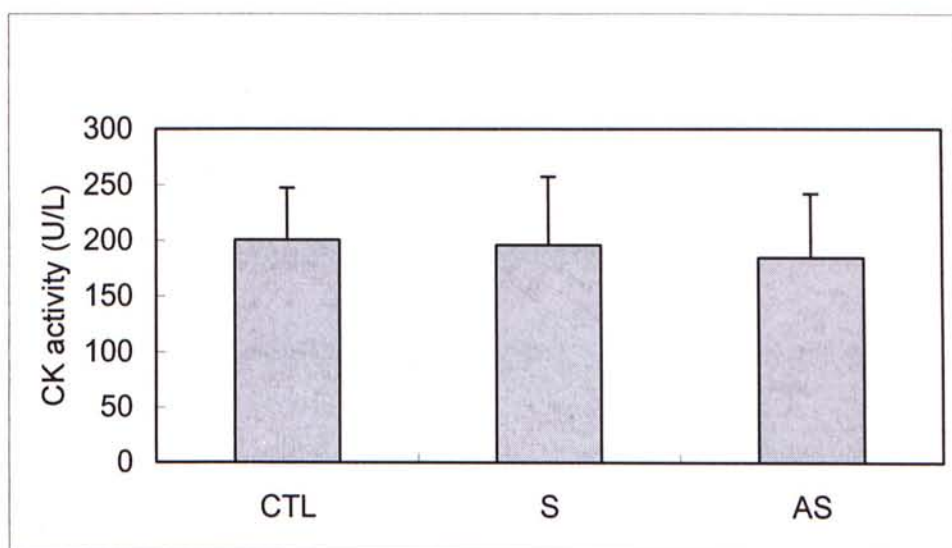
(A)



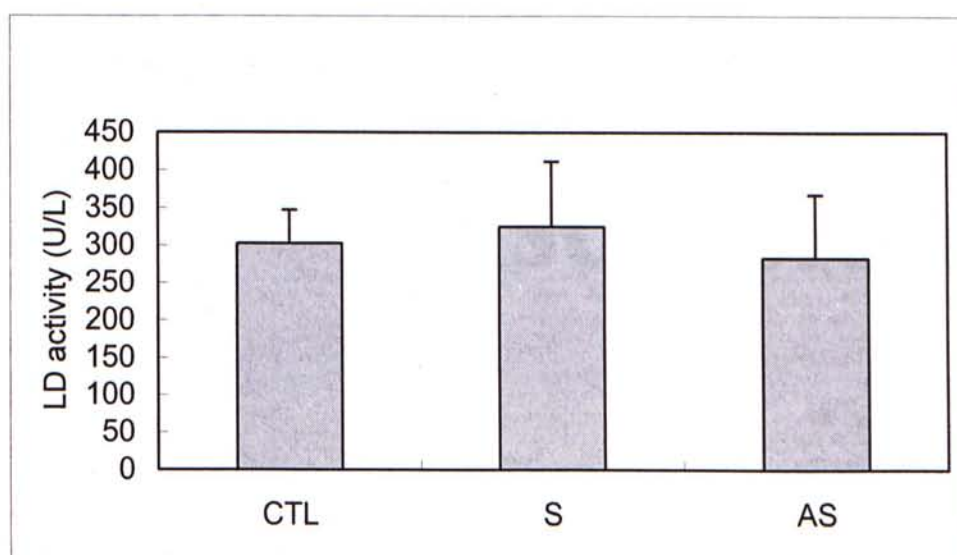
(B)

### Figure 3.22

Effect of AS on (A) AST, (B) ALT activities in the plasma of MCF-7 cells-bearing nude mice.  $1 \times 10^7$  MCF-7 cells in 0.1ml PBS was inoculated into the nude mice s.c. and allowed to grow until the tumor size reached about  $50\text{mm}^3$ . Treatment was started by injecting 20mg/kg/day of oligonucleotides adjacent to the tumor in each nude mice for 8 doses, every other day. For PBS-control group, 0.1ml of PBS was injected. The drugs were administrated into the tumor-bearing mice s.c., with constant volume of 0.1ml/mouse/injection. After 8 doses, the mice were sacrificed and the plasma was collected to perform enzyme assays. Data shown were mean  $\pm$  S.D.,  $n=10$ . (Student's  $t$ -test:  $P < 0.01$ ).



(A)



(B)

**Figure 3.23**

Effect of AS on (A) CK (B) LD activities in the plasma of MCF-7 cells-bearing nude mice. bearing nude mice.  $1 \times 10^7$  MCF-7 cells in 0.1ml PBS was inoculated into the nude mice s.c. and allowed to grow until the tumor size reached about  $50\text{mm}^3$ . Treatment was started by injecting 20mg/kg/day of oligonucleotides adjacent to the tumor in each nude mice for 8 doses, every other day. For PBS-control group, 0.1ml of PBS was injected. The drugs were administrated into the tumor-bearing mice s.c., with constant volume of 0.1ml/mouse/injection. After 8 doses, the mice were sacrificed and the plasma was collected to perform enzyme assays. Data shown were mean  $\pm$  S.D.,  $n=10$ . (Student's  $t$ -test:  $P < 0.01$ ).

# **Chapter 4**

## **Discussion**



## **4.1 Antisense Oligonucleotides against Glut 5 on Human Breast Cancer**

### **4.1.1 Antisense Oligonucleotides Strategy**

Antisense oligonucleotides provide a simple and efficient approach for developing highly specific drugs, as they can alter the gene expression sequence specifically. It is very useful to treat any diseases in which the disease causing genes have been identified. Once the disease causing genes, or genes related to growth of the disease have been defined, antisense oligonucleotides can be designed against the genes and alter the gene expression specifically.

There are many genes related to the development and growth of the cancer. For example, insulin-like-growth factors (IGFs) (Muti *et al.*, 2002) and glucose transporters (Gluts) (Chen *et al.*, 2002) are found to contribute to breast cancer development. If we use AS to alter the expression of these genes, it will lead to a change in a cascade of events, and finally causing anti-proliferative or cytotoxic effect on the cancer. Some findings suggested that AS against Glut 1 was effective in causing cytotoxic effect on MCF-7 and HepG-2 cells (Chen *et al.*, 2002).

The sequence selection is a critical factor in designing antisense oligonucleotides. Some studies suggested that phosphorothioated oligonucleotides (PS-Oligo) containing CpG motifs have immunostimulatory activity (Vollmer *et al.*,

2004). Also, the presence of secondary structures can interfere with antisense activity by allowing the AS to bind to unintended protein targets. AS is not easy to be designed and not as simple as designing primers for other assays, e.g. PCR reactions. Target site selection, choice of oligonucleotide sequences, chemical modification, minimization of protein binding and other competing factors should be addressed when designing the AS (Agrawal and Kandimalla, 2000). There are several limitations of using AS. The stability *in vivo* is the major problem. Ideally, it should be resistant to enzymes degradation, should induce RNase H activity, without altering the affinity for target gene and the specificity. To enhance the stability of the AS, modifications can be made (Section 1.3.4, Fig. 1.7). At the moment, there is no such modification that can fit the above criteria. The cost of using AS for therapeutic use is high. Although the AS with phosphorothioation at each base to enhance the stability, is commercially available, it is expensive.

The cellular uptake is another problem of AS strategy. Using cationic lipid as carrier system can improve the cellular uptake. Also, cationic, cell-penetrating peptide conjugated to the AS can enhance the membrane permeability and the resistance to nucleases. The peptide is 6-30 amino acids in length and linked to a 24-mer AS. The naked oligonucleotides are extensively taken up across the mammalian plasma membranes in a non-endocytic manner. It does not induce the

immune response *in vivo* (Oehlke *et al.*, 2002).

Although there are many limitations of AS strategy, AS is still an effective approach in down regulating the target gene expression in a sequence specific manner.

Antisense technology composed of different kinds, e.g. antisense DNA, siRNA and PNA, etc. Antisense DNA is single-stranded, negatively charged and complementary to the target gene. It triggers RNase H or steric blocking of ribosomes at some selected sequence of the mRNA. siRNA composed of small double-stranded RNA oligonucleotides with overhanging extremities and a length of 21/22 bases. It is the substrate of a natural intracellular protein complex called RNAi induced silencing complex (RISC), and can performing post-transcriptional gene silencing in mammalian cells (Hammond *et al.*, 2000). The gene silencing mechanism is totally different from that of antisense DNA. PNA is a nucleic acid mimic in which the deoxyribose phosphate backbone has been replaced by a peptide polymer to which the bases are linked (Larsen *et al.*, 1999). It is chemically related to DNA. The gene silencing mechanism is similar to that of antisense DNA.

In this project, antisense DNA was used. Antisense DNA is easily synthesized. A large variety of modifications can improve the stability, membrane permeability and the mode of action. It provides transient antisense effect to the cells.



Therefore, antisense DNA is suitable for inhibition of gene expression. 15 base pairs oligonucleotide was chosen. From previous study by our colleague Mr. Chan KK, it showed that 15 mer oligonucleotide was more efficient when compared with 21 mer, because of its shorter length. The uptake was increased from at least 2 folds in MCF-7 cells to 53 folds in MDA-MB-231 cells (The thesis of Chan KK, 2000). If shorter oligonucleotide was used, e.g. 6-12 mer, the specificity was decreased. The short oligonucleotide can bind to many important genes and this may affect the functions of our body. Since, statistically, the minimum number of nucleotides that occurs just once in the human genome is, on average, 13 (Alama *et al.*, 1997). Thus, 15 mer oligonucleotide is the best choice and should be able to bind selectively to a unique RNA species in cells.

#### 4.1.2 Role of Glut 5 in Breast Cancer

Glut 5 is expressed in the intestine and sperm, etc. Glut 5 helps in the entry of fructose into the cells and provide energy to support their high metabolic rate in addition to glucose. Fructose is phosphorylated on C-1 by fructokinase yielding fructose-1-phosphate (F1P). F1P is then converted to dihydroxyacetone phosphate (DHAP) and glyceraldehyde. The DHAP is converted, by triose phosphate isomerase, to glyceraldehyde-3 phosphate (G3P) and enters glycolysis. The glyceraldehyde can be phosphorylated to G3P by glyceraldehyde kinase. DHAP and G3P can then enter glycolysis (Elliott *et al.*, 2002).

Cancer cells exhibit enhanced rates of glycolysis when compared with normal cells (Warberg, 1956). The enhanced metabolic rate is supported by increased uptake of glucose or other hexoses. The hexoses enter cells via Gluts. It was found that Glut 1, 2, 4 and 5 were expressed in the breast cancer cells (Zamora-Leon *et al.*, 1996). The role of Glut 1 in human breast cancer has been studied extensively (Grover-McKay *et al.*, 1998, Laudanski *et al.*, 2003), but the role of Glut 5 in breast cancer has not been well studied. The only paper concerning Glut 5 in breast cancer was by Zamora-Leon *et al.* (1996). Therefore, it is a challenging task to study Glut 5 in breast cancer.

As mentioned in previous part, only Glut 5, also called fructose transporter,



was highly expressed in breast cancer cells, but absent in normal breast cells (Zamora-Leon *et al.*, 1996). Glut 5 exhibits selectivity for fructose transport, with a  $K_m$  of 6mM. In addition, fructose transport was not inhibited by cytochalasin B, a competitive inhibitor of glucose transporters (Tatibouet *et al.*, 2000). The result suggested that Glut 5 did not possess specificity toward glucose.

The expression of Glut 5 mRNA and protein are regulated by the fructose uptake by the cells. As mentioned before, the energy requirement of breast cancer cells is high because of their high metabolic rate. They do not fully utilize the glucose entered. The catabolism of glucose stops after glycolysis. Thus, small amount of energy is released by each glucose molecule. The presence of Glut 5 is important because this enables breast cancer cells to have a specialized ability to transport fructose, in which fructose is a metabolic substrate used by only a few human tissues. So, breast cancer cells can get more metabolic substrate, in addition to glucose, in meeting their energy requirements. Although the physiological concentration of fructose is low (50-200 $\mu$ mol/L) (Shiota *et al.*, 2002), fructose still has important physiological role for providing energy to the breast cancer cells. From my previous study, in the supply of different concentration of fructose, both cell lines grew in a dose dependent manner (Data not shown in the thesis). This can show that the growth of both MCF-7 cells and MDA-MB-231 cells depend on the

supply of fructose. During breast cancer development, the expression level of Glut 5 increased in breast cancer cells. It was observed from the cell lines MCF-7 cells and MDA-MD-231 cells (Fig.1.10). MCF-7 cells mimic the early stage of breast cancer, which is estrogen dependent and MDA-MB-231 cells mimic the late stage of breast cancer.

### 4.1.3 Effects of Tamoxifen on MCF-7 cells and MDA-MB-231 cells

Tamoxifen is the most common anti-cancer drug for treating breast cancer. It has been used for more than 20 years. The cytotoxic effects of tamoxifen on MCF-7 cell line and MDA-MB-231 cell line were investigated using MTT assay (Fig. 3.1). After 48 or 72 hour incubation, the  $IC_{50}$  of tamoxifen on MCF-7 cells were 15 $\mu$ M and 12.5 $\mu$ M respectively. For MDA-MB-231 cells, the  $IC_{50}$  of tamoxifen were 40 $\mu$ M and 35 $\mu$ M respectively.

From the results, it showed that tamoxifen is more effective in treating MCF-7 cell line, which is an ER-positive cell line and mimics the early stage of breast cancer, than MDA-MB-231 cell line, which is an ER-negative cell line and mimics the late stage of breast cancer. The results are not surprising as tamoxifen exerts its action through the estrogen receptor (ER). It acts as a competitive inhibitor of the estrogen. If the dosage is too high, it may cause many side effects e.g. occurrence of hot flashes, increase risk of endometrial cancer and thromboembolic disease, etc. Also, many tumors eventually become resistant to treatment with tamoxifen (Sainsbury, 2004). The possible causes of tamoxifen resistance are absence or loss of ER, mutant ER, tamoxifen-stimulated growth of tumor and cross-talk among growth factor signaling pathways (Osborne, 1998).

## 4.2 *In Vitro* Study of Antisense Oligonucleotides against Glut 5 on Breast Cancer Cells

The cytotoxic effects of AS 1 to AS 4, flanking different regions of the Glut 5 mRNA, were investigated by MTT assay. Sense sequence was complementary to AS 1, which flanking around the start codon. It was used to illustrate the non-specific effect. The non-specific effect was mainly due to the binding of sense sequence to some intracellular proteins in a sequence-independent manner. This would be toxic to the cells (Wagner, 1994). The cytotoxicity to MCF-7 cells and MDA-MB-231 cells of sense oligonucleotides increased when high concentrations were used. From the results, it showed that AS 1-4 against Glut 5 caused cytotoxic effect to MCF-7 cells and MDA-MB-231 cells in dose dependent manner, 72-hour post transfection. On MCF-7 cells, the  $IC_{50}$  of AS 1, AS 2, AS 3 and AS 4 were 220nM, 190nM, 300nM and 220nM, respectively. AS 2 is the most effective one in killing MCF-7 cells. On MDA-MB-231 cells, the  $IC_{50}$  of AS 1, AS 2, AS 3 and AS 4 were 410nM, 400nM, 400nM and 470nM, respectively. Both AS 2 and AS 3 are effective in killing MDA-MB-231 cells. In conclusion, AS 2 is the most effective antisense oligonucleotide. AS 2 is complementary to the coding region near 5' end. AS 2 was chosen to be used in *in vivo* study. The difference of  $IC_{50}$  in treating different cell lines was due to the fact that the expression level of Glut 5 is different in these two



cell lines (Fig.1.10). It is now known that MDA-MB-231 cells have more Glut 5 than that of MCF-7 cells (Zamora-Leon *et al.*, 1996). This means targeting Glut 5 by antisense oligonucleotide can be used for treating all stages of breast cancer.

The incubation time after transfection was chosen to be 72 hours (3 days). The oligonucleotides started to degrade after 72 hours *in vitro* (Crooke *et al.*, 1995). Therefore, the antisense effects should be detected before 72 hours.

MDA-MB-231 cells expresses more Glut 5 when compared with MCF-7 cells. Thus, it is reasonable to use a higher concentration of AS to cause 50% cytotoxicity. Although the concentration of AS used to cause 50% cytotoxicity was high in MDA-MB-231 cells, the concentration was still low when compared with using tamoxifen by 100 folds. As mentioned in previous part, the  $IC_{50}$  of tamoxifen in treating MCF-7 cells and MDA-MB-231 cells were 12.5 $\mu$ M and 35 $\mu$ M, respectively. Also, tamoxifen causes a lot of side effects. Therefore, AS is more effective in treating both early stage (estrogen responsive) and late stage (estrogen irresponsive) breast cancer. The probable side effects of AS were investigated *in vivo* and will be discussed in latter part of this thesis.

Glut 5 is responsible for transporting fructose. We hypothesized that AS against Glut 5 can down-regulate the gene expression of Glut 5 and affect the fructose uptake. Therefore, the effect of AS against Glut 5 on fructose uptake was



investigated. Also, glucose uptake was tested to see whether the glucose uptake is affected, using the 2-deoxy-D-[1-<sup>3</sup>H] glucose uptake assay. This can test the specificity of AS. If the AS is only specific for Glut 5, the glucose uptake should not be affected.

From the result, after AS 1-4 treatments with respective IC<sub>50</sub> concentration, the D-[U<sup>14</sup>C]-fructose uptake in MCF-7 cells were decreased when compared with the negative control and the sense control, after 72 hours of transfection (Fig. 3.7A). For MDA-MB-231 cells, a similar result was obtained (Fig. 3.7B). This suggested that the Glut 5 expression may be reduced and contributed to the decrease of D-[U<sup>14</sup>C]-fructose uptake.

For 2-deoxy-D-[1-<sup>3</sup>H] glucose uptake, after AS 1-4 treatments with respective IC<sub>50</sub> concentration, the 2-deoxy-D-[1-<sup>3</sup>H] glucose was not changed in both cell lines after 72 hours post transfection (Fig. 3.8). This implied that AS against Glut 5 was only specific to Glut 5, but not the other isoforms. Also, the decrease in fructose uptake did not cause an increase in glucose transport for compensation.

Glut 5 is highly expressed in breast cancer cells, but absent in normal breast cells. This finding indicated that breast cancer cells may have a specialized capacity to transport fructose which is a rare metabolic substrate to be used by only a few

human tissues. If fructose is the metabolic substrate for the breast cancer cells, after the inhibition of fructose uptake, the ATP content in the cells should be changed. Therefore, intracellular ATP assay was done to investigate the effect of AS on the breast cancer cells.

From the result, it showed that the intracellular ATP content decreased after AS 1-4 treatments with respective  $IC_{50}$  concentration, 72 hours post-transfection, in both cell lines. The percentage of reduction was about 30-40%. This suggested that AS against Glut 5 can inhibit the fructose uptake and reduce the catabolism of fructose to release ATP. Fructose may be the major metabolic substrate of breast cancer cells.

As mentioned before, the percentage of reduction of ATP content was about 30-40%, but it contributed to about 50% of cytotoxicity, as  $IC_{50}$  concentration were used. So, we speculated that Glut 5 may have functions other than transporting fructose, just like Glut 1 and Glut 3 can transport glucose and the metabolite of ascorbic acids (Rumsey *et al.*, 1997). Glut 1 can also transport D-mannose, water (Fischbarg *et al.*, 1990, Gould *et al.*, 1991), galactose (Takakura *et al.*, 1991) and glucosamine (Uldry *et al.*, 2002). Further investigation is needed to confirm this hypothesis.

Theoretically, AS can suppress the target gene expression in both

transcriptional and translational levels. To investigate whether AS against Glut 5 can suppress the Glut 5 mRNA level, traditional RT-PCR was performed to find out the amount of Glut 5 mRNA expression at the end-point. This can only provide the preliminary result. It would be further confirmed by real-time PCR. Real time PCR collects data in the exponential growth phase. The increase in reporter fluorescent signals is directly proportional to the number of amplicons generated. This is a more effective and accurate approach to detect the RNA expression.

We hypothesized that the reduction of fructose uptake and intracellular ATP content were accompanied by the reduction of Glut 5 mRNA and protein expression. Therefore, RT-PCR and Western blot analysis were done to test this hypothesis.

The results of traditional and real-time PCR showed that in both cell lines, there was down-regulation (~40-50%) of Glut 5 RNA after AS treatment with  $IC_{50}$  concentration, 72 hour post-transfection, when compared with the negative control. From the result of Western blot analysis, the Glut 5 protein level was decreased after AS treatment. These results suggested that the AS against Glut 5 can cause gene silencing by either inhibition of the transcription of target gene by DNA triplex formation, degradation of Glut 5 mRNA by RNase H or inhibition of translation by steric blocking which prevents ribosome from approaching the mRNA.

In the previous part, it can be shown that AS against Glut 5 possessed an



anti-tumor effect on breast cancer cell lines. The mechanism of the anti-tumor effect was investigated by flow cytometry. Propidium iodide (PI) was used to detect the change in cell cycle pattern. PI is the most common dye to assess the DNA content quantitatively. PI binds to DNA and emits red fluorescence and detected by flow cytometer FL-2 channel. We can estimate the percentage of cells in sub G<sub>1</sub>, G<sub>1</sub>, S and G<sub>2</sub>/M phases using a computer program WinMDI. Many anti-tumor drugs inhibit the growth of cancer cells by disturbing the cell cycle, causing cell cycle arrest in G<sub>1</sub> phase, e.g. tamoxifen blocks the transition from G<sub>1</sub> to S phase (Lykkesfeldt *et al.*, 1984).

From the results, it was found that there was no accumulation of cell population in G<sub>1</sub>, S and G<sub>2</sub>/M phase, but in sub G<sub>1</sub> phase (Fig. 3.12 and table 3.7). For MDA-MB-231 cells, similar results were obtained (Fig. 3.13 and table 3.8). For both cell lines, no cell cycle arrest was observed in all treatments, but there might be occurrence of apoptosis, as there was an accumulation of cells in sub G<sub>1</sub> phase. Apoptosis is programmed cell death which involved a cascade of events and signal transduction. Therefore, annexin V-FITC dye was used to find out whether apoptosis has occurred after AS treatment. Annexin V is a specific phosphatidylserine (PS) binding protein, in which PS are normally found in the inner membrane of the plasma membrane and is externalized to the outer surface of the membrane during

apoptosis. Annexin V is conjugated to FITC which emits green fluorescence and is detected by FL-1 channel of the flow cytometer. At the same time, PI was used to identify the dead cells and detected by FL-3. Early apoptotic cells are annexin V positive but PI negative, while late apoptosis and necrosis cells are both annexin V and PI positive. From the result, it suggested that all AS induced apoptosis after 72 hour recovery in both cell lines. Apoptosis resulted from nutrient deprivation, which may then induce activation of signal transduction, e.g. kinases like mitogen activation protein kinase (MAPK), c-Jun, etc., change in the redox state of the cell, or generation of free radicals (Aft *et al.*, 2002).

When compare the results of PI staining with annexin V-FITC staining, it was found that the percentage of cells present in sub G<sub>1</sub> phase in all AS treated cell lines was lower than that of early apoptotic phase in annexin V-FITC staining. As mentioned in previous part, PI stains DNA and sub G<sub>1</sub> phase represents cells present in late apoptotic in which the DNA was fragmented by the action of caspase 3. Caspase 3 is a key factor for initiation of DNA fragmentation. MCF-7 cells do not express caspase 3 gene (Kurokawa *et al.*, 1999). Therefore, DNA fragmentation was not detected during apoptosis, but still have PS externalization. Thus, it gave a little signal in sub G<sub>1</sub> phase (~10%) in PI staining, and high cell population in annexin V-FITC staining (~45%). MDA-MB-231 cells express caspase 3 (Yang *et al.*, 2003)



and DNA fragmentation occurs during apoptosis. Thus the percentages of cells present in sub G<sub>1</sub> phase in PI staining after AS treatment were similar in the early apoptotic phase in annexin V-staining.

### **4.3 *In Vivo* Study of Antisense Oligonucleotides against Glut 5 on Breast Cancer**

The effects of antisense oligonucleotides (AS) against Glut 5 have been tested *in vitro* and the result was encouraging. The probable side effects of AS should be investigated before clinical trial. Therefore, *in vivo* study was conducted to assess the effect of AS and the probable side effects to the internal organs of the MCF-7 cells-bearing nude mice.

Breast cancer is a solid tumor formed under the skin in breast. Drug can be directly injected adjacent to the tumor. This is more effective than intravenous (i.v.) injection as the AS would degrade rapidly in the bloodstream. Direct transmission of DNA into the tumor has proved to be feasible and safe at reducing tumor growth in experimental procedure in mice (Nable *et al.*, 1993).

Previous studies of the effect of tamoxifen on MCF-7 cells-bearing nude mice showed that it caused transient stimulation of tumor growth, followed by a prolonged stationary phase. The growth of tumor resumed. Growth inhibition was also observed with anti-estrogens and was dose dependent. The hormone-independent MDA-MB-231 cells were not influenced by anti-estrogen treatment. Endocrine therapy by anti-estrogen treatment inhibits tumor cell proliferation in nude mice, but does not cause tumor regression or loss of cell

### 4.3 *In Vivo* Study of Antisense Oligonucleotides against Glut 5 on Breast Cancer

The effects of antisense oligonucleotides (AS) against Glut 5 have been tested *in vitro* and the result was encouraging. The probable side effects of AS should be investigated before clinical trial. Therefore, *in vivo* study was conducted to assess the effect of AS and the probable side effects to the internal organs of the MCF-7 cells-bearing nude mice.

Breast cancer is a solid tumor formed under the skin in breast. Drug can be directly injected adjacent to the tumor. This is more effective than intravenous (i.v.) injection as the AS would degrade rapidly in the bloodstream. Direct transmission of DNA into the tumor has proved to be feasible and safe at reducing tumor growth in experimental procedure in mice (Nable *et al.*, 1993).

Previous studies of the effect of tamoxifen on MCF-7 cells-bearing nude mice showed that it caused transient stimulation of tumor growth, followed by a prolonged stationary phase. The growth of tumor resumed. Growth inhibition was also observed with anti-estrogens and was dose dependent. The hormone-independent MDA-MB-231 cells were not influenced by anti-estrogen treatment. Endocrine therapy by anti-estrogen treatment inhibits tumor cell proliferation in nude mice, but does not cause tumor regression or loss of cell

viability (Osborne *et al.*, 1985).

In the experiment, female nude mice were used, because their immune system is defective. The inoculation of human tumor cells will not cause any immune response to reject the xenograft. MCF-7 cells were inoculated into their back with a 60-day releasing  $17\beta$ -estradiol pellet to support its growth. The tumor cells were allowed to grow until a solid tumor was formed. The initial size of tumor was about  $50\text{mm}^3$ .

### **4.3.1 Effects of Antisense Oligonucleotides against Glut 5 on Body Weight and Tumor Size**

The effects of AS against Glut 5 on the body weight and tumor size of MCF-7 cells-bearing nude mice were investigated. We have demonstrated that the anti-tumor effect of AS against Glut 5 on tumor growth was due to specific antisense effect. Because there was no abrogation of tumor proliferation in any of the control groups.

After the injection of AS, it was absorbed and circulated in the bloodstream. The half-life is about 40-60 hours (Crooke *et al.*, 1994). This is the reason why the AS was injected in alternative days, but not in consecutive days. Plasma clearance of AS is rapid, broad tissue distribution occurs, and elimination is by nuclease metabolism. Metabolism is mediated by exo- and endonucleases that result in shorter oligonucleotides and nucleosides that are degraded by normal metabolic pathways (Crooke, 2004). A literature review suggested that in monkeys, rodents, and dogs, there was accumulation of AS and metabolites occurs in the form of basophilic granules in various tissues, including the kidney, lymph nodes and liver (Farman and Kornbrust, 2003), with the liver accumulating most rapidly.

The body weights of the mice were measured before each dose and it remained quite constant throughout the experiment. There was no significant change



of body weight with AS treatment when compared with the PBS and sense control.

For the tumor size, it was measured before each injection. The tumor in all group of mice grew progressively, but with less growth rate in AS treated group. The growth rate of PBS, sense control and AS treated groups were 7.4912, 7.2187 and 3.845 mm<sup>3</sup>/day respectively. The result showed that AS against Glut 5 is effective in treating breast cancer *in vivo*. Further investigation should be done on the mechanism, clearance of AS *in vivo*. Also, higher doses should be used to test whether AS is effective in a dose-dependent manner.

#### **4.3.2 Expression Level of Glut 5 of the Tumor**

The Glut 5 expression level was investigated using real-time PCR and Western blot analysis. From the result, it showed that after the injection of AS, the Glut 5 RNA and protein level decreased. This suggested that AS against Glut 5 can block the transcription and translation of Glut 5. The reduction of Glut 5 expression leads to decrease of fructose uptake or probably other important essential substrates for growth. Then, cell death occurred because of lack of nutrients (Fig. 4.1).

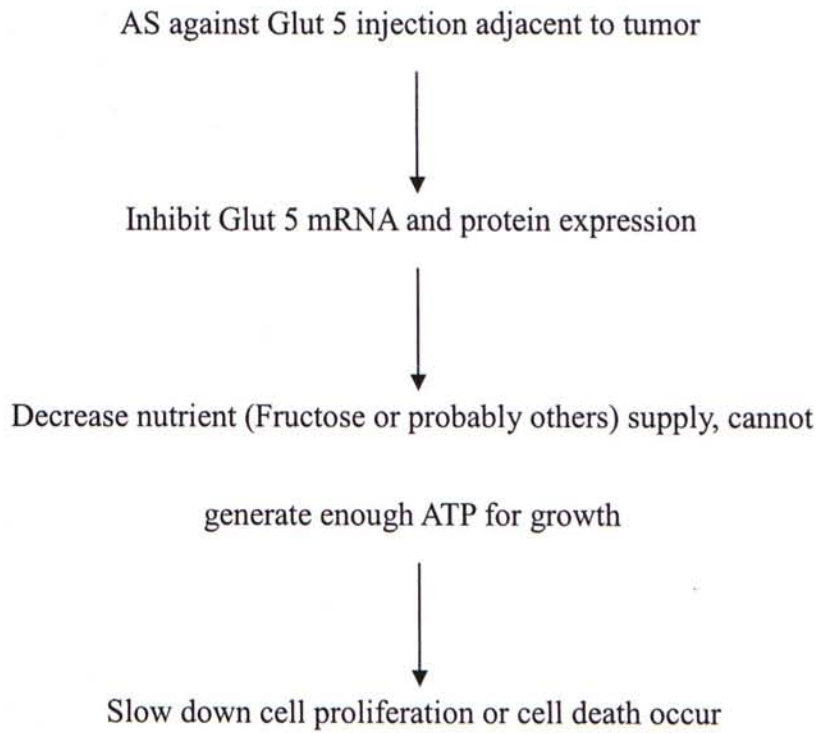


Figure 4.1

Flow chart of consequences of antisense oligonucleotides against Glut 5 treatment to MCF-7 cells-bearing nude mice.

### **4.3.3 Assessment of Side Effects of Antisense Oligonucleotides against Glut 5, by Measuring the Plasma Enzymes Level**

To assess the probable side effects of AS on the internal organs of MCF-7 cells-bearing nude mice, measurement of plasma enzymes activities can be used as diagnostic tool. To detect heart damage, creatine kinase (CK) and lactate dehydrogenase (LD) can be used. To detect liver damage, aspartate transaminase (AST) and alanine transaminase (ALT) can be used.

After AS treatment, there is no significant change of AST and ALT activities in the plasma, when compared with PBS control and sense control. This meant AS did not cause liver damage with this dosage. Similarly, there is no significant change of CK and LD activities in the plasma, when compared with PBS control and sense control. This meant AS treatment did not cause heart damage. In addition, no death and hemolysis occurred in all groups.

Note that only one dosage, 20mg/kg/day was used. The probable side effects of higher dosages e.g. 40mg/kg/day, should be assessed. High dosage of AS may cause splenomegaly, thrombocytopenia and severe elevation of AST and ALT (Sarmiento *et al.*, 1994). Actually the side effects of AS depends on the dosage and the duration of administration. Further studies should be done on higher dosage and longer treatment schedule.

#### **4.4 Possible Mechanisms of Antisense Oligonucleotides against Glut 5 on Breast Cancer**

The antisense oligonucleotides against Glut 5, AS 1-4, exert their effects on binding to the target nucleotide sequence directly through Watson and Cricks hybridization. The entry of AS was mediated by cationic liposomes. After the entry of an AS into the breast cancer cells, it binds to the target sequence and results in gene silencing, by inducing RNase H to degrade the DNA-RNA hybrid, forming DNA triplex or steric blocking of ribosome from binding to the mRNA. Thus, less amount of Glut 5 can be expressed and therefore, less fructose can be taken up by the breast cancer cells. From our study, fructose is an important metabolic substrate for breast cancer cells, this may induce energy deprivation and oxidative stress. Although the physiological concentration of fructose is low (50-200 $\mu$ mol/L) (Shiota *et al.*, 2002), fructose still has an important physiological role for providing energy to the breast cancer cells. In a colon cancer cell line Caco-2, fructose can serve as a carbon and energy source and common dietary monosaccharides affect the efficiency of fructose metabolism (Ellwood *et al.*, 1993).

During breast cancer development, the expression level of Glut 5 increased. For glucose deprivation-induced oxidative stress, these cause cytotoxic effect to the breast cancer cells by activating signal transduction and increased expression of



genes associated with malignancy (Spitz *et al.*, 2000). Glucose deprivation-induced energy depletion stimulated mitochondrial death pathway cascade (Moley and Mueckler, 2000). We hypothesized that the situation is similar in fructose-induced deprivation. Further investigations should be done to confirm the hypothesis.

AS against Glut 5 induced energy depletion. The reduction of intracellular ATP concentration may inhibit the action of P-glycoprotein, which is powered by ATP and pump drug out of the cells, results in drug resistance, e.g. usage of tamoxifen on late stage, hormone irresponsive breast cancer. The inhibition of p-glycoprotein pumping action can reduce multi-drug resistance in the cells. Ideally, combined treatment of antisense oligonucleotides against Glut 5 and the anti-cancer drug may have a synergistic effect. Glut 5 AS can reduce the gene expression of Glut 5 and then decrease the fructose uptake. Thus, energy deprivation results and the pumping action of p-glycoprotein were inhibited. Then the anti-cancer drug can exert its action on the cancer cells.



# **Chapter 5**

## **Future Prospectus and Conclusions**

## 5.1 Future Prospectus of Antisense Oligonucleotides

### 5.1.1 Antisense Oligonucleotides and Treatment of Breast Cancer

The antisense technology has been investigated extensively both *in vitro* and *in vivo*. It is a potential therapeutic agent in cancer, viral infections and genetic disorders, as well as a tool for studying the regulatory mechanisms in biological processes. But there are still many limitations for using antisense oligonucleotides, e.g. stability and delivery means, especially *in vivo*. These are the major hurdles to be overcome. It is necessary to create stronger and more selective affinity for RNA or duplex structures. Also, further investigation on antisense oligonucleotides should be done to provide the ability to cleave the target, and to enhance nuclease stability, cellular uptake and distribution, and *in vivo* tissue distribution, metabolism and clearance. The base, sugar and phosphate moieties of oligonucleotides can be modified. For clinical trial, the safety is the most important issue.

In the present study, the effects of antisense oligonucleotides against Glut 5 have been investigated. Further studies include usage of other forms of chemical modification, like conjugation to a short peptide to improve stability and membrane permeability, study of the inter-relationship between other glucose transporter isoforms and the usage of Glut 5 AS, microarray study to detect the gene expression profile after Glut 5 AS treatment and to see whether the mechanism is similar to that

of glucose-induced energy deprivation. For *in vivo* study, sufficient pharmacokinetics should be done to define rational dosing schedules. Also, it is important to try the inoculation of MDA-MB-231 cells into the mice to test the effect of AS. This can provide a significant clinical influence on the treatment of breast cancer. As mentioned before, MDA-MB-231 cells mimic the late stage, hormone irresponsive breast cancer and tamoxifen is unable to treat this kind of cancer (Osborne *et al.*, 1985). Therefore, the effect of AS on MDA-MB-231 cells should be done.

After evaluation of the antisense oligonucleotides against Glut 5, it can be hopefully used for treatment of breast cancer. Combined treatment with anti-cancer drugs, e.g. doxorubicin, tamoxifen may further improve the efficiency in treating breast cancer. As antisense oligonucleotides (AS) against Glut 5 can reduce intracellular ATP content and thus inhibit the pumping action of p-glycoprotein. As a result, the anti-cancer drug can enter the cells without any barrier and exerts their effects, even in multi-drug resistant tumor cells. At the same time, nutrient-deprivation induced energy depletion induces cascade of events and finally leads to apoptosis of cancer cells. Another approach is to combine antisense oligonucleotides against Glut 5 and Glut 1. AS against Glut 1 was studied extensively. The anti-tumor effects of Glut 1 AS on MCF-7 cells and HepG-2 cells

were investigated and it caused cytotoxic effect to both cell lines successfully (Chan *et al.*, 1999, Chen *et al.*, 2002). The combined treatment of AS against Glut 5 and Glut 1 may cause profound anti-tumor effects. But the toxicity and side effects on normal cells should be carefully addressed, as Glut 1 are present in almost all cells. AS against Glut 1 may affect the glucose uptake in the normal cells. If AS against Glut 1 is really cytotoxic to normal cells, it is not recommended to use as cancer therapeutic agent.



### 5.1.2 Role of Glut 5 in Breast Cancer

Glut 5 is a fructose transporter. Glut 5 exhibits selectivity for fructose transport, with a  $K_m$  of 6mM. In addition, fructose transport was not inhibited by cytochalasin B, a competitive inhibitor of glucose transporters (Tatibouet *et al.*, 2000). The result suggested that Glut 5 did not possess specificity toward glucose. The presence of Glut 5 is important because this enables breast cancer cells to have a specialized ability to transport fructose, in which fructose is a metabolic substrate used by only a few human tissues. This is a survival advantage for the breast cancer cells. So, breast cancer cells can get more metabolic substrate, instead of glucose, in meeting the great energy requirements of breast cancer cells.

Antisense oligonucleotides against Glut 5 can bring about effective cytotoxicity to the cells because of nutrient deprivation. It is speculated that Glut 5 may possess another functions instead of transporting fructose. It may transport some nutrients which are important for growth e.g. essential amino acids, fatty acids or vitamin, etc, just like Glut 1 and Glut 3 can transport glucose and the metabolite of ascorbic acids (Rumsey *et al.*, 1997). Up till now, there is no published paper about the substrate specificity of Glut 5. Further investigation should be done on Glut 5 kinetics study, to find out the  $K_m$  toward different important nutrients. This can help us understand the role of Glut 5 in breast cancer development.



## 5.2 Conclusions and Remarks

Antisense represents the regulation of gene expression by short oligonucleotides or oligonucleotide mimics, which relies on the formation of Watson and Crick hydrogen bonds between the antisense oligomer and the complementary mRNA strand, thereby providing target specificity of the agent. In the present study, antisense oligonucleotides against Glut 5 are effective to treat human breast cancer undoubtedly. Glut 5 AS binds to the target nucleotide sequence and results in gene silencing by either inducing RNase H to degrade the DNA-RNA hybrid, DNA triplex formation to block transcription, or steric blocking of ribosome to contact with mRNA. In *in vitro* study, Glut 5 AS caused cytotoxicity on MCF-7 cells and MDA-MB-231 cells by lowering the capacity to transport nutrients into the cells, and induced energy deprivation. The AS silencing mechanism was confirmed by the reduction of mRNA and protein expression. Apoptosis was the final step of energy deprivation. The flow of Glut 5 AS treatment was summarized in Fig. 5.1. In *in vivo* study, administration of Glut 5 AS reduced the tumor growth rate and it did not cause any side effect in mice, e.g. damage to internal organs, hemolysis and death.

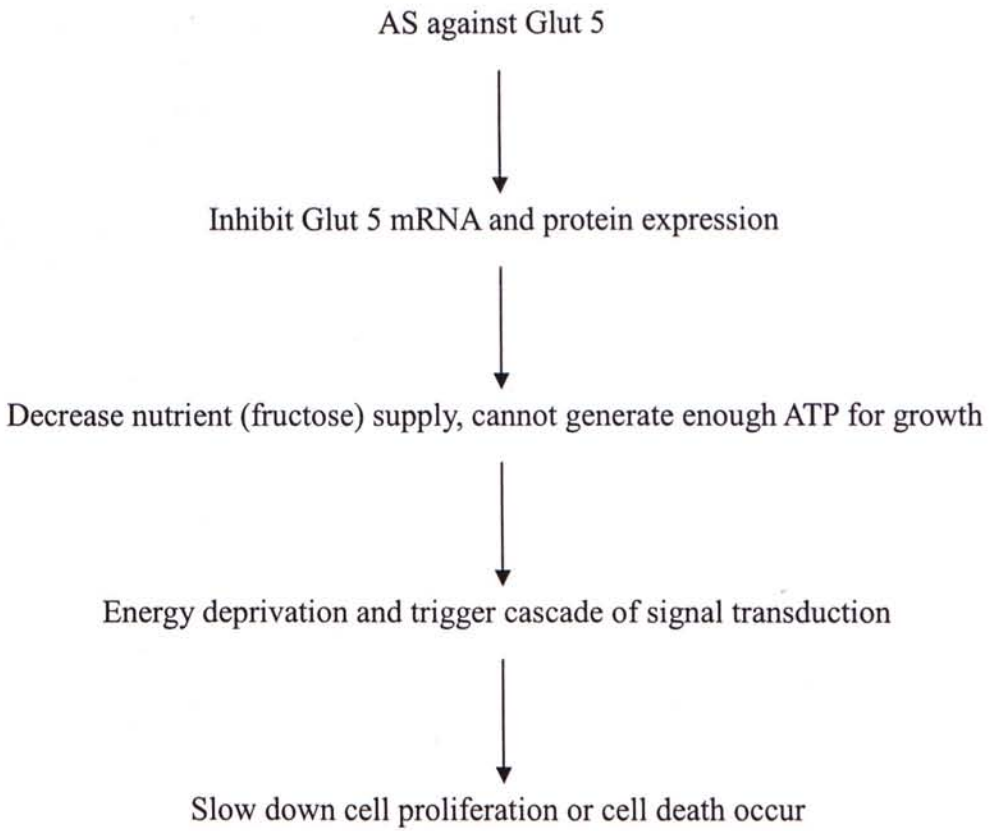


Figure 5.1

Flow chart of consequences of antisense oligonucleotides against Glut 5 treatments in MCF-7 cells and MDA-MB-231 cells.

The ultimate goal of our future works is to develop an effective approach to human breast cancer treatment by using novel chemically modified antisense oligonucleotides against Glut 5.

## References

- Aft RL, Zhang FW and Gius D. (2000). Evaluation of 2-deoxy-D-glucose as a chemotherapeutic agent: Mechanism of cell death. *Br J Cancer*. 87:805-812.
- Agrawal S. (1996). Antisense oligonucleotides: towards clinical trials. *Trends Biotechnol.* 14(10):376-387.
- Agrawal S and Kandimalla ER. (2000). Antisense therapeutics: Is It as Simple as Complementary base recognition. *Mol Med Today*. 6(3):103.
- Agrawal S, Tamsamani J and Tang JY. (1991). Pharmacokinetics, biodistribution, and stability of oligodeoxynucleotide phosphorothioates in mice. *Proc Natl Acad Sci USA*. 88:7595-7599.
- Agrawal S and Zhao Q. (1998). Antisense therapeutics. *Curr Opin Chem Biol*. 12(4):519-528.
- Aharinejad S, Abraham D, Paulus P, Abri H, Hofmann M, Grossschmidt K, Schafer R, Stanley ER and Hofbauer R. (2002). Colony-stimulating factor-1 antisense treatment suppresses growth of human tumor xenografts in mice. *Cancer Res*. 62(18):5317-5324.
- Alama A, Barbieri F, Cagnoli M and Schettini G (1997). Antisense oligonucleotides as therapeutic agents. *Pharmacol Res*. 36:171-178.
- Angeloni SV, Martin MB, Garcia-Morales P, Casro-Galache MD, Ferragut JA and Saceda M. (2004). Regulation of estrogen receptors- $\alpha$  expression by the tumor suppressor gene p53 in MCF-7 cells. *J Endocrinol*. 180(3):497-504.
- Au KK, Liong E, Li JY, Li PS, Liew CC, Kwok TT, Choy YM, Lee CY and Fung KP. (1997). Increases in mRNA levels of glucose transporters types 1 and 3 in Ehrlich ascites tumor cells during tumor development. *J Cell Biochem*. 67(1):131-135.
- Bao JJ, Le XF, Wang RY, Yuan J, Wang L, Atkinson EN, LaPushin R, Andreeff M, Fang B, Yu Y and Bast RC Jr. (2002). Re-expression of the tumor suppressor gene ARHI induces apoptosis in ovarian and breast cancer cells through a caspase-independent calpain-dependent pathway. *Cancer Res*. 62(24):7264-7272.



- Barrett MP, Walmsley AR and Gould GW. (1999). Structure and function of facilitative sugar transporters. *Curr Opin Cell Biol.* 11(4):496-502.
- Bertrand JR, Pottier M, Vekris A, Opolon P, Maksimenko A and Malvy C. (2002). Comparison of antisense oligonucleotides and siRNAs in cell culture and *in vivo*. *Biochem Biophys Res Commun.* 296(4):1000-1004.
- Brown GK. (2000). Glucose transporters: structure, function and consequences of deficiency. *J Inherit Metab Dis.* 23(3):237-246.
- Buchs AE, Sasson S, Joost HG and Cerasi E. (1998). Characterization of Glut 5 domains responsible for fructose transport. *Endocrinology.* 139(3):827-831.
- Burant CF, Takeda J, Brot-Laroche E, Bell GI and Davidson NO. (1992). Fructose transporter in human spermatozoa and small intestine is Glut 5. *J Biol Chem.* 267(21):14523-14526.
- Carmeci S, Thompson DA, Kuang WW, Lightdale N, Furthmayr H and Weigel RJ. (1998). Moesin expression is associated with the estrogen-receptor-negative breast cancer phenotype. *Surgery.* 124: 211-217.
- Chan JYW, Kong SK, Choy YM, Lee CY and Fung KP. (1999). Inhibition of glucose transporter gene expression by antisense nucleic acids in HL-60 leukemia cells. *Life Sci.* 65(1): 63-70.
- Chan KK, Chan JYW, Chung KW and Fung KP. (2004). Study of the effects of antisense oligonucleotides against glucose transporter 5 on human breast cancer. *J Cell Biochem.* In press.
- Chambard JM and Ashmore JF. (2003). Sugar transport by mammalian members of the SLC26 superfamily of anion-bicarbonate exchangers. *J Physiol.* 550.3:667-677.
- Chen CP, Li XX, Zhang LR, Min JM, Chan JY, Fung KP, Wang SQ and Zhang LH. (2002). Synthesis of antisense oligonucleotide-peptide conjugate targeting to Glut-1 in HepG-2 and MCF-7 Cells. *Bioconjug Chem.* 13(3):525-529.
- Claus EB, Stowe M and Carter D. (2003). Family history of breast and ovarian cancer and the risk of breast carcinoma in situ. *Breast Cancer Res Treat.* 78(1):7-15.



- Concha II, Velasquez FV, Martinez JM, Angulo C, Droppelmann A, Reyes AM, Slebe JC, Vera JC and Golde DW. (1997). Human erythrocytes express Glut 5 and transport fructose. *Blood*. 89(11):4190-4195.
- Crooke ST. (1999). Molecular mechanisms of action of antisense drugs. *Biochim Biophys Acta*. 1489(1):31-44.
- Crooke ST. (2004). Progress in antisense technology. *Annu Rev Med*. 55:61-95.
- Crooke ST, Grillone LR, Tendolkar A, Garrett A, Fratkin MJ, Leeds J and Barr WH. (1994). A pharmacokinetic evaluation of <sup>14</sup>C-labeled afovirsen sodium in patients with genital warts. *Clin Pharmacol Ther*. 56(6 Pt 1):641-646.
- Cutroneo KR and Chiu JF. (2003). Sense oligonucleotide competition for gene promoter binding and activation. *Int J Biochem Cell Biol*. 35(1):32-38.
- Dean N.M. and Bennett CF. (2003). Antisense oligonucleotide-based therapeutics for cancer. *Oncogene*, 22:9087-9096
- Devarajan E, Sahin AA, Chen JS, Krishnamurthy RR, Aggarwal N, Brun AM, Sapino A, Zhang F, Sharma D, Yang XH, Tora AD and Mehta K. (2002). Down-regulation of caspase 3 in breast cancer: a possible mechanism for chemoresistance. *Oncogene*. 21(57):8843-8851.
- Doisneau-Sixou SF, Sergio CM, Carroll JS, Hui R, Musgrove EA and Sutherland RL. (2003). Estrogen and antiestrogen regulation of cell cycle progression in breast cancer cells. *Endocr Relat Cancer*. 10(2):179-186.
- Elliott SS, Keim NL, Stern JS, Teff K and Havel PJ. (2002). Fructose, weight gain, and the insulin resistance syndrome. *Am J Clin Nutr*. 76(5):911-922.
- Ellmen J, Hakulinen P, Partanen A and Hayes DF. (2003). Estrogenic effects of toremifene and tamoxifen in postmenopausal breast cancer patients. *Breast Cancer Res Treat*. 82(2):103-111.
- Ellwood KC, Chatzidakis C and Failla ML. (1993). Fructose utilization by the human intestinal epithelial cell line, Caco-2. *Proc Soc Exp Biol Med*. 202(4):440-446.

- Fan Y, Borowsky AD and Weiss RH. (2003). An antisense oligodeoxynucleotide to p21(Waf1/Cip1) causes apoptosis in human breast cancer cells. *Mol Cancer Ther.* 2(8):773-782.
- Farman CA and Kornbrust DJ. (2003). Oligodeoxynucleotide studies in primates: antisense and immune stimulatory indications. *Toxicol Pathol.* 31 Suppl:119-122.
- Fernandez PM, Tabbara SO, Jacobs LK, Manning FC, Tsangaris TN, Schwartz AM, Kennedy KA and Patierno SR. (2000). Overexpression of the glucose-regulated stress gene GRP78 in malignant but not benign human breast lesions. *Breast Cancer Res Treat.* 59(1):15-26.
- Ferraris RP. (2001). Dietary and developmental regulation of intestinal sugar transport. *Biochem J.* 360:265-276.
- Fischbarg J, Kuang KY, Vera JC, Arant S, Silverstein SC, Loike J and Rosen OM. (1990). Glucose transporters serve as water channels. *Proc Natl Acad Sci USA.* 87(8):3244-3247.
- Flaherty KT, Stevenson JP and O'Dwyer PJ. (2001). Antisense therapeutics: lessons from early clinical trials. *Curr Opin Oncol.* 13: 499-505.
- Flanagan WM, Wolf JJ, Olson P, Grant D, Lin KY, Wagner RW and Matteucci MD. (1999) A cytosine analog that confers enhanced potency to antisense oligonucleotides. *Proc Natl Acad Sci USA.* 96(7):3513-3518.
- Freudenheim JL, Sieri S, Trevisan M and Berrino F. (2002). Fasting glucose is a risk factor for breast cancer: a prospective study. *Cancer Epidemiol Biomarkers Prev.* 11:1361-1168.
- Geary RS, Watanabe TA, Truong L, Freier S, Lesnik EA, Sioufi NB, Sasmor H, Manoharan M and Levin AA. (2001). Pharmacokinetic properties of 2'-O-(2-methoxyethyl)-modified oligonucleotide analogs in rats. *J Pharmacol Exp Ther.* 296(3):890-897.
- Gershon H, Ghirlando R, Guttman SB and Minsky A. (1993). Mode of formation and structural features of DNA-cationic liposome complexes used for transfection.



*Biochemistry*. 32: 7143-7151.

Girniene J, Tatibouet A, Sackus A, Yang J, Holman GD and Rollin P. (2003). Inhibition of the D-fructose transporter protein Glut5 by fused-ring glyco-1,3-oxazolidin-2-thiones and -oxazolidin-2-ones. *Carbohydr Res*. 338(8):711-719.

Godoy A, Vera JC, Aguayo L and Nualart F. (2000). Differential subcellular distribution of the glucose transporter Glut 1 and the fructose transporter Glut 5 in breast tumor cells. *J Physiol*. 523P:84P.

Good L. (2003). Translation repression by antisense sequences. *Cell Mol Life Sci*. 60(5):854-861.

Gould GW and Holman GD. (1993). The glucose transporter family: structure, function and tissue-specific expression. *Biochem J*. 295 (Pt 2):329-341.

Gould GW, Thomas HM, Jess TJ and Bell GI. (1991). Expression of human glucose transporters in *Xenopus* oocytes: kinetic characterization and substrate specificities of the erythrocyte, liver, and brain isoforms. *Biochemistry*. 30(21):5139-5145.

Grover-McKay M, Walsh SA, Seftor EA, Thomas PA and Hendrix MJ. (1998). Role for glucose transporter 1 protein in human breast cancer. *Pathol Oncol Res*. 4(2):115-120.

Hammond SM, Bernstein E, Beach D and Hannon GJ. (2000). An RNA-directed nuclease mediates post-transcriptional gene silencing in *drosophila*. *Nature*. 404:293-296.

Ho SP, Bao Y, Leshner T, Malhotra R, Ma LY, Fluharty SJ and Sakai RR. (1998). Mapping of RNA accessible sites for antisense experiments with oligonucleotide libraries. *Nat Biotechnol*. 16, 59-63.

Holen T, Amarzguioui M, Babaie E, and Prydz H. (2003). Similar behavior of single-strand and double-strand siRNAs suggests they act through a common RNAi pathway. *Nucl Acids Res*. 31: 2401-2407.

- Izuishi K, Kato K, Ogura T, Kinoshita T and Esumi H. (2000). Remarkable tolerance of tumor cells to nutrient deprivation: possible new biochemical target for cancer therapy. *Cancer Res.* 60(21):6201-6207.
- Jiang L and Ferraris RP. (2001). Developmental reprogramming of rat Glut-5 requires de novo mRNA and protein synthesis. *Am J Physiol Gastrointest Liver Physiol.* 280(1):G113-120.
- Joost HG and Thorens B. (2001). The extended Glut-family of sugar/polyol transport facilitators: nomenclature, sequence characteristics, and potential function of its novel members. *Mol Membr Biol.* 18(4):247-256.
- Kane S, Seatter MJ and Gould GW. (1997). Functional studies of human Glut5: effect of pH on substrate selection and an analysis of substrate interactions. *Biochem Biophys Res Commun.* 238(2):503-505.
- Kang SS, Chun YK, Hur MH, Lee HK, Kim YJ, Hong SR, Lee JH, Lee SG and Park YK. (2002). Clinical significance of glucose transporter 1 (Glut1) expression in human breast carcinoma. *Jpn J Cancer Res.* 93(10):1123-1128.
- Kawasaki H, Machida M, Komatsu M, Li HO, Murata T, Tsutsui H, Fujita A, Matsumura M, Kobayashi Y, Taira K and Yokoyama KK. (1996). Specific regulation of gene expression by antisense nucleic acids: a summary of methodologies and associated problems. *Artif Organs.* 20(8):836-848.
- Kayano T, Burant CF, Fukumoto H, Gould GW, Fan YS, Eddy RL, Byers MG, Shows TB, Seino S and Bell GI. (1990). Human facilitative glucose transporters. Isolation, functional characterization, and gene localization of cDNAs encoding an isoform (Glut 5) expressed in small intestine, kidney, muscle, and adipose tissue and an unusual glucose transporter pseudogene-like sequence (Glut 6). *J Biol Chem.* 265(22):13276-13282.
- Kretschmer-Kazemi Far R and Sczakiel G. (2003). The activity of siRNA in mammalian cells is related to structural target accessibility: a comparison with antisense oligonucleotides. *Nucleic Acids Res.* 31(15):4417-4424.
- Kurokawa H, Nishio K, Fukumoto H, Tomonari A, Suzuki T and Saijo N. (1999). Alteration of caspase-3 (CPP32/Yama/apopain) in wild-type MCF-7, breast cancer cells. *Oncol Rep.* 6(1):33-37.



- Kurreck J. (2003). Antisense technologies. Improvement through novel chemical modifications. *Eur J Biochem.* 270(8):1628-1644.
- Kurt RA, Urba WJ and Schoof DD. (2000). Isolation of genes overexpressed in freshly isolated breast cancer specimens. *Breast Cancer Res Treat.* 59(1):41-48.
- Larsen HJ, Bentin T and Nielsen PE. (1999). Antisense properties of peptide nucleic acid. *Biochim Biophys Acta.* 1489(1):159-166.
- Laudanski P, Swiatecka J, Kovalchuk O and Wolczynski S. (2003). Expression of Glut 1 gene in breast cancer cell lines MCF-7 and MDA-MB-231. *Ginek Pol.* 74(9):782-785.
- Lima WF, Wu H and Crooke ST. (2001). Human RNases H. *Methods Enzymol.* 341:430-440.
- Litzinger DC, Brown JM, Wala I, Kaufman SA, Van GY, Farrell CL and Collins D. (1996). Fate of cationic liposomes and their complex with oligonucleotide in vivo. *Biochim Biophys Acta.* 1281(2):139-149.
- Livak KJ and Schmittgen TD. (2001). Analysis of relative gene expression data using real-time quantitative PCR and the  $2^{-\Delta\Delta C_T}$  Method. *Methods.* 25(4):402-408.
- Lopes de Menezes DE, Hu Y and Mayer LD. (2003). Combined treatment of Bcl-2 antisense oligodeoxynucleotides (G3139), p-glycoprotein inhibitor (PSC833), and sterically stabilized liposomal doxorubicin suppresses growth of drug-resistant growth of drug-resistant breast cancer in severely combined immunodeficient mice. *J Exp Ther Oncol.* 3(2):72-82.
- Lykkesfeldt AE, Larsen JK, Christensen IJ and Briand P. (1984). Effects of the antioestrogen tamoxifen on the cell cycle kinetics of the human breast cancer cell line, MCF-7. *Br J Cancer.* 49(6):717-722.
- Ma XJ, Salunga R, Tuggle JT, Gaudet J, Enright E, McQuary P, Payette T, Pistone M, Stecker K, Zhang BM, Zhou YX, Varnholt H, Smith B, Gadd M, Chatfield E, Kessler J, Baer TM, Erlander MG and Sgroi DC. (2003). Gene expression profiles of human breast cancer progression. *Proc Natl Acad Sci USA.* 100(10):5974-5979.



- Makin G and Dive C. (2001). Apoptosis and cancer chemotherapy. *Trends Cell Biol.* 11(11):S22-26.
- Malide D, Davies-Hill TM, Levine M and Simpson IA. (1998). Distinct localization of Glut-1, -3, and -5 in human monocyte-derived macrophages: effects of cell activation. *Am J Physiol.* 274(3 Pt 1):E516-526.
- Matveeva O, Felden B, Audlin S, Gesteland RF and Atkins JF. (1997) A rapid *in vitro* method for obtaining RNA accessibility patterns for complementary DNA probes: correlation with an intracellular pattern and known RNA structures. *Nucl Acids Res.* 25, 5010–5016.
- Matveeva O, Felden B, Tsodikov A, Johnston J, Monia BP, Atkins JF, Gesteland RF and Freier SM. (1998) Prediction of antisense oligonucleotide efficacy by *in vitro* methods. *Nat Biotechnol.* 16, 1374–1375.
- Medina RA, Meneses AM, Vera JC, Guzman C, Nualart F, Astuya A, Garcia MA, Kato S, Carvajal A, Pinto M and Owen GI. (2003). Estrogen and progesterone up-regulate glucose transporter expression in ZR-75-1 human breast cancer cells. *Endocrinology.* 144(10):4527-4535.
- Mercatante DR and Kole R. (2002). Control of alternative splicing by antisense oligonucleotides as a potential chemotherapy: effects on gene expression. *Biochim Biophys Acta.* 1587(2-3):126-132.
- Moley KH, and Mueckler MM. (2000). Glucose transport and apoptosis. *Apoptosis.* 5(2):99-105.
- Mueckler M. (1994) Facilitative glucose transporters. *Eur J Biochem.* 219:713-725.
- Muti P, Quattrin T, Grant BJ, Krogh V, Micheli A, Schunemann HJ, Ram M, Nable GJ, Nable EG, YangZY, Fox BA, Plautz GE, Gao X, Huang L, Shu S, Gordon D and Chang AE. (1993). Direct Gene Transfer with DNA-Liposome Complexes in Melanoma: Expression, Biologic Activity, and Lack of Toxicity in Humans. *Proc Natl Acad Sci USA*, 90:11307-11311.
- Noguchi Y, Saito A, Miyagi Y, Yamanaka S, Marat D, Doi C, Yoshikawa T, Tsuburaya A, Ito T and Satoh S. (2000). Suppression of facilitative glucose transporter 1 mRNA can suppress tumor growth. *Cancer Lett.* 154(2):175-182.

- Oehlke J, Birth P, Klauschenz E, Wiesner B, Beyermann M, Oksche A and Bienert M. (2002). Cellular uptake of antisense oligonucleotides after complexing or conjugation with cell-penetrating model peptides. *Eur J Biochem.* 269(16):4025-4032.
- Olson AL and Pessin JE. (1996). Structure, function and regulation of the mammalian facilitative glucose transporter gene family. *Annu Rev Nutr.* 16:235-256.
- Osborne CK, Hobbs K and Clark GM. (1985). Effect of estrogens and antiestrogens on growth of human breast cancer cells in athymic nude mice. *Cancer Res.* 45(2): 584-590.
- Osborne CK. (1998). Tamoxifen in the treatment of breast cancer. *N Engl J Med.* 339(22):1609-1618.
- Parton M, Dowsett M and Smith I. (2001). Studies of apoptosis in breast cancer. *BMJ.* 322(7301):1528-1532.
- Paterson BM, Roberts BE and Kuff EL (1977) Structural gene identification and mapping by DNA-mRNA hybrid-arrested cell-free translation. *Proc Natl Acad Sci USA.* 74(10):4370-4.
- Rogers S, Docherty SE, Slavin JL, Henderson MA and Best JD. (2003). Differential expression of Glut12 in breast cancer and normal breast tissue. *Cancer Lett.* 193(2):225-233.
- Rosok O and Sioud M. (2003). Systematic identification of sense-antisense transcripts in mammalian cells. *Nat Biotechnol.* 22(1):104-108.
- Rumsey SC, Daruwala R, Al-Hasani H, Zarnowski MJ, Simpson IA and Levine M. (1997). Dehydroascorbic acid transport by Glut4 in *Xenopus* oocytes and isolated rat adipocytes. *J Biol Chem.* 275(36):28246-28253.
- Salatino M, Schillaci R, Proietti CJ, Carnevale R, Frahm I, Molinolo AA, Iribarren A, Charreau EH and Elizalde PV. (2004). Inhibition of *in vivo* breast cancer growth by antisense oligodeoxynucleotides to type I insulin-like growth factor receptor mRNA involves inactivation of ErbBs, PI-3K/Akt and p42/p44 MAPK signaling pathways



but not modulation of progesterone receptor activity. *Oncogene*. 23(30):5161-5174.

Sarmiento UM, Perez JR, Becker JM and Narayanan R. (1994). In vivo toxicological effects of rel A antisense phosphorothioates in CD-1 mice. *Antisense Res Dev*. 4(2):99-107.

Shadidi M and Sioud M. (2003). Identification of novel carrier peptides for the specific delivery of therapeutics into cancer cells. *FASEB J*. 17(2):256-258.

Shim H, Chun YS, Lewis BC and Dang CV. (1998). A unique glucose-dependent apoptotic pathway induced by c-Myc. *Proc Natl Acad Sci USA*. 95(4):1511-1516.

Shiota M, Moore MC, Galassetti P, Monohan M, Neal DW, Shulman GI, and Cherrington AD. (2002). Inclusion of low amounts of fructose with an intraduodenal glucose load markedly reduces postprandial hyperglycemia and hyperinsulinemia in the conscious dog. *Diabetes*. 51:469-478.

Song RX, Santen RJ, Kumar R, Adam L, Jeng MH, Masamura S and Yue W. (2002). Adaptive mechanisms induced by long-term estrogen deprivation in breast cancer cells. *Mol Cell Endocrinol*. 193(1-2):29-42.

Spitz DR, Sim JE, Ridnour LA, Galoforo SS and Lee YJ. Glucose deprivation-induced oxidative stress in human tumor cells. A fundamental defect in metabolism? *Ann N Y Acad Sci*. 899:349-362.

Summerton J. (1999). Morpholino antisense oligomers: the case for an RNase H-independent structural type. *Biochim Biophys Acta*. 1489(1):141-158.

Takakura Y, Kuentzel SL, Raub TJ, Davies A, Baldwin SA and Borchardt RT. (1991). Hexose uptake in primary cultures of bovine brain microvessel endothelial cells. I. Basic characteristics and effects of D-glucose and insulin. *Biochim Biophys Acta*. 1070(1):1-10.

Tatibouet A, Yang J, Morin C and Holman GD. (2000). Synthesis and evaluation of fructose analogues as inhibitors of the D-fructose transporter Glut 5. *Bioorg Med Chem*. 8(7):1825-1833.

Toth J, Boszormenyi I, Majer ZS, Laczko I, Malvy C, Hollosi M and Bertrand JR. (2002). A two step model aimed at delivering antisense oligonucleotides in targeted

cells. *Biochem Biophys Res Commun.* 293(1):18-22.

Uldry M, Ibberson M, Hosokawa M and Thorens B. (2002). GLUT2 is a high affinity glucosamine transporter. *FEBS Lett.* 524(1-3):199-203.

Vollmer J, Weeratna R, Payette P, Jurk M, Schetter C, Laucht M, Wader T, Tluk S, Liu M, Davis HL and Krieg AM. (2004). Characterization of three CpG oligodeoxynucleotide classes with distinct immunostimulatory activities. *Eur J Immunol.* 34(1):251-262.

Wagner RW. (1994). Gene inhibition using antisense oligodeoxynucleotides. *Nature.* 372: 333-335.

Wang H, Yu D, Agrawal S and Zhang R. (2003). Experimental therapy of human prostate cancer by inhibiting MDM2 expression with novel mixed-backbone antisense oligonucleotides: in vitro and in vivo activities and mechanisms. *Prostate.* 54(3):194-205.

Warberg O. (1956). On the origin of Cancer cells. *Science.* 123:306-314.

Wasserman D, Hoekstra JH, Tolia V, Taylor CJ, Kirschner BS, Takeda J, Bell GI, Taub R and Rand EB. (1996). Molecular analysis of the fructose transporter gene (Glut 5) in isolated fructose malabsorption. *J Clin Invest.* 98(10):2398-2402.

Wu L, Fritz JD and Powers AC. (1998). Different Functional Domains of Glut2 Glucose Transporter Are Required for Glucose Affinity and Substrate Specificity. *Endocrinology.* 139(10): 4205-4212.

Yang L, Cao Z, Yan H and Wood WC. (2003). Coexistence of high levels of apoptotic signaling and inhibitor of apoptosis proteins in human tumor cells: implication for cancer specific therapy. *Cancer Res.* 63(20):6815-24.

Yang SP, Song ST and Song HF. (2003). Advancements of antisense oligonucleotides in treatment of breast cancer. *Acta Pharmacol Sin.* 24(4):289-295.

Zamecnik PC and Stephenson ML (1978). Inhibition of Rous sarcoma virus replication and cell transformation by a specific oligodeoxynucleotide. *Proc Natl Acad Sci USA.* 75(1):280-284.



Zamora-Leon SP, Golde DW, Concha II, Rivas CI, Delgado-Lopez F, Baselga J, Nualart F and Vera JC. (1996). Expression of the fructose transporter Glut 5 in human breast cancer. *Proc Natl Acad Sci USA*. 93:1847-1852.

Zapata JM, Krajewska M, Krajewski S, Huang RP, Takayama S, Wang HG, Adamson E and Reed JC.(1998). Expression of multiple apoptosis-regulatory genes in human breast cancer cell lines and primary tumors. *Breast Cancer Res Treat*. 47(2):129-140.

Zelphati O and Szorka Jr FC. (1996). Mechanism of oligonucleotide release from cationic liposomes. *Proc Natl Acad Sci USA*. 93(21):11493-11498.

Zhang HY, Mao J, Zhou D, Xu Y, Thonberg H, Liang Z and Wahlestedt C. (2003). mRNA accessible site tagging (MAST): a novel high throughput method for selecting effective antisense oligonucleotides. *Nucleic Acids Res*. 31, No. 14 e72.

Website:

<http://www.cancernet.co.uk/tamoxifen.htm>



CUHK Libraries



004146103